1-1-2015

Drosophila Cyclin J And The Somatic Pirna Pathway Cooperate To Regulate Germline Stem Cells

Paul Michael Albosta
Wayne State University,

DROSOPHILA CYCLIN J AND THE SOMATIC piRNA PATHWAY COOPERATE TO REGULATE GERMLINE STEM CELLS

by

PAUL MICHAEL ALBOSTA

DISSERTATION

Submitted to the Graduate School

of Wayne State University,

Detroit, Michigan

in partial fulfillment of the requirements

for the degree of

DOCTOR OF PHILOSOPHY

2015

MAJOR: MOLECULAR MEDICINE AND GENETICS

Approved by:

_____

Advisor Date

_____

_____

_____

DEDICATION

This work is dedicated to my mother Janet, father Robert, sister Kristina, and brother Philip Albosta. Most importantly, this dedication goes out to my wife Merra and son Gabriel Albosta, who encouraged me to be the best scientist I can be. The love and support of my family will keep me strong for many years to come.

ACKNOWLEDGMENTS

First and foremost, I would like to thank my advisor, Dr. Russell L. Finley, Jr. Russ has guided me on my journey, provided the right balance of encouragement and constructive criticism, and most importantly, taught me how to think. I am also grateful for my committee; Dr. Michael Tainsky, Dr. George Brush, and Dr. Victoria (Vicky) Meller. They have been wonderful, insightful, flexible, and have contributed to my graduate experience being somewhat pleasant. I want to thank the graduate director, Dr. Gregory Kapatos. None of this would be possible without the Center for Molecular Medicine and Genetics, namely the chair, Dr. Lawrence (Larry) Grossman, the best secretary in the world, Suzanne Shaw, and our fearless financial administrator, David Wissbrun. I must also thank god, through whom all things are possible.

I would like a moment of silence for the millions of flies who gave their lives for this study… And a huge thanks to the fantastic fly community here at WSU starting with the fly food technician, Charles Hogan, for making my job easier. Some of my best presentations and feedback came from fly club, organized by Dr. Vicky Meller. I would say more, but the first rule of fly club is you don't talk about fly club (just kidding, that is a movie reference). Finally, I would like to thank the former members of the Finley lab, namely Nermin Gerges, Phillip Selman M.S., Dr. Thilakam Murali, Dr. Dumrong Mairiang, Dr. Dongmei Liu, Dr. George Roberts III, Dr. Steven Guest, and Huamei (Heidi) Zhang, all of who provided constructive conversations and/or reagents for my project and results. Above all, I must thank Dr. Govindaraja (Raj) Atikukke. His work with Cyclin J provided me with a running start on my project. His findings and interpretations have been absolutely essential to this study.

TABLE OF CONTENTS

LIST OF TABLES

LIST OF FIGURES

CHAPTER 1: INTRODUCTION

1.1 Summary

My goal for this project was to determine and characterize a role for Cyclin J (CycJ) in oogenesis. CycJ is conserved in all metazoans and is homologous to well-characterized cell cycle regulators, but its function is unknown. In *Drosophila*, it is expressed exclusively in ovaries and early embryos, suggesting a possible role in one or both of these tissues. Initial analyses in *Drosophila* revealed that *CycJ* might regulate embryogenesis, but is dispensable during oogenesis under normal conditions (Kolonin and Finley 2000; Althoff, Viktorinova et al. 2009; Atikukke 2009). Further characterization showed that *CycJ* genetically interacted with two piRNA pathway members, *armitage (armi)* and *aubergine (aub);* a *CycJ* null enhanced the oogenesis defects of *armi* or *aub* single mutants (Atikukke 2009). I extended these analyses by demonstrating a genetic interaction between *CycJ* and a third piRNA pathway member, *piwi,* as well as quantifying the resulting oogenesis defects of all *CycJ*-piRNA pathway double and single mutants. The key findings are that *piwi* and *armi* are required for packaging of germline cells into egg chambers and *CycJ* contributes to this process as discussed in Chapter 2 (Atikukke, Albosta et al. 2014). I went on to demonstrate that *piwi* and *armi* function from somatic cells to regulate bone morphogenetic protein (BMP) signaling and the number of germline stem cells (GSCs), and that *CycJ* interacts with this somatic piRNA pathway as described in Chapter 3 [Albosta 2015 in prep]. These data suggest that the piRNA pathway in ovarian somatic cells controls GSCs via BMP signaling and this leads to a requirement for *CycJ* limiting these excess GSCs, indicating that CycJ may be a conserved stem cell regulator.

1.2 Cyclins are highly conserved serine/threonine kinase regulators

Cyclins are a superfamily of highly conserved eukaryotic regulatory proteins. The defining feature of cyclins is a cyclin box, which is a domain that interacts with cyclin-dependent kinases (Cdks) (Hadwiger, Wittenberg et al. 1989; Jeffrey, Russo et al. 1995). Cyclin binding is required for the activation of kinase activity and contributes to the substrate specificity of Cdks (Kobayashi, Stewart et al. 1992; Lees and Harlow 1993; Horton and Templeton 1997). The founding member of this protein superfamily, Cyclin B (CycB), was originally identified as a protein that oscillated with the cell division cycles of sea urchin embryos and was aptly named Cyclin (Evans, Rosenthal et al. 1983). This protein was later identified as CycB after cloning and sequencing, and was found to be the only sea urchin mRNA capable of inducing frog (*Xenopus*) oocyte maturation upon injection, suggesting a conserved specific role for this molecule in driving the cell cycle (Pines and Hunt 1987). Further studies in *Xenopus* demonstrated that CycB was required for transition from the Gap 2 cell cycle phase to Mitosis (i.e., the G2→M transition) (Minshull, Blow et al. 1989). Finally, CycB destruction was shown to be required for the exit of mitosis (Murray, Solomon et al. 1989). CycB is a conserved cell cycle regulator in most eukaryotic organisms including unicellular *Dictyostelium* (Cao, Chen et al. 2014). In metazoans, cyclins are named with letters and multiple cyclins in addition to Cyclin B (e.g., Cyclin A, D, E) are known to have conserved roles in regulating the cell cycle by activating Cdks and phosphorylating specific substrates that are required for cell cycle transitions (reviewed in (Hochegger, Takeda et al. 2008)). Other cyclins (e.g., Cyclin C, H, T) have conserved roles in regulating Cdks involved in transcription or other cellular processes, and some have multiple functions, like Cyclins

D and E that function in both cell cycle and transcription regulation (reviewed in (Lim and Kaldis 2013)). In *Drosophila,* there are 16 highly conserved unique cyclins and only a few of them, including CycY and CycJ, have poorly or uncharacterized functions.

1.3 Cyclin J is a poorly characterized and highly conserved putative cell cycle regulator specifically expressed in *Drosophila* ovaries

CycJ is a poorly characterized highly conserved cyclin specifically expressed in ovaries and early embryos. It was identified originally in *Drosophila* as a Cdk interacting protein in yeast-two-hybrid screens (Finley and Brent 1994; Finley, Thomas et al. 1996). CycJ has been shown to physically interact with both Cdk1 and Cdk2 *in vivo,* and the kinase activity of CycJ immunoprecipitates has been verified *in vitro* with an H1 kinase assay (Finley, Thomas et al. 1996; Kolonin and Finley 2000; Althoff, Viktorinova et al. 2009). Based on amino acid sequence, CycJ is more closely related to the A and B type cyclins, which are known cell cycle regulators, but a definitive role for CycJ in regulating the cell cycle has not been established. Sequence alignment of CycJ amino acid sequences reveals high conservation between *Drosophila*, human, mouse, and frog, indicating that CycJ likely has an important function (Atikukke 2009). In *Drosophila*, *CycJ* mRNA is present in ovaries and very early embryos suggesting a function in one or both of these tissues (Finley, Thomas et al. 1996; Kolonin and Finley 2000). Two studies looked for a potential role for CycJ in regulating the *Drosophila* early embryo cell cycles, but came to different conclusions. In one study, injection of CycJ antibodies or peptide aptamers into early embryos caused chromatin bridges during the rapid nuclear divisions of the early syncytial embryo suggesting that CycJ is required for cell cycle progression and chromosome segregation (Kolonin and Finley 2000). Contrary to these

results, the Lehner lab showed that in early embryos, CycJ-EGFP fusion proteins were not expressed and the syncytial cell cycles in early embryos of *CycJ* null were not disrupted (Althoff, Viktorinova et al. 2009). Both groups agree that *CycJ* null exhibited reduced egg-hatching rates compared to controls (Althoff, Viktorinova et al. 2009; Atikukke 2009). Considering that the *CycJ* null embryos that fail to hatch are fragile, making them difficult to isolate and examine, it is possible that the Lehner group only examined the good embryos rather than those that were defective. Despite the differing results, these studies suggest that CycJ is conserved and specifically expressed in ovaries and/or early embryos of *Drosophila*, but its function remains elusive.

The expression of *Drosophila CycJ* is unique and somewhat conserved between organisms. Figure 1 shows mRNA expression from all 16 *Drosophila* cyclins across 55 stages and tissues from two high-throughput sources, modENCODE and Fly Atlas (Arbeitman, Furlong et al. 2002; Graveley, Brooks et al. 2011; Chintapalli, Wang et al. 2013), demonstrating that *CycJ* is specifically expressed in ovaries and early embryos, a pattern that is unique among the cyclins and suggests a possible function in one or both of these tissues. The unique mRNA expression pattern is also conserved in the mosquito (*Aedes aegypti*) ortholog of *CycJ* (Cyclin A3 in mosquito, AAEL008256), which is only expressed in early embryos and ovaries after a blood meal when oogenesis becomes active (Akbari, Antoshechkin et al. 2013). In *Drosophila*, *CycJ* is also in ovaries and early embryos, and also demonstrates that it is up-regulated in ovaries when germline stem cell (GSC) number is increased by mutations that inhibit differentiation of GSCs (Kai, Williams et al. 2005). Furthermore, *CycJ* expression is not

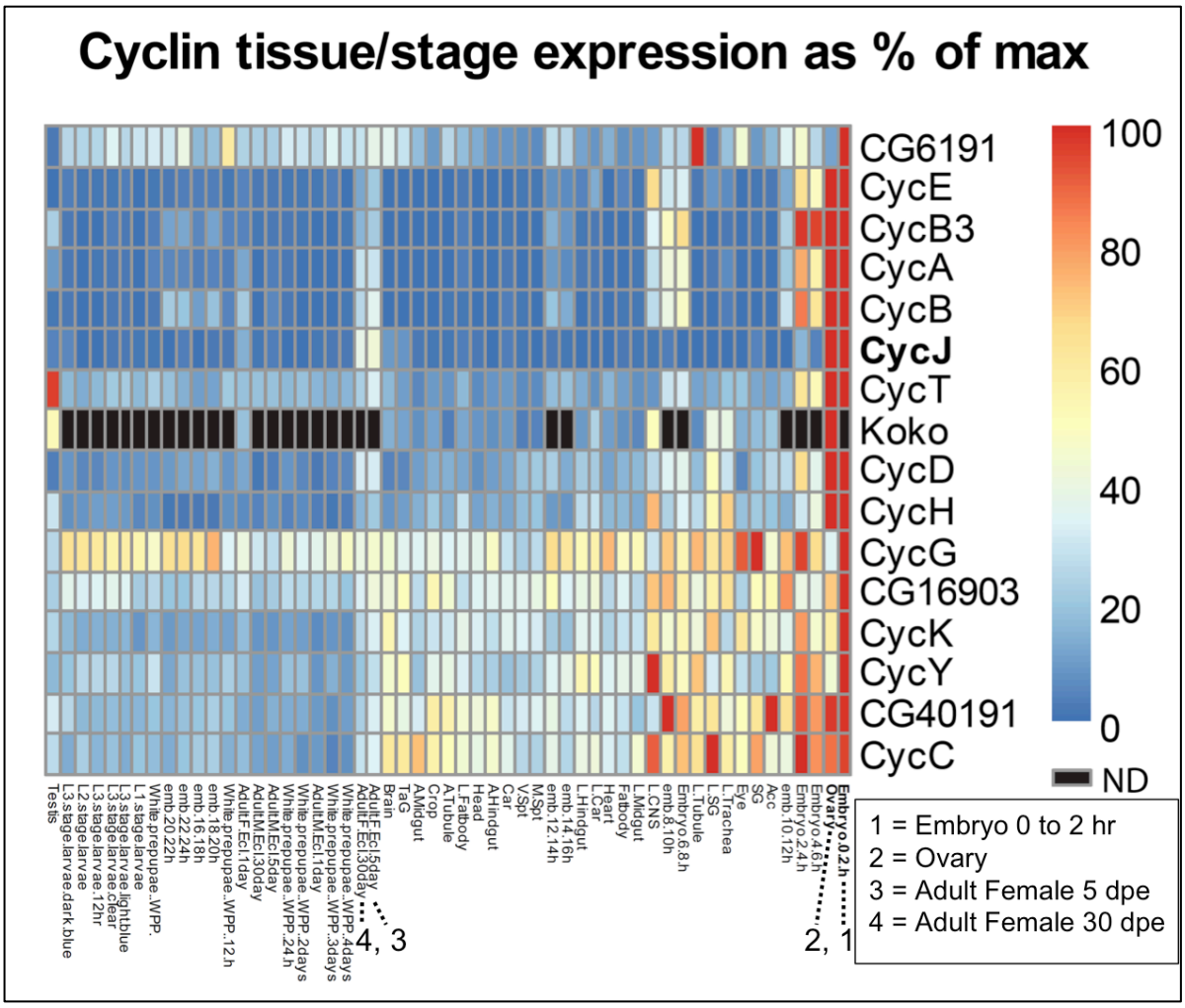

Figure 1: *CycJ* is expressed almost exclusively in *Drosophila* ovaries, a pattern that is unique among the superfamily of cyclins. This is a heatmap of cyclin expression in 55 stages and tissues of *Drosophila* as a percentage of each gene's maximal expression (% max). Expression data were acquired from two high throughput repositories, FlyAtlas for tissue expression (Chintapalli, Wang et al. 2013) and modENCODE for stage expression (Graveley, Brooks et al. 2011). Raw values were obtained from each source, the highest value for each gene was determined, and that gene's expression was scaled as a percent of this maximal value as described (Murali, Pacifico et al. 2014). Percent max was determined for FlyAtlas and modENCODE data independently from one another. *CycJ* is maximally expressed only in early 0-2 hour old embryos (column 1) and ovaries (column 2), and unlike all other cyclins, it is not expressed above ~20% of its maximum at any other time or in any other tissue. Columns labeled 3 and 4 represent adult females 5 and 30 days post eclosion (dpe), respectively, where *CycJ* is expressed above 50% max. Since all parts of the fly have been dissected, analyzed individually, and most demonstrate little to no *CycJ* expression, this increase in adult females is due to high ovary expression. ND = no data for Koko. This figure has been published in (Atikukke, Albosta et al. 2014) and is presented here with minor modifications.

normally detected in testis, but is expressed in testis of *benign gonial cell neoplasm (bgcn)* mutants and *bgcn* mutants over-expressing the Jak/STAT ligand *outstretched*, which inhibits germline differentiation and promotes accumulation of GSCs, respectively (Terry, Tulina et al. 2006). These data suggest that *CycJ* is expressed in stem cell populations and expression can be induced when stem cell populations are expanded. Interestingly, the expression pattern of human *CycJ* (*CCNJ*) is also associated with stem cells. Meta analysis of genome-wide expression studies found in the NCBI GEO database demonstrate that *CCNJ* is expressed at low levels in many tissues, including oocytes and early embryos, as well as embryonic stem cells. Strikingly, *CCNJ* is expressed in induced pluripotent stem cells from multiple sources, whereas expression is significantly lower in the cells of origin (Ohi, Qin et al. 2011). Together, these data demonstrate conserved expression of *CycJ* in oocyte, early embryo, and stem cells, both endogenous and induced. These unique conserved expression profiles suggest that CycJ may play a role in oogenesis, early embryogenesis, and/or stem cell regulation.

Although virtually nothing is known about CycJ function in any organism, multiple studies suggest that aberrant *CycJ* regulation may be associated with human cancers. Human *CCNJ* is up-regulated in three cancers, and one study suggests that it may contribute to the cell cycle under tumorous conditions. In one study, patients with high-risk B-precursor acute lymphoblastic leukemia that had high expression of a five-gene cluster, which included *CCNJ*, exhibited a superior outcome and higher rates of 4-year relapse-free survival, but they did no further validation or characterization of *CCNJ* in this cancer (Harvey, Mullighan et al. 2010). It has also been shown that *CCNJ* is down-

regulated by two separate miRNAs, which are inhibited in two other human cancers. In prostate cancer cells, Vitamin D promoted expression of miR-98, which down-regulated *CCNJ* and inhibited cell growth via G2/M arrest, but the causal relationship between *CCNJ* down-regulation and G2/M arrest was not investigated any further (Ting, Messing et al. 2013). Finally, miR-125b, which down-regulated *CCNJ*, was found to be decreased in a miRNA expression profile of 50 breast cancer patients (Feliciano, Castellvi et al. 2013). Further analyses confirmed that *CCNJ* was over-expressed in breast cancer patients and forced expression of miR-125b in MCF7 breast adenocarcinoma cultured cells resulted in a G2/M arrest. They also demonstrated that siRNA knockdown of *CCNJ* in MCF7 cells resulted in a G2/M arrest similar to that seen under forced expression of miR-125b. Two of these studies suggest that CCNJ may be a G2/M regulatory cyclin in the cultured tumor cells analyzed, suggesting that its function as a cell cycle regulator is revealed in cells with stem cell-like qualities. Nevertheless, more detailed analyses are required to understand the function of this conserved cyclin.

Surprisingly, in *Drosophila* a *CycJ* null displays relatively normal oogenesis (Althoff, Viktorinova et al. 2009; Atikukke 2009). Despite this fact, we have recently shown that *CycJ* regulates oogenesis in the absence of the piRNA pathways (discussed in detail in Chapters 2 and 3 (Atikukke 2009; Atikukke, Albosta et al. 2014)), which suggests that *CycJ* functions in this tissue under specific conditions. We propose a non-redundant function for *CycJ* in oogenesis based on our data showing that *CycJ* is required in piRNA pathway mutants to limit GSC abundance or accumulation and to

prevent severe oogenesis defects; i.e., *CycJ* is responding to some condition created by piRNA pathway inhibition (Atikukke 2009).

1.4 Oogenesis: The making of an oocyte

Oogenesis is a process that starts from a stem cell and results in production of a gamete known as an oocyte. In *Drosophila* this takes place in ovaries composed of a series of parallel tubular structures called ovarioles. Oogenesis begins with the asymmetric mitotic division of a germline stem cell (GSC) located at the anterior tip of a germarium, giving rise to a new stem cell and a daughter cell called a cystoblast (Schupbach, Wieschaus et al. 1978; Wieschaus and Szabad 1979; Spradling 1993) (Figure 2 A). The new stem cell remains in the stem cell niche at the anterior tip of the germarium where signaling (e.g., Bone Morphogenetic Protein (BMP) signaling) from neighboring somatic terminal filament and cap cells leads to repression of differentiation factors in the germline (e.g., Bag of Marbles (Bam)) (Xie and Spradling 1998; King and Lin 1999; King, Szakmary et al. 2001; Song, Smith et al. 2004) (Figure 3). The cystoblast is positioned posteriorly away from the GSC niche, where it is free from BMP signaling thereby allowing differentiation. The cystoblast differentiates by undergoing exactly four rounds of division with incomplete cytokinesis giving rise to 16 cells interconnected by structural cell-cell connections known as fusomes and ring canals. The fusome originates from a spherical spectrin-containing structure called a spectrosome found in GSCs and cystoblasts. The spectrosome is required for the formation of ring canals, which maintain the permanent connection between the cells of a cyst (Lin, Yue et al. 1994; Huynh 2000). The 16-cell cyst eventually reaches the middle of the germarium where it comes in contact with somatic stem cells (SSCs),

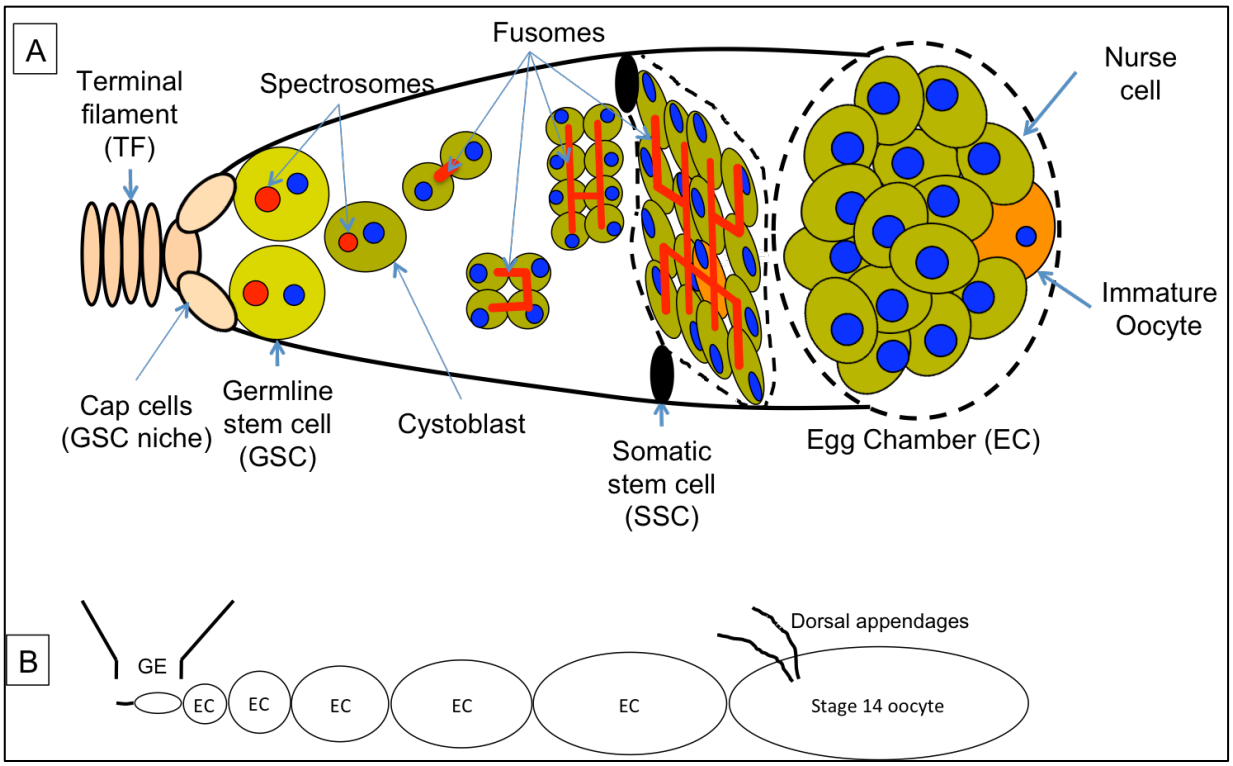

Figure 2: *Drosophila* oogenesis. (A) *Drosophila* germarium (GE). Oogenesis begins in the GE, which functions to produce egg chambers (ECs). The process beginnings with germline stem cells (GSCs) that reside in a well-defined niche composed of terminal filament (TF) and cap cells. GSCs produce daughter cells called cystoblasts. GSCs and cystoblasts each contain a characteristic spherical spectrosome. The cystoblast becomes an interconnected 16-cell cyst, which initially contains a fusome (to establish long term cell-cell connectivity) created by transmission and elongation of the spectrosome. One of the 16 cells will become the oocyte and the other 15 become nurse cells, which undergo extra rounds of DNA replication without cell division resulting in nuclei that get larger with time. Cysts are surrounded by follicle cells from somatic stem cells (SSCs), resulting in an egg chamber. (B) The GE continuously produces egg chambers, which grow and mature into stage 14 oocytes, which contains characteristic dorsal appendages. The GE, ECs, and stage 14 oocyte all constitute a single ovariole. This figure has been modified from (Atikukke, Albosta et al. 2014).

which produce follicle cells that encapsulate the cysts to form egg chambers (Goode, Wright et al. 1992; de Cuevas, Lilly et al. 1997; Nystul and Spradling 2010). One of the original 16 germline cells undergoes meiosis and becomes the oocyte, while the other 15 undergo multiple cycles of DNA replication without cell division (i.e., endocycles) to become polyploid nurse cells that eventually donate their cytoplasm to the oocyte through the ring canals. Fully formed egg chambers are continuously produced, bud off from the germarium, and populate ovarioles, creating long chains of egg chambers that mature and increase in size, culminating in the formation of a mature stage 14 oocyte (Figure 2 B).

Drosophila oogenesis is a well-characterized model for stem cell biology including the supporting cells that constitute a stem cell niche. Oogenesis begins with GSCs in a well-defined somatic niche, and there are many studies characterizing the pathways that regulate maintenance of these cells. GSC maintenance is partly achieved by localized inhibition of differentiation facilitated by BMP signaling (Figure 3) (Song, Wong et al. 2004; Zhang and Li 2005). Production, secretion, and diffusion of the BMP ligands glass bottom boat (Gbb) and Decapentaplegic (Dpp) from somatic niche cells is restricted so they only bind to GSCs and activate the BMP signaling pathway. For example, the number and maintenance of somatic niche cells is regulated by Notch signaling between the soma and germline (Song, Call et al. 2007). The niche cells express engrailed (en), which is required for the production and secretion of the morphogen Hedgehog (Hh) that signals to adjacent niche cells and promotes the production of Dpp (Rojas-Rios, Guerrero et al. 2012). Furthermore, expression of the glypican Dally in cap cells promotes localization of Dpp at GSCs,

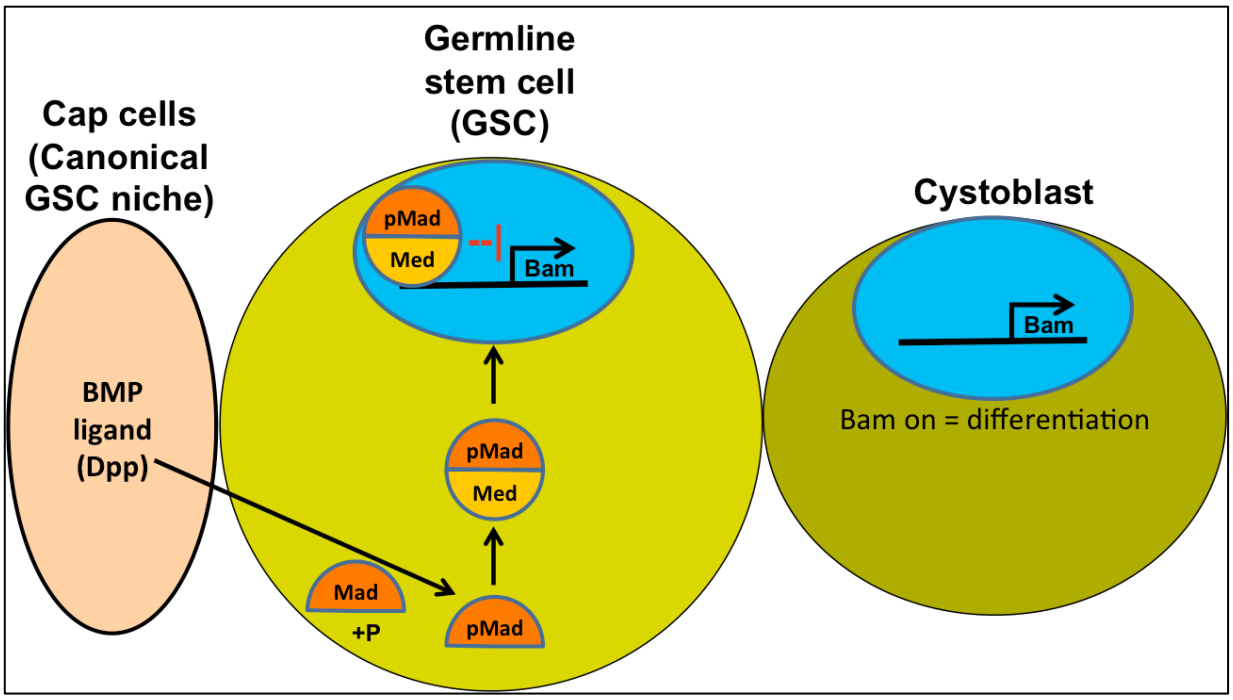

Figure 3: BMP signaling represses GSC differentiation. The primary function of the GSC niche is to produce signals that promote stem cell self-renewal mainly by inhibiting differentiation. This is partly achieved with bone morphogenetic protein (BMP) signaling. Ligand, e.g. decapentaplegic (Dpp), is produced and secreted from niche cells, followed by binding to GSCs and initiation of the BMP signal transduction pathway. This signaling begins with phosphorylation of receptors and substrates including phosphorylation of the transcription factor Mothers against Dpp (Mad). pMad binds to the co-mediator protein Medea (Med) and the protein pair translocates to the nucleus where they inhibit the transcription of the differentiation factor Bag of Marbles (Bam), thereby promoting self-renewal. Daughter cells, also known as cystoblasts, migrate away from the niche and its stem cell maintenance signaling, where they can then produce the differentiation factor Bam.

whereas ectopic expression of Dally leads to expansion of Dpp diffusion and excessive inhibition of differentiation (Guo and Wang 2009). With the help of these other pathways, Dpp is produced in niche cells, secreted, and targeted to GSCs (Figure 3). Upon ligand binding, GSCs activate the BMP signaling pathway, which initiates a series of intracellular signaling events, namely phosphorylation of receptors and pathway components (Miyazono, Maeda et al. 2005). One such phosphorylation occurs on the transcription factor Mothers Against Decapentaplegic (Mad). Phosphorylated Mad (pMad) then binds to the co-mediator protein Medea (Med) and the protein pair translocates to the nucleus. This protein pair can bind to regulatory DNA 5' of *Bam* and inhibit its transcription, which inhibits differentiation in GSCs (Song, Wong et al. 2004; Slaidina and Lehmann 2014). It is not surprising that mutations resulting in increased BMP signaling (e.g., over-expression of *dpp* or *dally*) also result in an increase of undifferentiated GSC-like cells at the anterior of the germarium; although they are no longer restricted to the niche, these cells are like GSCs in that they contain a spherical spectrosome and do not express differentiation factors like Bam. This can lead to egg chambers packaged with too many germline cells (Xie and Spradling 1998; Muzzopappa and Wappner 2005). Together, these data illustrate regulation of GSCs by somatic niche cells and show that disruption of pathways that control GSCs can lead to disruption of other oogenesis processes, like egg chamber packaging.

1.5 The piRNA pathways are conserved protectors of germline genome integrity and regulators of oogenesis

The piRNA pathways are also required during oogenesis for maintenance of germline genome integrity from both germline and ovarian somatic cells (Figure 4).

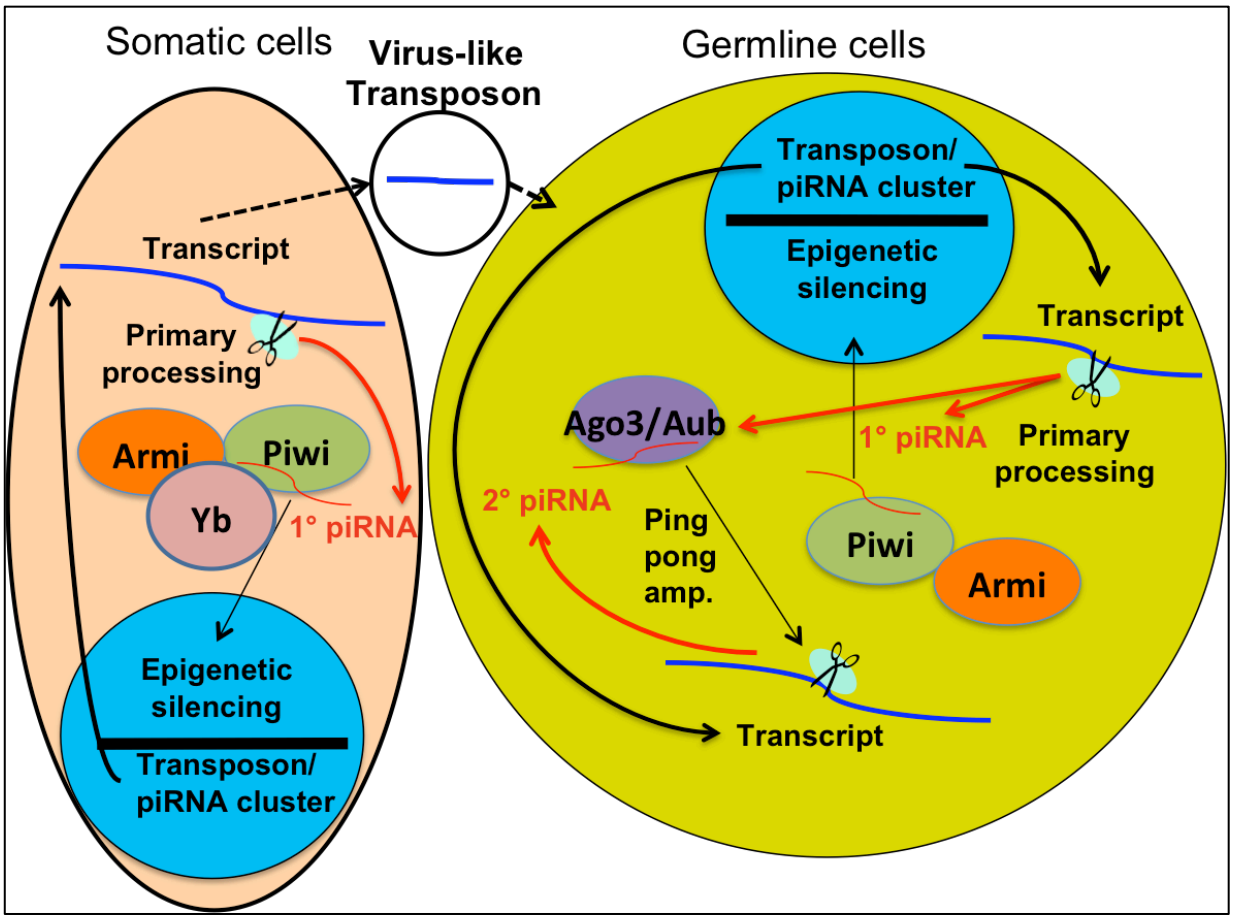

Figure 4: The piRNA pathways are conserved RNA silencing mechanisms that function to maintain and regulate germline development. The pathway proteins do this by repressing transposons with the help of small RNAs, called piRNAs, which are complementary to transposon transcripts. Two key classes of proteins found in these pathways are depicted. The argonaute class, including Piwi, Argonaute 3 (Ago3) and Aubergine (Aub), which bind the piRNAs and use them for guided transposon silencing, and the putative RNA helicase Armi, which is in a complex with Piwi functioning to process piRNAs and load them onto Piwi. There are two distinct silencing mechanisms that this pathway uses. The first targets transposon transcripts for degradation facilitated by transcript degradation. In the germline, Aub participates in a piRNA recycling process known as ping-pong amplification used to possibly amplify the amount of piRNAs available for transposon silencing. The pathway can also function in the nucleus targeting transposon producing loci and causing epigenetic modification, which silences transcription of these loci. Out of these three proteins, only piwi has been shown to regulate epigenetic modification. The pathway must function in both the somatic cells and the germline cells with the common goal of protecting germline genome integrity. It is believed that the somatic piRNA pathway does this by preventing the transmission of virus-like transposons from the somatic cells to the germline (Song, Kurkulos et al. 1997; Malone, Brennecke et al. 2009).

They are conserved transposon RNA silencing mechanisms that produce small 24-30nt RNAs called piRNAs, which are loaded onto PIWI clade Argonaute proteins (Ago3, Aub, and Piwi in *Drosophila*). The piRNAs are used for complementary base pair recognition of transposon-producing loci or transposon transcripts followed by transcriptional or posttranscriptional silencing of the targeted transposon (Vagin, Sigova et al. 2006; Klattenhoff and Theurkauf 2008) (Figure 4). The pathways require many families of proteins including the Argonaute proteins mentioned above, RNA helicases (e.g., Armitage (Armi)), Tudor proteins (e.g., fs(1)Yb (Yb)), nucleases (e.g., Zucchini (Zuc)), and many others (Olivieri, Sykora et al. 2010). Small RNA pathways, like the piRNA pathway, that inhibit transposon mobilization are conserved from plants and fungi to humans (Aravin, Hannon et al. 2007). In fact, humans and other vertebrates like mouse share with *Drosophila* many common pathway proteins (including PIWI clade Argonaute proteins) and mechanisms. The Argonaute proteins of the piRNA pathways silence transposons by targeted transcript cleavage via endonuclease activity (Ago3 and Aub), or by epigenetic silencing of transposon-producing loci in the genome via recruitment of epigenetic modification proteins (Piwi) (Gunawardane, Saito et al. 2007; Yin and Lin 2007; Malone, Brennecke et al. 2009; Rangan, Malone et al. 2011). The proper silencing of transposons is thought to limit DNA damage in the germline by repressing the movement of these selfish genetic elements (Klattenhoff, Bratu et al. 2007). Theurkauf and colleagues have shown that mutants of *armi* or *aub* accumulate germline DNA double stranded breaks and this leads to DNA damage checkpoint activation, which in turn disrupts establishment of the anterior-posterior and dorsal-ventral patterning of developing oocytes. piRNA pathways must function in both germline cells

and associated somatic cells with the common goal of maintaining germline genome integrity (Malone, Brennecke et al. 2009; Zamore 2010). Aub and Ago3 are germline specific and function in a cycle that produces piRNAs from genomic clusters transcribed from both strands (dual-strand clusters) in a process known as ping-pong amplification (Li, Vagin et al. 2009; Malone, Brennecke et al. 2009). Antisense piRNAs associated with Aub target transposon transcripts for degradation facilitated by Aub endonuclease activity.

Piwi, on the other hand, functions in both somatic and germline cells in pathways distinct from the germline specific ping-pong amplification. In somatic cells, a protein complex containing Piwi, Armi, Zuc, Vreteno (Vret), and Yb functions in perinuclear Yb bodies to produce antisense piRNAs from genomic clusters transcribed from a single strand (uni-strand clusters) (Olivieri, Sykora et al. 2010; Murota, Ishizu et al. 2014). piRNA/Piwi complexes enter the nucleus and associate with transposon loci, possibly by complementary base pair recognition of nascent transposon transcripts or recognition of DNA at transposon loci. Once in position, Piwi recruits epigenetic modifying proteins resulting in silencing of these loci. Unlike Ago3 and Aub, Piwi silences transposons without cleaving transposon transcripts. Yb is a Tudor-domain containing protein that acts as a scaffold to localize piRNA pathway proteins and piRNA cluster transcripts for piRNA processing and RNA induced silencing complex (RISC) assembly (Murota, Ishizu et al. 2014). Vret is also a Tudor-domain containing protein that specifically interacts with and stabilizes Piwi (Zamparini, Davis et al. 2011). Zuc has endonuclease activity and has been implicated in processing and maturation of 5' piRNA ends, which are loaded onto Piwi (Nishimasu, Ishizu et al. 2012). Finally, Armi is

an RNA helicase required for loading of piRNAs onto Piwi (i.e., RISC assembly), which is a prerequisite of nuclear localization of piRNA/Piwi complexes (Murota, Ishizu et al. 2014). Piwi and Armi also facilitate production of piRNAs in the perinuclear nuage of germline cells through similar mechanisms, though the germline cells lack Yb and Yb bodies. These data suggest that Armi and Piwi may have unique functions in somatic cells compared to germline cells, even though they are involved in piRNA production and transposon silencing in both cell types.

In *Drosophila,* the piRNA pathway members Yb, Vret, and Piwi limit GSC accumulation and promote egg chamber packaging and several lines of evidence indicate that this is a somatic-specific function of the piRNA pathway. First, Yb is only expressed in the soma and homozygous Yb^{72} ovaries exhibit GSC accumulation and production of egg chambers with too many germline cells (i.e., mispackaged egg chambers) (Swan, Hijal et al. 2001). Second, homozygous $vret^{148\text{-}60}$ ovaries also over-accumulate GSCs and produce egg chambers with abnormal nurse cell numbers, and these defects can be rescued by expression of wild-type *vret* specifically in somatic cells (Zamparini, Davis et al. 2011). Furthermore, germline $vret^{148\text{-}60}$ clones do not exhibit GSC accumulation or loss, indicating that limiting GSCs is a somatic-specific function of Vret (Zamparini, Davis et al. 2011). Third, multiple *piwi* mutants and RNAi knockdowns of *piwi* specifically in somatic cells result in GSC accumulation, which can be rescued with somatic expression of wild-type *piwi* (Jin, Flynt et al. 2013). In contrast, germline knockdown of *piwi* does not result in extra GSCs (Ma, Wang et al. 2014). The excess GSCs in these Piwi studies also exhibited BMP signaling activity and somatic escort cells had increased *dpp* expression, suggesting that Piwi may limit GSC accumulation

by limiting BMP signaling. The *piwi*^{NT} mutant, which lacks nuclear localization, is not able to repress transposons, yet exhibits normal GSC regulation, suggesting that Piwi's role in GSC regulation is independent of transposon silencing (Klenov, Sokolova et al. 2011). These data suggest that multiple piRNA pathway members limit GSC accumulation, promote egg chamber packaging, and/or limit BMP signaling from ovarian somatic cells. These proteins physically associate with one another, as well as with other piRNA pathway members, including Armi (Haase, Fenoglio et al. 2010; Qi, Watanabe et al. 2011). Germline knockdown and germline-specific mutants of *armi* were found to have normal GSC numbers, but the role of Armi regulating GSCs from somatic cells has not been examined (Ma, Wang et al. 2014). These studies suggest a potential common role for piRNA pathway proteins in ovarian somatic cells regulating oogenesis possibly independent of transposon regulation, but a more comprehensive analysis is required.

1.6 Overview

I used a previously generated deletion of the genomic region containing *armi* and *CycJ*, as well as null mutants for each gene created by adding back individual transgenes for each gene to the deletion. In Chapter 2, I show that CycJ regulates egg laying and hatching, but appears to be dispensable during oogenesis under normal conditions. In the absence of the piRNA pathway, however, CycJ plays a role in regulating egg chamber packaging and maturation. Most of the data in Chapter 2 have been published (Atikukke, Albosta et al. 2014). In Chapter 3, I demonstrate that the somatic piRNA pathway regulates multiple aspects of oogenesis by limiting BMP

signaling and that CycJ enhances these functions. Finally, Chapter 4 contains conclusions and future directions.

CHAPTER 2: A ROLE FOR *DROSOPHILA* CYCLIN J IN OOGENESIS REVEALED BY GENETIC INTERACTIONS WITH THE piRNA PATHWAYS

Part of the work described in this chapter has been published in *Mechanisms of Development* 133: 64-76, 2014.

2.1 Introduction

Cyclin J (CycJ) is a poorly characterized member of the cyclin superfamily of proteins specifically expressed in ovaries and early embryos. Cyclins are eukaryotic proteins that contain a cyclin box, a domain that interacts with cyclin-dependent kinases (Cdks) (Hadwiger, Wittenberg et al. 1989; Jeffrey, Russo et al. 1995). Many cyclins are known to have conserved roles in regulating the cell cycle. In metazoan species from *Drosophila* to human, for example, A and B cyclins regulate mitotic events, D cyclins regulate progression through G1, and E cyclins regulate entry into S phase (Minshull, Blow et al. 1989; Murray 2004). Other cyclins have conserved roles in regulating transcription or other cellular processes (Lim and Kaldis 2013). CycJ is conserved in all metazoans, yet it has only been studied in *Drosophila* were it was originally identified as a Cdk-interacting protein (Finley and Brent 1994; Finley, Thomas et al. 1996). The RNA expression pattern of *CycJ* is unique among *Drosophila* cyclins and suggests a possible role in oogenesis or embryogenesis. *CycJ* mRNA is present almost exclusively in ovaries and early embryos, whereas all other cyclins are expressed in multiple tissues and stages of development (Figure 1) (Finley, Thomas et al. 1996; Arbeitman, Furlong et al. 2002; Graveley, Brooks et al. 2011; Chintapalli, Wang et al. 2013). A potential role for CycJ in embryogenesis was suggested in a study showing that injection of syncytial embryos with CycJ-inhibitory antibodies or peptide aptamers resulted in delays of the early nuclear division cycles (Kolonin and Finley 2000). I set out to determine whether

CycJ also plays a role in ovaries where both the RNA and protein appear to be maximally expressed.

Here, I set out to determine whether or not *CycJ* plays a role in oogenesis. I used a previously generated deletion of the genomic region containing *armi* and *CycJ*, as well as null mutants for each gene created by adding back individual transgenes for each gene to the deletion (Atikukke 2009). We show that while oogenesis is normal in the *CycJ* null, the *armi* null produces few egg chambers and mature eggs, all of which have axis specification defects. Surprisingly, in the *armi-CycJ* double null there was a further decrease in the number of egg chambers per ovariole, a drastic increase in the number of differentiated germline cells in each egg chamber, and no mature eggs. The *armi* null defects could be suppressed by mutation in the Chk2 checkpoint kinase gene as shown previously, but the *armi-CycJ* double null defects could not (Atikukke 2009). I observed a similar genetic interaction between *CycJ* and two other piRNA pathway genes, *piwi* and *aub*, suggesting that *CycJ* plays a nonredundant role in oogenesis when the piRNA pathways are compromised.

2.2 Materials and Methods

2.2.1 *Drosophila* strains

Flies were maintained and crosses conducted at 25°C unless heat shock (37°C) is indicated. Many stocks were used in a previous project from our lab (Atikukke 2009). w1118 is wild type for this study. $armi^{72.1}$ (Cook, Koppetsch et al. 2004) was obtained from William E. Theurkauf. $mnkP^{6}$ (Takada, Kelkar et al. 2003; Brodsky, Weinert et al. 2004) was obtained from Andrew Swan. Stocks for w^{1118}, P{hsFLP}1, y^{1} w^{1118}; $Dr^{Mio}/TM3$, ry^{*} Sb^{1}, *aub* mutants, aub^{HN} cn^{1} bw^{1} and w^{1118}; aub^{QC42} cn^{1} bw^{1} (Schupbach

and Wieschaus 1991), *eIF5B*^{09143}, *VP16::nos-Gal4,* Df(3L)Exel6064, Df(3L)Exel6065, balancer strains, y[1] M{vas-int.Dm}ZH-2A w[*]; M{3xP3-RFP.attP'}ZH-51C, P{ry[+t7.2]=PZ}piwi[06843] cn[1]/CyO; ry[506], and w[1118] ; Df(2L)BSC145/CyO were obtained from the Bloomington *Drosophila* Stock Center. We obtained P1 clone DS01105 and BAC clone B22N9 from the Berkeley *Drosophila* Genome Project (BDGP) resource center. All flies are listed in Appendix A.

2.2.2 Creation of *Df(3L)armi-J* and transgenic constructs for rescue experiments

A genomic deletion, named the *Df(3L)armi-J*, was created removing *CycJ* and two adjacent genes, *armi* and *CG14971* as previously described (Atikukke 2009) (Figure 5). Briefly, the region was deleted by inducing recombination between two FRT-bearing transposon insertions flanking the genomic region. Creation of genomic transgenes for each of the genes in the three-gene deletion was also previously described (Atikukke 2009). New transgene construction for this study includes pCaSpeR-*HZ14-CycJ* constructed by cutting pCaSpeR-*CycJ* with SpeI, which uniquely digests in *armi* exon 8, filling in with Klenow (New England Biolabs), and religating. This introduced a frame shift 12 codons into the *armi* coding region in exon 8. High fidelity polymerase, (Herculase, Stratagene Inc.) was used for all PCR and the resultant constructs were verified by DNA sequencing. Constructs were microinjected into *w*^{1118} *Drosophila* embryos to induce P-element mediated germline transformation as described (Rubin and Spradling 1982). Injections were performed by the Model System Genomics facility at Duke University. Individual progeny bearing the transgenes as identified by eye color and verified by PCR were selected and mated with flies carrying

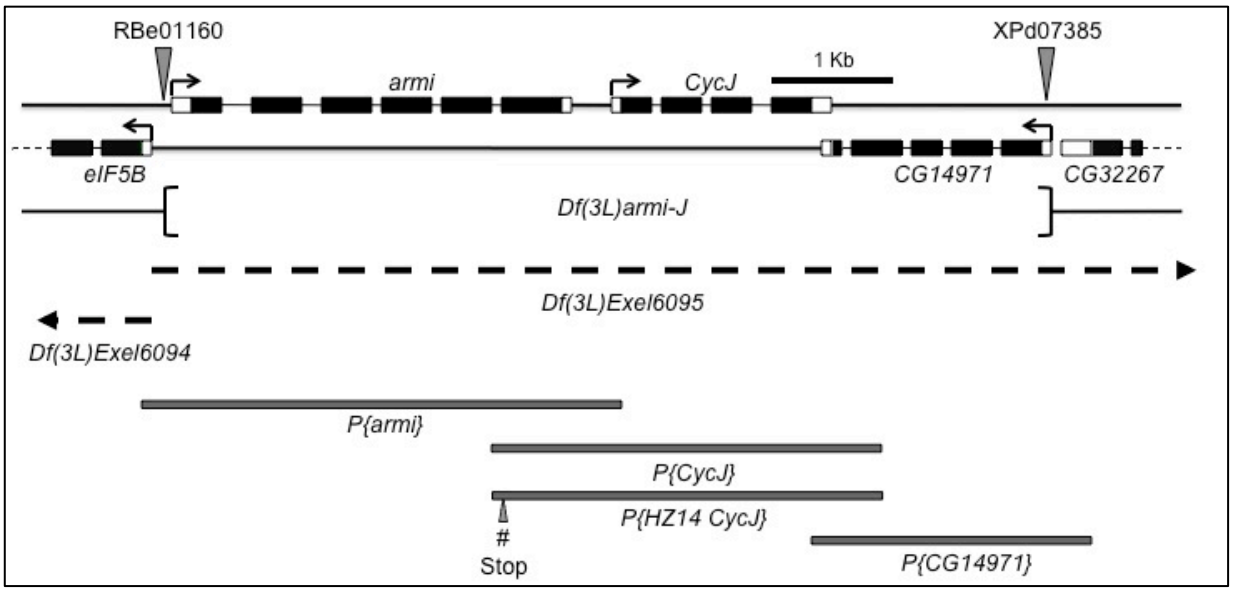

Figure 5: Genomic tools used for analysis of *CycJ*. Schematic representation of the genomic region corresponding to *CycJ, armi*, and the neighboring genes on chromosome 3L. The region shown corresponds to estimated cytological band 63E1. Black boxes represent coding regions and open boxes represent 5' and 3' untranslated regions. *armi* and *CycJ* are transcribed left to right while all other genes shown are transcribed right to left (arrows). FRT-bearing transposon insertions *RBe00161* and *XPd07385* (shown by triangles) were used to delete the intervening genomic region. The deleted genomic region is represented as *Df(3L)armi-J*. Rescue experiments were conducted by using independent transgenes, *P{armi}, P{CycJ},* and *P{CG14971}* that were generated using the indicated genomic regions (shaded boxes). Rescue experiments also used a second *CycJ* genomic transgene, *P{HZ14CycJ}*, which introduced stop codons (# stop) in the *armi* coding region eliminating *armi* coding potential. Regions missing in the deficiency chromosomes *Df(3L)Exel6094* and *Df(3L)Exel6095* are indicated by dashed lines and extend beyond the region shown (arrowheads). This figure has been previously published in (Atikukke 2009; Atikukke, Albosta et al. 2014) and is represented here with modifications.

marked balancer chromosomes to obtain balanced stocks. Chromosomes containing the transgenes are referred to as *p{CycJ}*, p{HZ14*CycJ*}, *p{armi}*, and *p{CG14971}*. To express the CycJ open reading frame (ORF) from a UAS we used pHZ12 (Mairiang, Zhang et al. 2013), a vector derived from *pUASattB* (Bischof, Maeda et al. 2007) that contains an attB site, the mini-white gene, and a UAS driving expression of ORFs with an N-terminal 6His-3Myc tag. The *CycJ* ORF was amplified from a yeast two-hybrid clone (Stanyon, Liu et al. 2004) using recombination tag primers 5RT and 3RT and recombined into the 5RT and 3RT sites of vector pHZ12 as described (Parrish, Limjindaporn et al. 2004) to create *pUAS-Myc-CycJ*. The *CycJ* ORF in *pUAS-Myc-CycJ* was verified by sequencing and includes from the ATG to the stop codon of *Cyclin J* isoform A. *pUAS-Myc-CycJ* was inserted into the attP site at 51C in Drosophila line *y[1] M{vas-int.Dm}ZH-2A w[*]; M{3xP3-RFP.attP'}ZH-51C* (Bischof, Maeda et al. 2007). All fly lines are listed in Appendix A.

2.2.3 Ovary dissection and staining

Ovary dissection and staining was conducted as previously described (Atikukke 2009). Briefly, ovaries were removed in a ringer solution on ice, fixed with a formaldehyde solution, washed with PBS followed by PBT. Ovaries were incubated in primary antibody for either 2 hours at room temp or overnight at 4°C. They were washed in PBT and incubated in secondary antibody at room temperature for 1 to 2 hours. They were washed with PBT, counterstained with DAPI, washed with PBT followed by PBS, equilibrated with PBS:Glycerol (1:1), and finally in antifade mounting solution (PBS:Glycerol 1:4 containing DABCO). Primary antibodies from Developmental Studies Hybridoma Bank and dilutions include hts-RC (1:50), α-spectrin (1:50) and Orb

6H4 and 4H8 (1:50). Primary anti-GFP (1:50) was obtained Invitrogen. Secondary antibodies from Sigma and dilutions include Goat anti-mouse IgG FITC (1:200) and Goat anti-rabbit IgG Texas Red (1:200). Nuclei of all ovaries were counterstained with DAPI (1μg/ml) from Sigma. Microscopy was conducted with a Zeiss Axio imager upright microscope that had an apotome for background reduction and optical sectioning.

2.2.4 Hatch rates

Experiments analyzing hatch rates were conducted as previously described (Atikukke 2009) and with the following modifications. To assess embryo hatching rates and morphology, equal numbers of newly emerged virgin females of each genotype were mated with w^{1118} males and the eggs were collected on apple juice plates or grape juice plates every day for 4 days. Plates were 2.2% w/v Agar (USB 10906), 2.5% w/v Sucrose (Domino Table Sugar), 25% v/v apple or grape juice, and 0.075% w/v Tegosept (p-hydroxy-benzoic acid methyl ester, Sigma H-3647). Agar and sugar were mixed with 75% of the total volume of water and autoclaved. Tegosept must first be dissolved in ethanol (21% w/v) prior to addition to liquid agar. Juice was added immediately after autoclaving, solution was cooled to 60°C and Tegosept/alcohol mixture was added. Liquid agar was cooled to roughly 40°C and poured into 60 mm Petri dishes. Prior to use, yeast paste (1 g of yeast in 1.3 mL water) was added in a thin layer on five spots covering 10% of the plate surface. Flies were allowed to lay eggs on plates for 20-24 hours at 25°C and 50% humidity for four days total. Plates were changed each day and the number of eggs laid was counted. Eggs were given at least 24 hours to hatch followed by counting of the eggs that did not hatch. The number of eggs laid vs. eggs that did not hatch was used to calculate hatch rate. The number of

eggs hatched was determined by counting the number of eggs that failed to hatch after aging for 24 hours at 25°C. Eggs were counted and categorized based on dorsal appendage morphology. At least 200 eggs were examined for each genotype except the *armi* null for which repeated collections provided 50 eggs to examine.

2.2.5 Whole fly DNA extraction, PCR, and agarose gel electrophoresis

DNA was extracted from individual flies for genotyping according to Michael Ashburner's protocol as previously described with modification (Ashburner 1989; Atikukke 2009). A single fly was collected and added to a 1.7 mL microcentrifuge tube (Denville C2170) containing 50 µL homogenization buffer [Tris-HCl (pH7.5) 10mM, NaCl 60mM, EDTA 10mM, Spermine 0.15mM, Spermidine 0.15mM, Sucrose 5%]. Flies were mechanically homogenized with a small plastic pestle (Fisher nc9907525). After homogenization, 50 µL of lysis buffer [Tris-HCl (pH 9.0) 300mM, EDTA 100mM, SDA 0.63%, Sucrose 5%] was added followed by a 15 minute incubation at 70°C. Tubes were removed from heat and cooled to room temperature, then 15 µL of 8M potassium acetate (KAc) was added followed by a 30 minute incubation on ice. Tubes were centrifuged for 5 minutes at 13,000 RPM. The supernatant was transferred to a new tube and 230 µL of 100% ethanol was added followed by a 5 minute incubation at room temperature. Tubes were centrifuged for 5 minutes at 13,000 RPM. The supernatant was discarded and the pellet was washed with 230 µL of 70% ethanol followed by centrifugation for 5 minutes at 13,000 RPM. The supernatant was discarded and pellets were air dried. The pellet was resuspended in 50 µL of Tris-EDTA [TE, 10 mM Tris pH 6.8: 1 mM EDTA pH 8.0]. DNA was amplified with the polymerase chain reaction (PCR) using either Invitrogen reagents (kit 10342-020) or Promega GoTaq Green (M7122).

Invitrogen reagents were used as follows; 1x PCR buffer, 0.25 µM dNTPs, 2.5 mM $MgCl_2$, 0.083 µM each primer, 1 U Taq, 1 ng template DNA, and water to 30 µL. GoTaq was used as follows; 1x GoTaq master mix, 0.2 µM primers, 2 ng template DNA, and water to 10 µL. PCR was performed with a BioRad DNA Engine Tetrad2. Parameters are as follows; 1) Denaturation at 96°C for 5 minutes, 2) Denaturation at 94°C for 30 seconds, 3) Annealing at 60°C for 30 seconds, 4) Extension at 72°C for 1 minute per Kb of product (no less than 1 minute), 5) Repeat cycles two thru four 29 more times, 6) final extension at 72°C for 5 minutes, and 7) cool down to 25°C for 5 minutes. PCR was analyzed on 1% w/v agarose TBE gel at 100 V for roughly 30 minutes.

2.2.6 PCR verification of *Df(3L)armi-J*

Strains with *Df(3L)armi-J* (Figure 5) were subjected to genomic PCR and cDNA amplification for verification of the absence of *armi, CycJ,* and *CG14971*. First, genomic DNA was prepared from *Df(3L)armi-J/Df(3L)armi-J* and *w1118*. This DNA was used as template for a PCR reaction with diagnostic primers specific for *armi, CycJ,* or *CG14971* designed in adjacent exons resulting in a larger PCR product when compared to cDNA as template. The primer pairs were: *armi*=PA02F/PA02R, *CycJ*=PA01F/PA01R, and *CG14971*=PA03F/PA03R. To verify that transcription was also abolished in the *Df(3L)armi-J*, cDNA was synthesized from *Df(3L)armi-J/Df(3L)armi-J*. RNA was extracted using the RiboPure Kit (Ambion AM1924). A single homozygous fly was homogenized mechanically with a plastic pestle in 0.2 mL TRI reagent and incubated at room temperature for 5 minutes. 0.1 mL of chloroform was added followed by 15 seconds of vortexing and a 5 minute incubation at room temperature. Mixture was centrifuged at 13000 rpm and 4°C for 10 minutes. The top

layer (clear, ~0.15 mL) was transferred to a new tube with 0.075 mL EtOH and vortexed for 5 seconds. The RNA was then purified using the GeneJET RNA Purification Kit (Thermo Scientific K0731) beginning with addition of RNA/EtOH to a filtration column. The column was centrifuged at 13000 rpm for 1 minute and the flow through discarded. The column was washed twice with wash buffer followed by centrifugation. The column was transferred to a 1.5 mL microcentrifuge tube and 25 µL of elution buffer was added followed by incubation at room temperature for 2 minutes. The column was centrifuged at 13000 rpm and 4°C for 1 minute. RNA concentration was quantified using the NanoDrop and an aliquot was diluted with water to 5 µg in a total volume of 21.5 µL. The RNA was then subjected to DNase treatment with 2.5 µL 10x DNase buffer and 1 µL DNase 1 for a total of 25 µL. The mixture was gently finger mixed and incubated at 37°C for 30 minutes. DNase was removed with the addition of 6 µL DNase inactivation reagent and incubation at room temperature for 2 minutes with periodic vortexing. Tubes were centrifuged at 14000 rpm for 1 minute and the supernatant was transferred to a new tube. Single stranded cDNA was synthesized using the Roche Transcriptor First Strand cDNA Synthesis Kit (Roche 04379012001). Reverse Transcription of polyadenylated RNA was performed with the following parameters: 1X RT buffer, 1 mM dNTPs, 2.5 µM oligo dT primers, 20 U Protector RNase Inhibitor, 10 U Reverse Transcriptase, 2.4 µg purified RNA template, and water to 20 µL. Reverse transcription reaction was performed at 50°C for 1 hour followed by 85°C for 5 minutes. cDNA was used as template in a PCR reaction with the same diagnostic primers for the three genes of the deletion used previously with genomic DNA template. These primers are

designed to produce a noticeably smaller PCR product when amplifying cDNA. All primers and their sequences are listed in Appendix B.

2.2.7 Sequence verification of *Df(3L)armi-J*

The sequence of *Df(3L)armi-J* was verified by sequencing inward from both breakpoints with 4 primers. The first set of primers did not generate enough sequence information to cover the transposon remnants left behind from recombination that created the deletion. Once the sequence was known for the first half of the deletion, another set of primers was created and used to complete sequencing. The transposon remnant is ~2,100 bp in length and does not disrupt the flanking genes *eIF5B* and *CG32267*. The first sequencing primers were used to target the left end with RF305 and the right end with RF304. The second primers designed from the first round of sequence data were used to target the left end with PARB1 and the right end with PAXP1. Sequence data was aligned and combined with the Geneious program (Figure 6). All primers and their sequences are listed in Appendix B.

2.2.8 Tissue specific expression with *Gal4>UAS*

Tissue specific expression of transgenes was accomplished with the *Gal4-UAS* binary system of expression (Brand and Perrimon 1993). Gal4 is a yeast transcription factor that binds to and activates genes containing a regulatory Upstream Activation Sequence (*UAS*). The system works by attaching a specific enhancer/promoter to *Gal4* and a desired target gene to *UAS*. A fly containing a *promoter-Gal4* construct is mated to a fly containing a *UAS-gene* construct. The progeny that contain *Gal4* and *UAS* will express the target gene in the desired pattern governed by the promoter linked to Gal4. This chapter utilized fly lines containing the germline-specific *VP16::nos.UTR-Gal4*

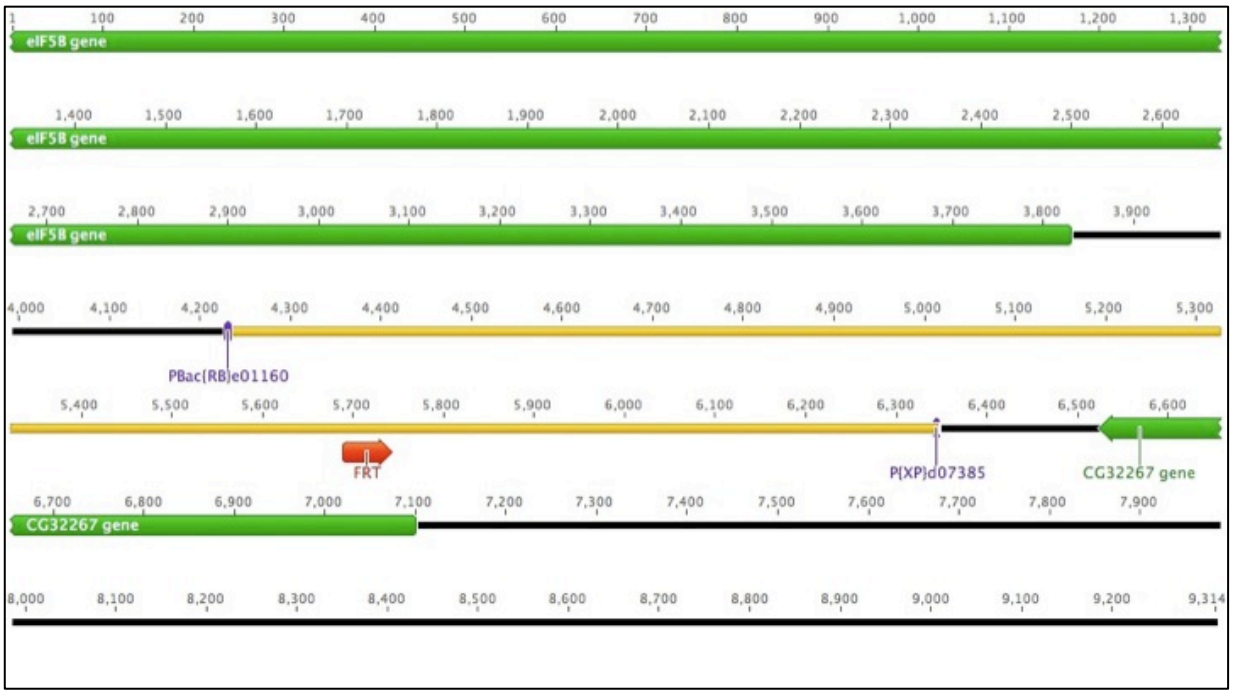

Figure 6: The *Df(3L)armi-J* chromosome contains a 2,100 bp transposon remnant left behind from transposon-mediated deletion. *Df(3L)armi-J* was created with flippase mediated recombination between FRT sites in two different transposon insertions annotated in purple, PBac{RB}e01160 flanking the left of armi and P{XP}d07385 flanking the right of CG14971. Recombination between the transposons left a large DNA remnant, which was sequenced and is represented by the yellow line including an FRT site indicated in red. This image was produced with the Geneious program using sequencing data from *Df(3L)armi-J* homozygotes. This indicates that the deletion successfully removed *armi, CycJ,* and *CG14971* (depicted in their genomic environment in Figure 5) while leaving the flanking genes *eIF5B* and *CG32267* intact with their ORFs annotated in green. The black lines represent non-coding DNA.

(*nos-Gal4*) or the soma-specific *e22c-Gal4* drivers to express *UAS-CycJ.cDNA.myc*. All flies are listed in Appendix A.

2.2.9 Oogenesis phenotype quantification

To quantify oogenesis defects, females were aged for 2-4 days post eclosion and ovaries from at least 10 flies per genotype (with two exceptions as noted) were extracted and stained with DAPI as described above. *piwi* mutant females were only aged for 0-2 days post eclosion due to rapid egg chamber loss. All ovarian material was transferred to a slide and ovarioles were mechanically separated from one another with forceps or insulin syringes for analysis. Number of mature oocytes per fly, number of egg chambers per ovariole, and percent of mispackaged egg chambers per fly were quantified and averaged. Error bars represent standard error of the mean (SEM) calculated by dividing the average by the square root of n (the number of flies). Statistical differences between single and double mutants for each phenotype were calculated using a type 3 student's T-test, which accounts for unequal sample sizes.

2.3 Results

2.3.1 Loss of both *armi* and *CycJ* results in oogenesis defects characterized by severely disorganized ovarioles containing mispackaged egg chambers

CycJ analysis began with a previously described genomic deletion encompassing *armi, CycJ,* and *CG14971*, referred to here as the three-gene deletion or *Df(3L)armi-J*, which revealed a possible role for CycJ in oogenesis or embryogenesis (Atikukke 2009). I verified the absence of *armi, CycJ,* and *CG14971* in *Df(3L)armi-J* with genomic and cDNA PCR (Figure 7) along with sequencing and mapping of the transposon remnants on the *Df(3L)armi-J* chromosome. The homozygous *Df(3L)armi-J*

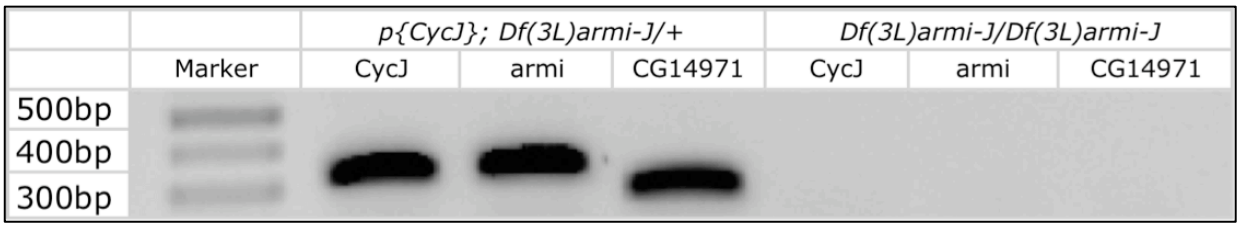

Figure 7: Diagnostic *Df(3L)armi-J* PCR using cDNA as template verifies that transcripts of the three genes are absent in the deletion. *CycJ, armi,* and *CG14971* are not transcribed in *Df(3L)armi-J/Df(3L)armi-J.* RNA was purified from *Df(3L)armi-J* homozygotes and *Df(3L)armi-J/+* flies containing a *p{CycJ}* transgene followed by cDNA synthesis. The cDNA was used as template for PCR. The absence of bands in homozygotes indicates that mRNA was not produced. Primers used are as follows; CycJ=PA01F/PA01R, armi=PA02F/PA02R, and CG14971=PA03F/PA03R. Primers are their sequences are listed in Appendix B.

mutant flies were viable indicating that *armi*, *CycJ,* and *CG14971* are not essential for viability or development to adulthood, a conclusion that was also reached in previous studies (Althoff, Viktorinova et al. 2009; Atikukke 2009; Olivieri, Sykora et al. 2010). The deletion, however, resulted in complete male and female sterility, and the females did not lay any eggs (Table 1). As described in detail below, the three-gene deletion resulted in major defects in oogenesis. To analyze the contributions of individual genes to these phenotypes, transgenic lines containing genomic clones of each gene individually and in different combinations were previously constructed and tested for their ability to modify the *Df(3L)armi-J* phenotypes (Atikukke 2009; Atikukke, Albosta et al. 2014) (Figure 5). Several lines of evidence suggest that all of the oogenesis defects observed with *Df(3L)armi-J* are due to loss of *armi*, *CycJ*, or both genes and not to loss of *CG14971* or disruption of the immediate upstream gene, *eIF5B*. First, *Df(3L)armi-J* complemented a lethal deficiency (*Df(3L)Exel6094*) that removes *eIF5B*, which is an essential gene (Carrera, Johnstone et al. 2000), suggesting that *eIF5B* is not affected in the mutant that we generated. Transheterozygous *Df(3L)armi-J*/*Df(3L)Exel6094* males and females are viable and fertile, as are animals with *Df(3L)Exel6094* over a deficiency (*Df(3L)Exel6095*) that removes *CycJ*, *armi*, and several downstream genes. Furthermore, ovaries from Df(3L)Exel6094 over Df(3L)armi-J or Df(3L)Exel6094 over Df(3L)Exel6095 females showed no signs of oogenesis defects (Figure 8). Second, it was previously found that addition of the *CG14971* transgene into *Df(3L)armi-J* females either in the presence or absence of the *CycJ* and *armi* transgenes had no effect on any of the phenotypes that I observed (Table 1) (Atikukke 2009). Finally, the combination of both *armi* and *CycJ* transgenes was sufficient to fully

Table 1: Embryogenesis defects

Maternal Genotype	Genotype abbreviation	Eggs laid[a]	Egg morphology[b] (dorsal appendages) Two	One	None	Hatching rate[e]
Df(3L)armi-J /+		100%	100%	0%	0%	96%
Df(3L)armi-J or Df(3L)armi-J/Df(3L)Exel6095	$armi^{1null}$ $CycJ^{null}$ ($CG14971^{null}$)	NONE	NA	NA	NA	NA
P{CG14971}; Df(3L)armi-J	$armi^{1null}$ $CycJ^{null}$	NONE	NA	NA	NA	NA
P{CycJ}; Df(3L)armi-J	$armi^{1null}$ ($CG14971^{null}$)	<1%	0%	0%	100%	0%
P{CG14971}; P{CycJ} ; Df(3L)armi-J	$armi^{null}$	<1%	0%	0%	100%	0%
P{armi}; Df(3L)armi-J	$CycJ^{null}$ ($CG14971^{null}$)	65.3%	92%	7%	1%	30%
P{armi} / P{CG14971}; Df(3L)armi-J	$CycJ^{null}$	65.1%	91%	8%	1%	30%
P{armi}; P{CycJ}; Df(3L)armi-J	$CG14971^{null}$	66.7%	94%	6%	0%	73%
P{armi}; P{HZ14-CycJ}3-2; Df(3L)armi-J/Df(3L)Exel6095	$CG14971^{null}$	79.2%	90.3%	6.3%	3.4%	76%
P{armi} / P{CG14971}; P{CycJ};Df(3L)armi-J	Fully complemented deficiency	67.4%	93%	7%	0%	75%
Df(3L)armi-J / $armi^{72.1}$	$armi^{72.1}$ (hypomorph)	35.3%	0%	28%	72%	0%
aub^{HN} / aub^{QC}	*aub*	75.0%	8%	68%	24%	0%
P{armi}; aub^{HN} / aub^{QC}; Df(3L)armi-J	$CycJ^{null}$, *aub*	NONE	NA	NA	NA	NA
mnk^{P6}; *Df(3L)armi-J / $armi^{72.1}$*	$armi^{72.1}$, *mnk*	89.4%	85%	8%	7%	0%
mnk^{P6}; *Df(3L)armi-J*	$armi^{1null}$ $CycJ^{null}$, *mnk*	NONE	NA	NA	NA	NA
P{CycJ}; mnk^{P6};Df(3L)armi-J	$armi^{1null}$, *mnk*	16.8%	77%	12%	9%	0%

[a] Percent of the number eggs laid by *Df(3L)armi-J/+* (n=1118) over the same period of time. For the two *armi* null genotypes, repeated collections yielded only 4 or 5 eggs per collection. *armi-CycJ* null and *CycJ* null *aub* double mutants laid no eggs.
[b] Number of dorsal appendages per egg (wild-type is two). Axis establishment defects lead to ventralized eggs, which have fewer than two dorsal appendages. NA, not applicable (no eggs laid).
[e] Embryo hatching rates relative to wild-type (Materials and Methods).
*This table has been previously published in (Atikukke 2009; Atikukke, Albosta et al. 2014) and is represented here with minor modifications.

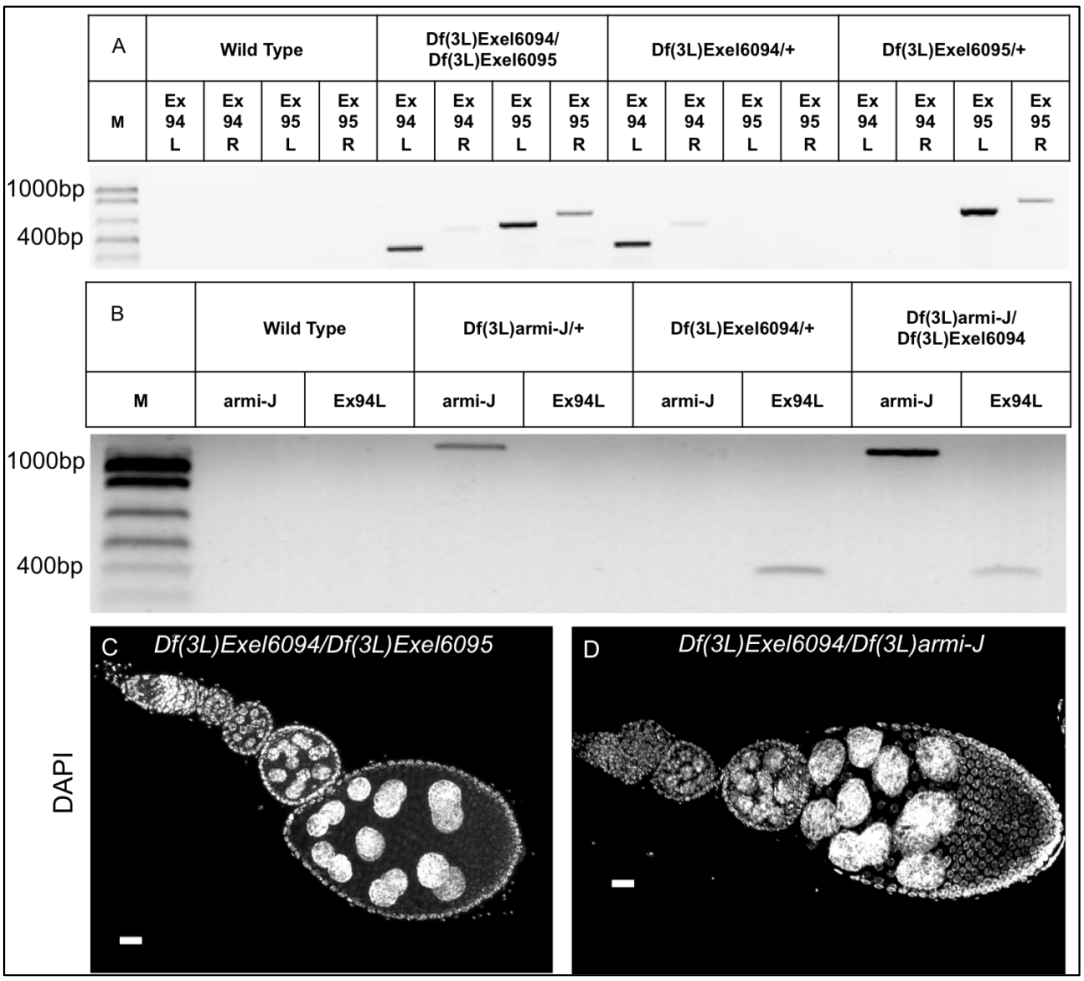

Figure 8: A deficiency removing eIF5B (Df(3L)Exel6094) is fully complemented by both *Df(3L)armi-J* and a deficiency also removing these three genes (Df(3L)Exel6095). Transheterozygous females *Df(3L)Exel6094* over *Df(3L)armi-J* or *Df(3L)Exel6095* are viable and have normal oogenesis. (A) and (B) Diagnostic PCR showing that *Df(3L)Exel6094/Df(3L)Exel6095* (A) and *Df(3L)Exel6094/Df(3L)armi-J* (B) contain both deficiencies and confirming the endpoints of these deficiencies. (C) and (D) DAPI stained ovarioles from *Df(3L)Exel6094/Df(3L)Exel6095* (C) and *Df(3L)Exel6094/Df(3L)armi-J* (D) females. Oogenesis occurs without obvious defects in these transheterozygotes suggesting that eIF5B does not contribute to the three-gene deletion. Size bar = 20 μm. PCR was conducted on template DNA prepared from whole adult flies of the indicated genotypes. Gen=Genotype, Pri=primer pair, M=DNA marker ladder (see methods). Ex94* are primer pairs specific for the *L left end (6094Gpfor/TnLeft) and *R right end (6094Gprev/TnRight) of Exel6094; Ex95* are primer pairs specific for the *L left end (6095Gpfor/TnLeft) and *R right end (6095Gprev/TnRight) of Exel6095. “armi-J” is primer pairs (RB/PA_Df(3L)armiJ_R) specific for *Df(3L)armi-J*. All primer pairs consisted of one transposon specific and one genome primer, sequences listed in Appendix B. Figure has been published in (Atikukke, Albosta et al. 2014) and is represented here with minor revisions.

suppress all of the oogenesis defects described below, suggesting that *CG14971* does not play a role in these phenotypes. Thus, I refer to either homozygous *Df(3L)armi-J* or transheterozygous *Df(3L)armi-J* over *Df(3L)Exel6095* animals as *armi-CycJ* double null.

To characterize oogenesis defects that may explain the lack of eggs from *armi-CycJ* double null females, I analyzed ovaries at various time points during the first week after eclosion as previously described (Atikukke 2009). This analysis revealed that *armi-CycJ* double null females have oogenesis defects that were different from either single null fly (described below and in (Atikukke 2009)). Germaria from *armi-CycJ* double null animals were disorganized and the ovarioles generally contained only one egg chamber with many more than the normal number of germline cells (Figure 9 A&B). The single egg chamber usually had a terminal filament (Figure 9 C&D), suggesting that the germarium failed to package individual cysts and became the only egg chamber. The germline nuclei were of different sizes suggesting that they have undergone different numbers of endoreplicative cycles. Many egg chambers also showed an intense punctate DAPI staining pattern that increased as the females aged beyond 3 days, suggestive of increasing cell death (arrows in Figure 9 E&F). I observed identical phenotypes in ovaries from animals homozygous for *Df(3L)armi-J or* transheterozygous for *Df(3L)armi-J* over the deficiency *Df(3L)Exel6095* that uncovers *armi*, *CycJ,* and a number of additional genes (Figure 9 B&C). Ovaries from *Df(3L)armi-J* mutants that were over 1 week old contained ovarioles with disorganized germaria, no developing egg chambers, and few visible nuclei (Figure 9 G). These observations suggest that as females age, further development ceases and the few egg chambers that initially developed are eliminated, leaving only disorganized germaria.

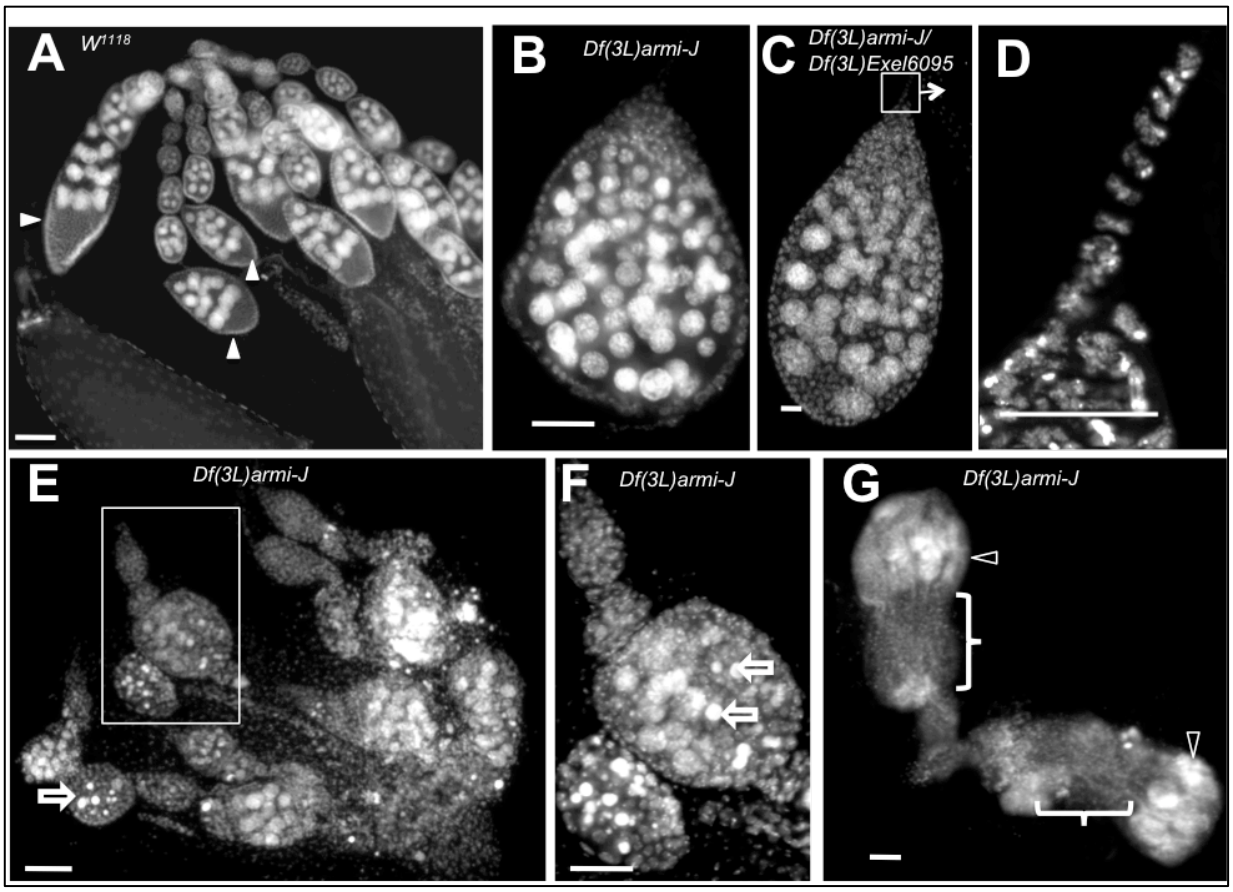

Figure 9: Deletion of both *armi* and *CycJ* results in accumulation of egg chambers with excess germline cells. Ovaries from wild type (w^{1118}) and *Df(3L)armi-J* mutant females were stained with DAPI to visualize nuclei. (A) Wild-type ovarioles from 3-day old or 8-day old females (not shown) consist of chains of developing egg chambers (arrows). Each egg chamber has 15 nurse cells undergoing endoreplication (large nuclei) and a single oocyte located at the posterior end (arrowheads). (B) A typical cyst from 3-day old *Df(3L)armi-J* females has many more than 16 nuclei undergoing endoreplicative cycles along with pycnotic nuclei. (C) An ovariole from a *Df(3L)armi-J*/*Df(3L)Exel6095* transheterozygote, which have a phenotype identical to *Df(3L)armi-J.* (D) A higher magnification of the terminal filament region in C. (E) Ovaries from 3-day old *Df(3L)armi-J* females contain abnormal egg chambers with more than the normal number of endoreplicating nuclei. Some cells appear to be undergoing cell death as indicated by the characteristic pycnotic nurse cell nuclei (open arrows), which is evident at higher magnification in (F). (G) Ovaries from 8-day old *Df(3L)armi-J* females contain empty ovarioles (bracket) with disorganized germaria (open arrowheads). Anterior is generally toward the top of each figure; in (G) the anterior of the lower ovariole is toward the right. Size bar is 50 μm in all panels except C, D, F, and G, in which it is 20 μm. This figure is published in (Atikukke, Albosta et al. 2014). Images A, B, E, F, and G of this figure have been previously published in (Atikukke 2009).

To determine whether the germline cells in homozygous *Df(3L)armi-J* were differentiated we stained ovaries with antibodies against Hts-RC, a component of the ring canals that connect cystocytes (Robinson, Cant et al. 1994; Atikukke 2009), and Orb, an oocyte-specific marker (Lantz, Chang et al. 1994). In wild-type ovaries, each cystoblast undergoes four rounds of cell division with incomplete cytokinesis resulting in 16 cystocytes that are connected by 15 ring canals (Figure 10 A&B) (Spradling 1993). One of the two cystocytes with four ring canals eventually adopts the oocyte fate, as is evident from Orb staining, while the other 15 cystocytes undergo endoreduplication to become nurse cells (Figure 10 E&H). In the *Df(3L)armi-J* mutant, ring canals appear to develop normally at least initially, though there are far more than the normal number in each egg chamber (Figure 10 C&D). Orb staining revealed that the process of oocyte selection takes place, though again there were two or more Orb-staining cells in each egg chamber of the *armi-CycJ* double null, suggesting that multiple cysts are enclosed in a single follicular layer (Figure 10 F&G). Combined, these results indicate that in the *armi-CycJ* double null, cystoblast division and differentiation occur, giving rise to several groups of germline cells consisting of nurse cells and an oocyte all contained in a single compound, or mispackaged, egg chamber.

2.3.2 *CycJ* transgenes suppress oogenesis defects in the *armi-CycJ* double mutant

Oogenesis defects in *Df(3L)armi-J* homozygotes may be due to loss of any one, a combination, or all of the three genes in this deletion. To determine whether the absence of *CycJ* contributes to defects observed in the armi-CycJ null, *CycJ* transgenes were introduced into *Df(3L)armi-J* homozygotes and

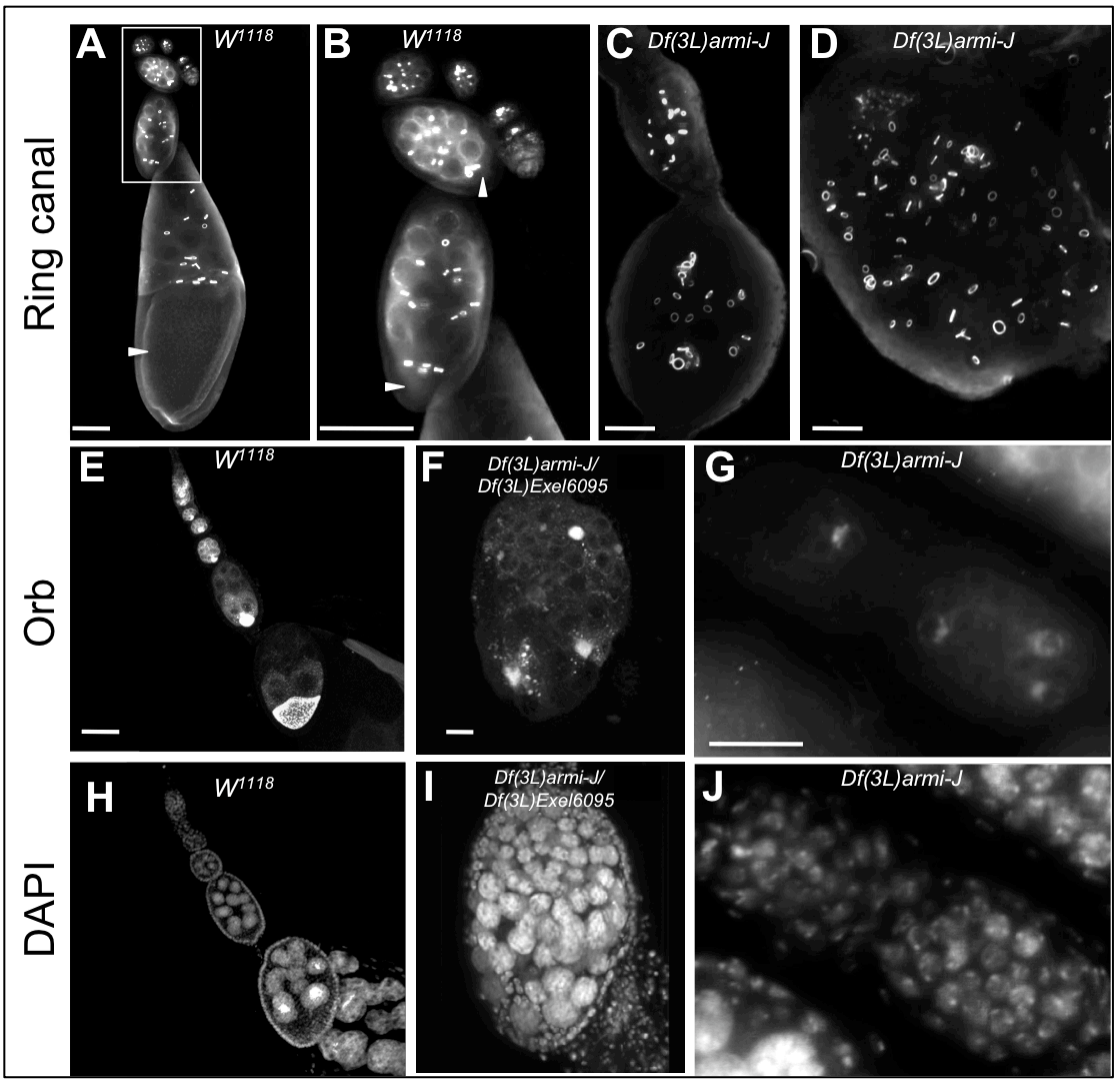

Figure 10: Multiple cystoblasts divide and differentiate within a single egg chamber in *armi-CycJ* mutants. Ovaries from wild type (w^{1118}) (A, B) and *Df(3L)armi-J* (C,D) adults were stained with anti-hts-RC antibody to visualize ring canals. In wild-type ovarioles each egg chamber contains a single posteriorly located oocyte (arrowheads) with 4 ring canals. (B) shows the boxed region in A at higher magnification. The *Df(3L)armi-J* mutant ovarioles show multiple abnormalities (C and D). Germarial patterning is disrupted and each egg chamber carries a giant cyst with multiple clusters of 16 cells interconnected by ring canals. (E-J) Ovarioles from wild-type (w^{1118}) (E, H), *Df(3L)armi-J*/*Df(3L)Exel6095* ovarioles (F, I), and *Df(3L)armi-J* (G, J) stained with DAPI (H-J) and Orb (E-G) to visualize oocytes. In wild-type ovarioles each egg chamber contains one Orb-staining oocyte. In the mutant, each giant cyst contains multiple Orb-staining nuclei adjacent to endoreplicating nurse cells. Anterior is towards the top in A and upper left in the rest of the images. Size bars are 50 μm in A-E and H, and 20 μm in F, G, I, and J. This figure has been published in (Atikukke, Albosta et al. 2014). Images A-D, G, and J of this figure have been previously published in (Atikukke 2009).

*Df(3L)armi-J/Df(3L)*Exel6095 transheterozygotes (described below and in (Atikukke 2009)). I used two different genomic *CycJ* transgenes and obtained similar results with each. One transgene contained *CycJ* and its upstream region including *armi* exon 9 and part of *armi* exon 8 (Figure 5). The other transgene included the same region but had stop codons introduced into *armi* exon 8 to guard against the possible expression of a C-terminal fragment of *armi*. I found that introduction of the *CycJ* transgenes significantly suppressed the *armi-CycJ* double null phenotypes (Figure 11 C&D). Unlike *Df(3L)armi-J*, the *Df(3L)armi-J* females containing a *CycJ* transgene were capable of producing fully developed stage 14 egg chambers and of laying eggs, albeit at a dramatically reduced rate compared to heterozygotes (Table 1). Introduction of the *CycJ* transgenes also resulted in a dramatic decrease in the frequency of mispackaged egg chambers (Figure 12 and Table 2). I observed similar results with the two different *CycJ* transgenes and with multiple independent insertion lines. Germline and somatic expression of a myc-tagged Cyclin J in the *Df(3L)armi-J* mutant also reduced the frequency of mispackaged egg chambers (Figure 13 and Table 2). This indicates that it is likely the coding region of *CycJ* that modifies the *armi-CycJ* phenotypes and suggests that *CycJ* can function in the germline and somatic cells. A *CG14971* transgene did not modify the oogenesis phenotypes in any background. Combined, these results indicate that the oogenesis defects observed in *Df(3L)armi-J* are due to the absence of both *armi* and *CycJ*.

These results also suggest that the defects observed in the *Df(3L)armi-J* animals that contain a *CycJ* transgene are due to the complete loss of *armi*; i.e., they represent the phenotype of an *armi* null (Atikukke 2009). These *armi* null females produced

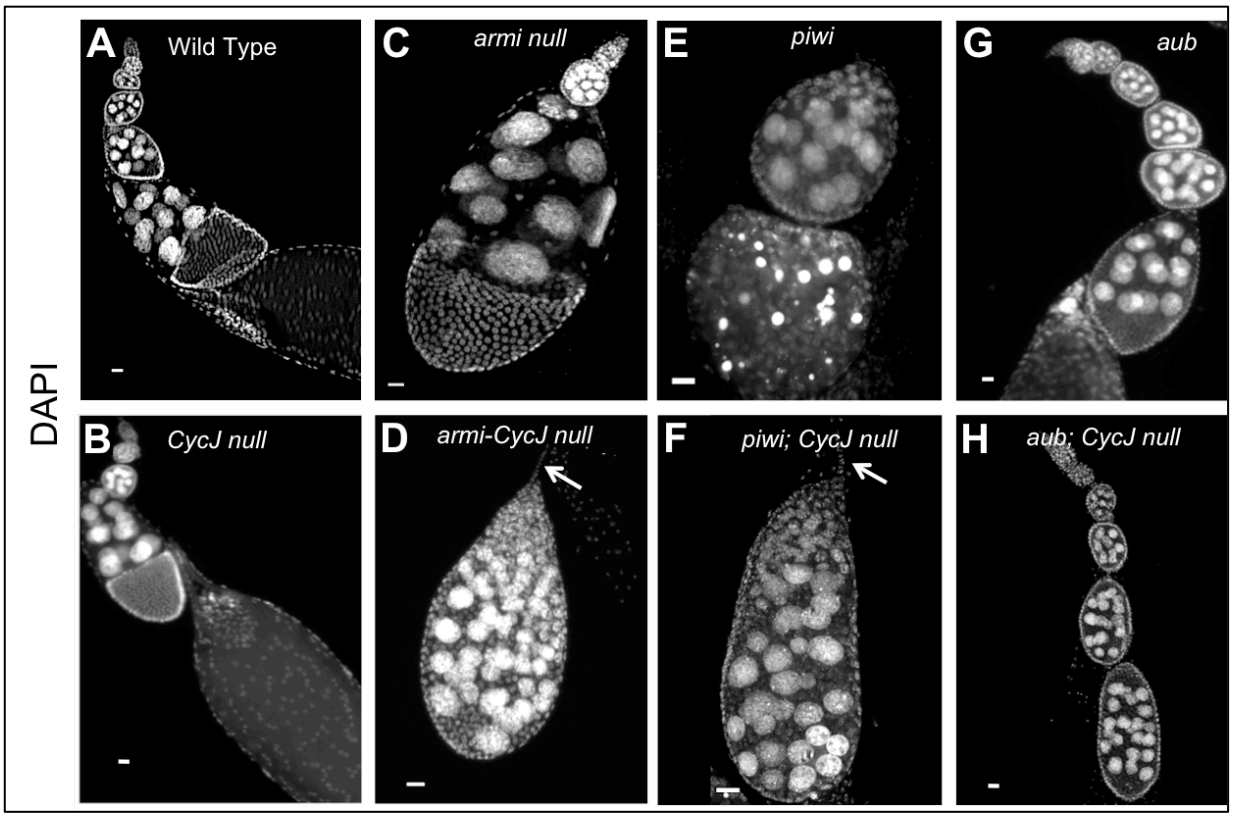

Figure 11: *CycJ* genetically interacts with *armi*, *piwi*, and *aub*. As in wild type (A), ovarioles from the *CycJ* null (*Df(3L)armi-J* with the P{*armi*} transgene appear normal (B), with long chains of egg chambers each containing 15 nurse cell nuclei. Ovarioles from the *armi* null (C) (*Df(3L)armi-J* with a P{*CycJ*} transgene frequently have just two egg chambers per ovariole, and egg chambers have 15 nurse cell nuclei. The *armi-CycJ* null (D) exhibits drastic oogenesis defects epitomized by production of ovarioles with one egg chamber that often has many more than 15 nurse cells. Like the *armi* null, *piwi* mutants (E) (*piwi[06843]/Df(2L)BSC145)* exhibit a decreased number of egg chambers per ovariole. *piwi-CycJ* double mutants (F) phenocopy the *armi-CycJ*, producing mispackaged egg chambers with more than 15 nurse cells. The *aub* mutant (G) (aub^{HN}/aub^{QC42}) showed all stages of egg chamber development each with the normal number (15) of nurse cell nuclei. In *aub-CycJ* double mutants (H), oogenesis arrested prior to stage 8 with some egg chambers harboring many more than 15 nurse cells. Arrows in D and F point to the terminal filament. Anterior is towards the top and size bars are 20 μm in all panels. This figure has been published in (Atikukke, Albosta et al. 2014) and is presented here with minor modifications.

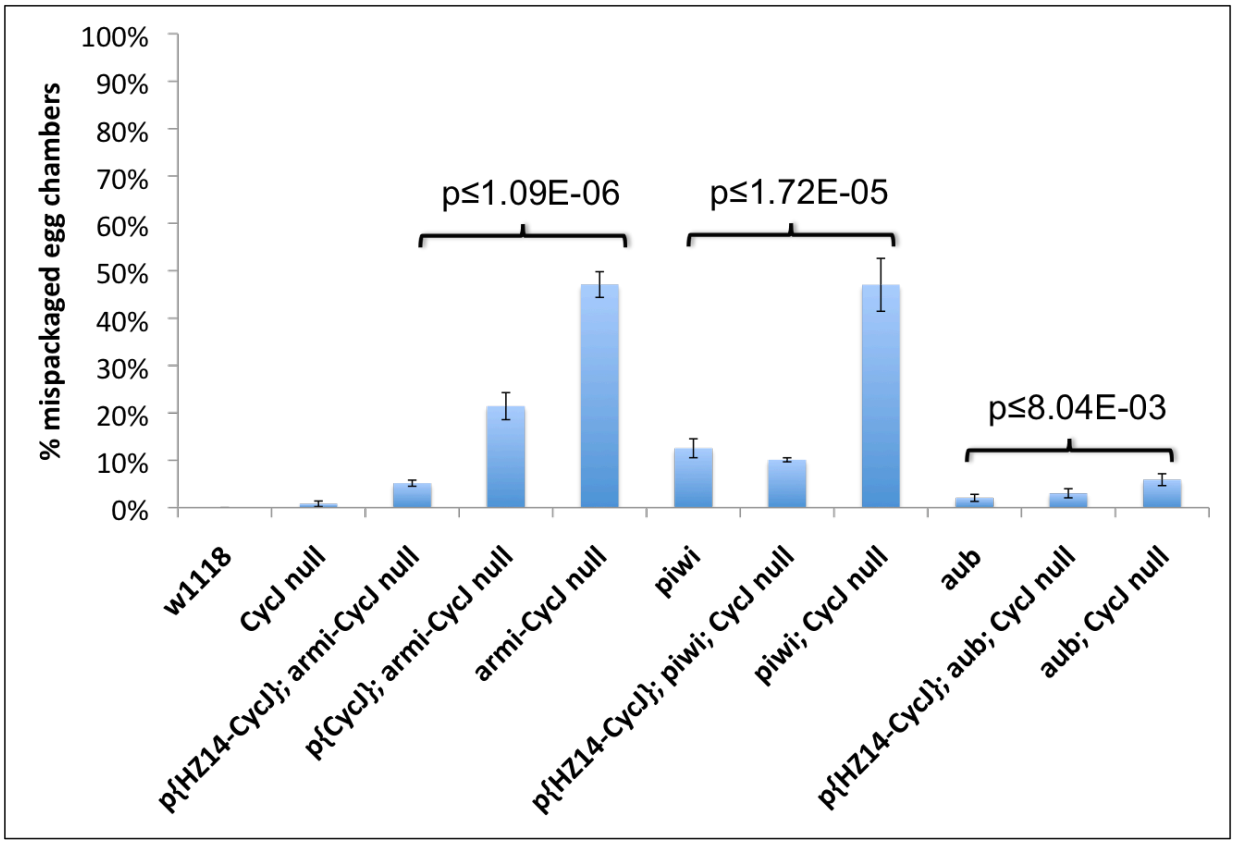

Figure 12: *CycJ* expression suppresses mispackaged egg chamber production in *armi-CycJ, piwi-CycJ,* and *aub-CycJ*. The percent of egg chambers with more than 15 nurse cell nuclei is shown, error bars = SEM (0.00% to 5.58%). Transgenes are in bold. *CycJ* null egg chambers are the same as wild type with respect to the number of nurse cell nuclei. In *armi-CycJ* null ovaries, 47.1%±2.7% of egg chambers have an excess of germline cells, which is indicative of a mispackaged egg chamber (see examples in Figure 12). *CycJ* genomic transgenes (p{*CycJ*} or p{*HZ14-CycJ*}) added to the *armi-CycJ* null significantly decreased the frequency of mispackaged egg chambers back to both *piwi-CycJ* and *aub-CycJ* was able to rescue mispackaged egg chamber production back to the level of the *piwi* and *aub* single mutants, respectively. Note that *armi-CycJ* and *piwi-CycJ* exhibit the same high level of mispackaged egg chamber production. The *CycJ* null is *P{armi}, Df(3L)armi-J/Df(3L)Exel6095*. The *armi-CycJ* double null in each case is *Df(3L)armi-J/Df(3L)Exel6095*. The *piwi* mutant is *piwi[06843]/Df(2L)BSC145*. The *aub* mutant is aub^{HN}/aub^{QC42}. P-values are shown in Table 2. All ovaries are from females 2-4 days post eclosion except *piwi* mutants, which are 0-2 days. At least 10 flies per genotype were examined, except for *p{HZ14-CycJ}; piwi; CycJ* null (n=2) and *p{HZ14-CycJ}; aub; CycJ* null (n=4). This figure has been published in (Atikukke, Albosta et al. 2014) and is presented here with minor modifications.

Table 2: *CycJ* differentially regulates egg chamber formation, packaging, and maturation in the absence of the piRNA pathways

Genotype	Alias	# of mature oocytes per fly		# of egg chambers per ovariole		% mispackaged egg chambers	
w1118	Wild Type	31.4 ±0.8	P=5.32 E-1	4.4±0.05	P=2.32 E-2	0.0% ±0.0%	P=1.81 E-1
p{armi}, Df(3L)armi-J/Df(3L)Exel6095	*CycJ null*	30.1 ±1.8		4.3±0.05		0.8% ±0.6%	
VP16::nos-Gal4>UAS-myc-CycJ; Df(3L)armi-J/Df(3L)Exel6095	***Germline armi null***	**0.2 ±0.1**	**P=8.05 E-2**	**1.5±0.07**	**P=1.23 E-3**	**19.4% ±1.9%**	**P=1.41 E-4**
VP16::nos-Gal4; Df(3L)armi-J/ Df(3L)Exel6095	**sibling control *armi-CycJ null***	**0.0 ±0.0**		**1.0±0.1**		**37.7% ±3.8%**	
e22c-Gal4>UAS-myc-CycJ; Df(3L)armi-J/ Df(3L)Exel6095	***Somatic armi null***	**0.2 ±0.2**	**P=6.23 E-1**	**2.6±0.3**	**P=1.95 E-3**	**13.2% ±2.9%**	**P=1.25 E-3**
>UAS-myc-CycJ; Df(3L)armi-J/ Df(3L)Exel6095	**sibling control *armi-CycJ null***	**0.4 ±0.4**		**1.3±0.03**		**38.3% ±2.5%**	
p{CycJ} or *p{HZ14-CycJ}; Df(3L)armi-J/ Df(3L)Exel6095*	***armi null***	**7.7 ±0.5**	**P=8.86 E-29**	**2.0±0.06**	**P=1.20 E-13**	**9.9% ±1.0%**	**P=1.22 E-15**
Df(3L)armi-J/Df(3L)Exel6095	***armi-CycJ null***	**0.3 ±0.1**		**1.2±0.07**		**47.1% ±2.7%**	
aub[HN]/aub[QC42]	***aub***	**7.5 ±1.8**		**3.8±0.4**		**2.1% ±1.8%**	
P{HZ14-CycJ}; aub[HN]/aub[QC42]; p{armi}, Df(3L)armi-J/Df(3L)Exel6095	**aub; CycJ rescue**	**6.8 ±0.9**	**P=2.11E-3**	**3.7±0.4**	**P=4.23E-1**	**1.7% ±0.1%**	**P=2.83E-3**
aub[HN]/aub[QC42]; p{armi}, Df(3L)armi-J/ Df(3L)Exel6095	***aub; CycJ null***	**0.0 ±0.0**	**P=8.20E-4**	**3.8±0.2**	**P=4.97E-1**	**5.9% ±1.3%**	**P=8.01E-3**
piwi[06843]/Df(2L)BSC145	***piwi***	**0.0 ±0.0**		**1.2±0.1**		**12.5% ±2.0%**	
P{HZ14-CycJ}; piwi[06843]/Df(2L)BSC145; p{armi}, Df(3L)armi-J/Df(3L)Exel6095	**piwi; CycJ rescue**	**0.0 ±0.0**	**P=1.20E-1**	**2.5±0.07**	**P=1.14E-4**	**10.1% ±0.4%**	**P=1.21E-5**
piwi[06843]/Df(2L)BSC145; p{armi}, Df(3L)armi-J/Df(3L)Exel6095	***piwi; CycJ null***	**0.4 ±0.3**	**P=1.20E-1**	**1.5±0.2**	**P=6.90E-2**	**47% ±5.6%**	**P=1.72E-5**

Quantification of oogenesis defects in *armi-CycJ, piwi-CycJ,* and *aub-CycJ* mutants. Three oogenesis phenotypes were affected in *CycJ-piRNA* pathway double mutants; number of mature oocytes per fly, number of egg chambers per ovariole, and percent of mispackaged egg chambers per fly. *armi-CycJ* ovaries displayed significantly worse defects in all three phenotypes compared to *armi* null. Germline expression of *UAS-myc-CycJ* in an *armi-CycJ* background was able to increase egg chambers per ovariole and decrease mispackaged egg chambers per fly, but did not affect mature oocyte production. *aub-CycJ* ovaries had more severe defects in mature oocyte and mispackaged egg chamber production, but not in egg chambers per ovariole compared to *aub* mutants. *piwi-CycJ* ovaries had significantly more mispackaged egg chambers than *piwi* mutants. *CycJ* transgenes were able to rescue all genetic interactions. All single and double null phenotypes are significantly worse than *CycJ* null and wild type. See Methods for details on quantification of these phenotypes and calculation of p values. For all genotypes excpet those noted, ovaries were scored at 2-4 days post eclosion. This table is published in (Atikukke, Albosta et al. 2014).

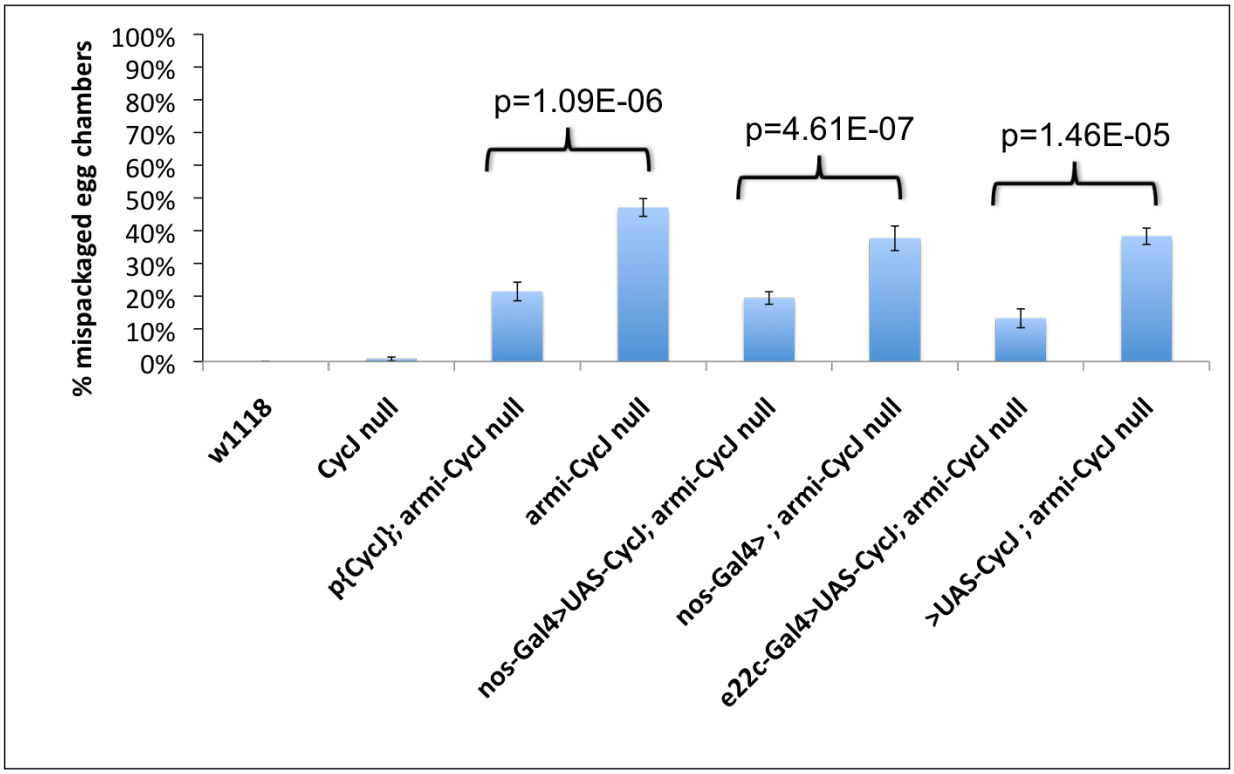

Figure 13: Expression of *CycJ* in germline and somatic cells in an *armi-CycJ* null background resulted in a significant reduction of egg chambers with too many germline cells. *UAS-CycJ.cDNA.myc (UAS-CycJ)* was expressed in escort cells, early premature follicle cells, and differentiated cells of developing egg chambers with *e22c-Gal4* and in the germline with *VP16::nos-Gal4 (nos-Gal4)* in an *armi-CycJ* null. Germline expression of *UAS-CycJ* in *armi-CycJ* null decreased the percent of mispackaged egg chambers to 19.4%±1.9% compared to sibling controls with the *nos-Gal4*, but not *CycJ,* with 37.7%±3.8%, p=4.61E-07. Somatic expression also decreased mispackaged egg chambers to 13.2%±2.9% compared to sibling controls with *UAS-CycJ*, but not *e22c-Gal4*, with 38.3%±2.5%, p=1.46E-05. At least 10 flies per genotype were examined except for *e22c-Gal4>UAS-CycJ; armi-CycJ* null (n=6). This figure has been published in (Atikukke, Albosta et al. 2014) and is presented here with minor modifications.

mature eggs that were often collapsed and that had dorso-ventral axis establishment defects (Table 1), a phenotype previously observed for a strong *armi* loss-of-function allele, *armi*$^{72.1}$ (Cook, Koppetsch et al. 2004). The *armi* null ovaries also showed frequent mislocalization of oocytes within egg chambers (Figure 14 D&E). Wild-type ovarioles exhibit posterior oocyte positioning in egg chambers, whereas oocyte positioning was random in the *armi* null. Oocyte positioning defects have been characterized in mutants of the spindle-class of genes including *spindle C (spn-C), spn-A, spn-B, spn-D* and *spn-E* (Gonzalez-Reyes and St Johnston 1994; Gonzalez-Reyes, Elliott et al. 1997). While this severe patterning defect was not reported for the previous *armi* loss of function mutant, it is consistent with the established role for *armi* in axis specification (Cook, Koppetsch et al. 2004).

2.3.3 *CycJ* is not essential for oogenesis

Next, we generated a *CycJ* null to address the potential function of CycJ (Atikukke 2009). Previously it was shown that an *armi* transgene was able to restore fertility to animals with the same three-gene deletion (Althoff, Viktorinova et al. 2009). We further found that addition of P*{armi}* to the *Df(3L)armi-J* deletion suppressed all oogenesis defects (Figures 11, 12, and Table 2). Specifically, cyst development was normal, as indicated by 15 large nurse cell nuclei and 15 ring canals as well as normal production of a chain of egg chambers with a posteriorly located oocyte (Figure 14). The *P{armi}; Df(3L)armi-J/Df(3L)armi-J* (*CycJ* null) females were fertile and laid eggs with two properly positioned dorsal appendages, but only 30% of the eggs hatched (Table 1). Providing a *CycJ* transgene along with the *armi* transgene in *Df(3L)armi-J/Df(3L)armi-J* or *Df(3L)armi-J*/*Df(3L)Exel6095* significantly improved the hatching rate

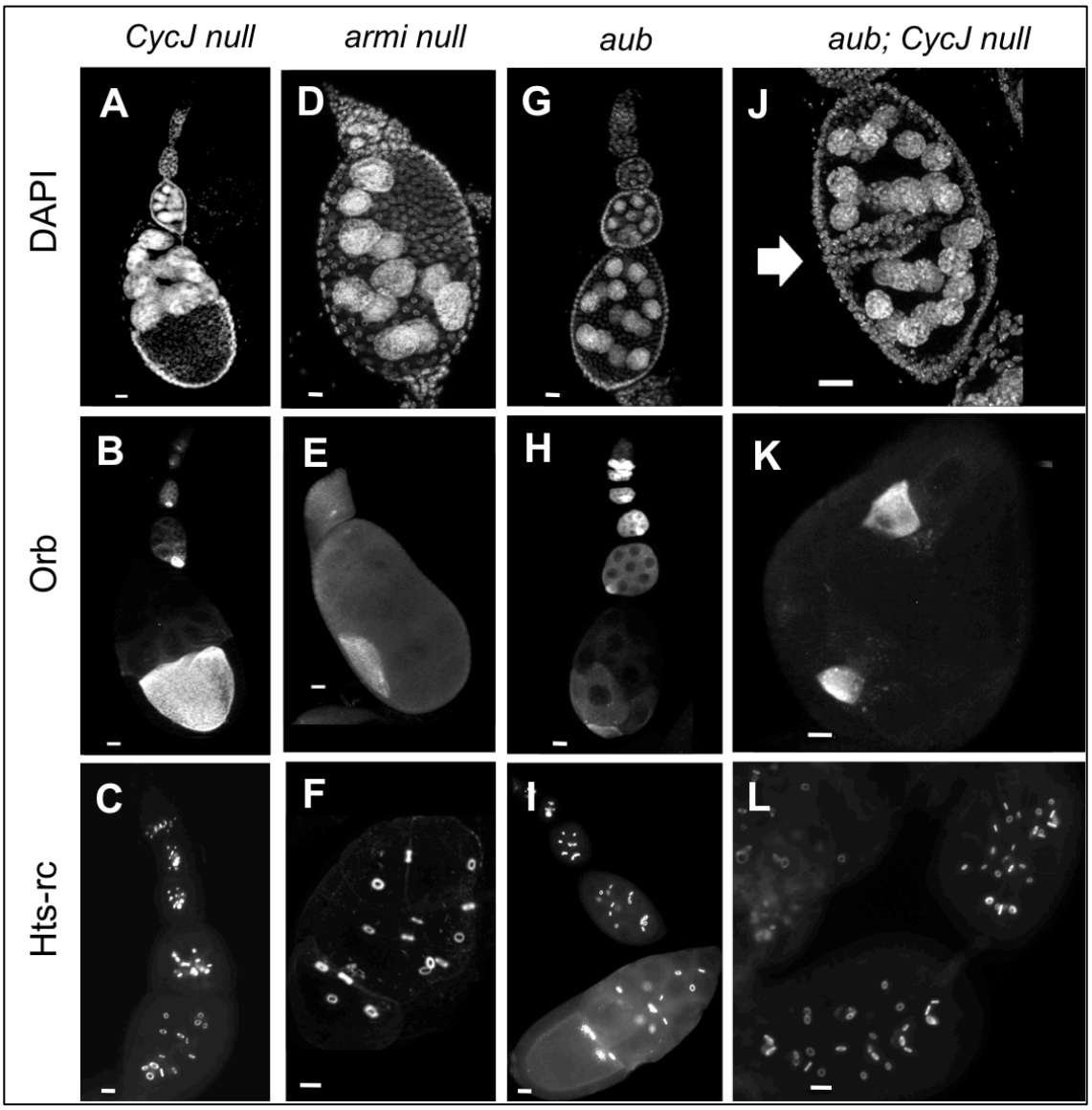

Figure 14: Cystoblast division, differentiation, and packaging are relatively normal in *CycJ* null, *armi* null, and *aub* mutants, but not in *aub-CycJ* double mutants, which often have multiple cysts in one egg chamber. Ovaries from *CycJ* null (A-C), *armi* null (D-F), and *aub* mutant (G-I) egg chambers all have a single orb staining oocyte (B, E, H) and 15 ring canals (C, F, I). Note that the *armi* null (D, E, F) exhibits oocyte mislocalization to the middle of the egg chamber. *aub-CycJ* double mutants (J-L), on the other hand, have egg chambers containing multiple cysts as indicated by more than 15 nurse cell nuclei (J), two orb staining foci (K), and more than 15 ring canals (L). The arrow in J marks a group of somatic cells partially dividing two adjacent egg chambers that appear to have undergone fusion resulting in one mispackaged egg chamber. The *CycJ* null is P{*armi*}, *Df(3L)armi-J*/*Df(3L)Exel6095*. The *armi* null is P{CycJ}; *Df(3L)armi-J*/*Df(3L)Exel6095*. The *aub* mutant is aub^{HN}/aub^{QC42}. All size bars = 20 μm. This figure has been published in (Atikukke, Albosta et al. 2014).

to 73 - 76% (Table 1). *CG14971* did not contribute to these phenotypes or hatching rates (Table 1). These data suggest that while *CycJ* regulates egg laying and hatching, it is dispensable for oogenesis under normal conditions. Combined with our previous data, *CycJ* appears to play a role in egg chamber formation, packaging, or maturation, but only in the absence of *armi*.

2.3.4 *CycJ* genetically interacts with multiple members of the piRNA pathways

The strong genetic interaction between *CycJ* and *armi* suggested that *CycJ* might be required when a piRNA pathway is compromised. To further test this possibility *CycJ* was removed in an *aub* mutant background (Atikukke 2009), and I also removed it from a *piwi* mutant background (Figure 11). First, I examined a piwi loss-of-function mutant *piwi[06843]* over a deficiency *Df(2L)BSC145* lacking *piwi*; hereafter I refer to *piwi[06843]/ Df(2L)BSC145* as the *piwi* mutant. *piwi* mutant ovaries were examined between zero and two days post eclosion because beyond two days they frequently contained agametic germaria and lacked egg chambers. Similar to the *armi* null, the *piwi* mutant produced only one to two egg chambers per ovariole and occasional mispackaged egg chambers (Figures 11, 12, and Table 2). Significantly, the *piwi-CycJ* double mutants exhibited a dramatic increase in the frequency of mispackaged egg chambers to a level identical to that seen in *armi-CycJ* double null. Addition of a *CycJ* transgene to the *piwi-CycJ* double mutant decreased the frequency of mispackaged egg chambers to the levels seen in *piwi* mutants (Figure 12). These results define a strong genetic interaction between *CycJ* and a second piRNA pathway member.

We also tested for a genetic interaction between *CycJ* and *aub* (Atikukke 2009). *aub* is required for synthesis of piRNAs and for silencing of transposons specifically in germline cells (Aravin, Klenov et al. 2004; Vagin, Sigova et al. 2006; Li, Vagin et al. 2009; Malone, Brennecke et al. 2009). *aub* mutants are similar to *armi* hypomorphs with respect to egg morphology, axis defects, accumulation of DNA double strand breaks, and checkpoint activation (Schupbach and Wieschaus 1991; Klattenhoff, Bratu et al. 2007). To test for a genetic interaction between *aub* and *CycJ* I generated females that were *CycJ* null and transheterozygous for the *aub* alleles, aub^{HN} and aub^{QC42} (hereafter referred to as *aub* mutants). While the *aub* mutants exhibited a modest decrease in egg laying capacity (75% of wild-type), the *aub-CycJ* double mutants laid no eggs (Table 1). Ovaries from the *aub* mutants had fully developed ovarioles with egg chambers at all stages of development (Figures 11 and 14). In contrast, oocyte development in the *aub-CycJ* double mutant was arrested at early stages, with egg chambers rarely advancing beyond stage 8 (Figure 11). The *aub-CycJ* ovaries had a significant number of mispackaged egg chambers with multiple oocytes and more than 15 nurse cell nuclei and ring canals (Figures 12, 14, and Table 2). Unlike the *armi-CycJ* and *piwi-CycJ* double mutants, the mispackaged egg chambers in *aub-CycJ* ovaries often included a disorganized layer of follicle cells nearly separating two fully developed cysts (Figure 14). The *aub-CycJ* double mutant phenotypes could be fully suppressed by introduction of a *CycJ* transgene (Figure 12). These observations define a genetic interaction between *CycJ* and *aub*, similar to the genetic interactions of *CycJ* with *armi* and *piwi*. The phenotypes of the respective double mutants have several similarities such that those of *armi-CycJ* and *piwi-CycJ* could be interpreted as more severe than those of

aub-CycJ; e.g., *armi-CycJ* and *piwi-CycJ* egg chambers arrested at earlier stages of development and produced more mispackaged egg chambers compared to the *aub-CycJ* mutants.

2.3.5 *armi* null defects, but not *armi-CycJ* null, were suppressed by a checkpoint pathway mutation

It has been previously shown by Theurkauf and colleagues (Klattenhoff, Bratu et al. 2007) that mutation of *armi* results in DNA double stranded breaks and activation of a DNA damage checkpoint dependent on the Chk2 kinase gene (known as *loki* or *mnk* in Drosophila) (Abdu, Brodsky et al. 2002; Masrouha, Yang et al. 2003). They found that the axis specification defects in *armi* mutants result from checkpoint activation, since loss of *mnk* function can rescue these defects. We performed the same analysis by introducing the mnk^{p6} allele into *armi* null or *armi-CycJ* double nulls followed by analysis of axis specification defects (Atikukke 2009). As previously demonstrated, *mnk* mutation suppressed the patterning defects of the *armi* hypomorph, $armi^{72.1}$ (Table 1) (Klattenhoff, Bratu et al. 2007). Whereas none of the eggs laid by $armi^{72.1}$/*Df(3L)armi-J* mothers had the normal number (two) of dorsal appendages, 85% of those from mnk^{P6} $armi^{72.1}$/*Df(3L)armi-J* double mutant mothers were normal. The *mnk* mutation also suppressed the patterning defect in the *armi* null, where 77% of the eggs from the mnk^{P6}; *armi* null had normal egg morphology compared to 0% in the *armi* null (Table 1). Whereas the *armi* null produced only rare eggs (<1% of the number laid by heterozygous *Df(3L)armi-J* mothers), introduction of the *mnk* mutation resulted in a >17-fold increase in egg production (Table 1). The *mnk* mutant also rescued egg production in the *armi* hypomorph by >2-fold (Table 1). These results suggest that

checkpoint activation contributes to not only the patterning defects but also the decrease in oocyte maturation associated with loss of *armi* function. In contrast, the *mnk* mutation did not suppress the developmental abnormalities of the *armi-CycJ* double null mutants (Table 1). This suggests that axis specification in *armi* is checkpoint dependent, whereas *armi-CycJ* double null may be downstream or independent of the DNA damage checkpoint.

2.4 Discussion and Summary

Cyclin J is highly conserved and specifically expressed in ovaries and early embryos, suggesting that it may function in one or both of these tissues. Cyclin J was originally identified in Drosophila where its mRNA was detected in adult females and embryos prior to cellularization but at no other stages (Finley, Thomas et al. 1996). This pattern has been confirmed and further refined in several transcriptome studies, which have invariably shown that the *CycJ* message is highest in ovaries and early embryos and virtually absent in other tissues and developmental stages (Arbeitman, Furlong et al. 2002; Graveley, Brooks et al. 2011; Chintapalli, Wang et al. 2013). Interestingly, the mosquito (*Aedes aegypti*) ortholog of *CycJ* is also expressed exclusively in ovaries and early embryos (Akbari, Antoshechkin et al. 2013). The conserved sequence and expression pattern suggest that Cyclin J might play an important role in oogenesis or early embryogenesis. Surprisingly, however, *CycJ* null Drosophila have no obvious defects and are fertile, albeit at a somewhat reduced rate compared to heterozygous controls. This could be explained if Cyclin J has an important function that is redundant with that of another protein, such as another cyclin. Althoff et al. explored this possibility testing for genetic interactions between *CycJ* and *CycE*, *CycA*, *CycB*, and *CycB3* by

removing a copy of each cyclin individually in a *CycJ* null followed by analysis of fertility (Althoff, Viktorinova et al. 2009). They observed no genetic interactions, though their results could not exclude the possibility of redundancy with one of these or another cyclin. Instead of being fully redundant with another gene, it may be that *CycJ* is required only under specific conditions. Such condition-specific requirements have been observed for many genes in a number of organisms, most notably in yeast where only 17% of the genes are essential for growth in standard rich medium, whereas 97% of genes have been shown to be required under one or more specific environmental conditions (Giaever, Shoemaker et al. 1999; Winzeler, Shoemaker et al. 1999; Hillenmeyer, Fung et al. 2008). Our findings that a *CycJ* null mutant modifies the phenotypes of piRNA pathway mutants are consistent with a nonredundant role for Cyclin J in oogenesis under specific conditions; i.e., when some aspect of a piRNA pathway is compromised.

I have shown that mutation of *CycJ* alters the mutant oogenesis phenotypes of *armi*, *piwi*, and *aub*. In the case of *armi*, the *armi-CycJ* double mutants have dramatic oogenesis defects, including only one egg chamber per ovariole, egg chambers with excess germline cells (mispackaged egg chambers), and a complete failure to produce fully developed eggs. These defects can be partially rescued with *CycJ* transgenes, including a *CycJ* open reading frame driven by a germline promoter. These observations define a genetic interaction between *CycJ* and *armi* and indicate that *CycJ* plays some role in oogenesis. I observed a similar genetic interaction with *piwi*, where *piwi-CycJ* double mutants produced egg chambers with excess germline cells and this phenotype was rescued with *CycJ* transgenes back to levels observed in *piwi* mutants.

The genetic interaction with *aub* was also dramatic. While *aub* or *CycJ* mutant mothers produced eggs at 75% and 65% the rate of wild type, respectively, the double mutant produced no eggs.

The disruption of a piRNA pathway has a number of consequences, any of which could create a requirement for *CycJ*. *piwi* and *armi* are required for production of primary piRNAs in both the germline and associated somatic cells (Malone, Brennecke et al. 2009; Olivieri, Sykora et al. 2010; Muerdter, Guzzardo et al. 2013). Germline cells also possess a unique piRNA production mechanism known as ping-pong amplification that uses the germline-specific argonaut proteins Aub and Ago3 (Aravin, Hannon et al. 2007; Li, Vagin et al. 2009; Siomi, Sato et al. 2011). The requirement for *CycJ* may result from defects that these distinct pathways have in common since *CycJ* genetically interacts with members of each (e.g., *armi* and *piwi*, or *aub*). For example, loss of function mutations of members of either pathway result in increased transposon activity that can be accompanied by DNA double strand breaks in the germline (Klattenhoff, Bratu et al. 2007). The DNA damage results in activation of checkpoint kinases such as Chk2 (encoded by *loki/mnk*) that in turn lead to defects in the localization of axis determinants. While any of these conditions may create a requirement for *CycJ*, the finding that an *mnk* mutant can suppress the *armi* null but not the *armi-CycJ* double mutant, suggests that *CycJ* is not required specifically as a result of Chk2 activation. A similar analysis will be needed to test whether *CycJ* is required when other DNA damage responses are activated. Alternatively, it is possible that the genetic interactions I observe are a consequence of misregulation of genes other than transposon genes. The piRNA pathways, for example, have been shown to repress a

small set of cellular genes (Sienski, Donertas et al. 2012), any one of which could be responsible for creating a requirement for *CycJ*.

A common feature of the double mutants of *CycJ* and *armi*, *piwi*, or *aub* is the increased frequency of mispackaged egg chambers. In both *armi-CycJ* and *piwi-CycJ* ovarioles there is often only one egg chamber and it has a terminal filament (Figure 11 D&F), suggesting that packaging of individual egg chambers has completely failed and the germarium has itself become an egg chamber. These egg chambers contain an excess of differentiated germline cells including multiple oocytes, indicating that germline differentiation has occurred (Figure 10). Thus, they are unlike mutants that only affect germline differentiation, which lead to germaria with an excess of undifferentiated GSC-like cells (McKearin and Ohlstein 1995; Chen and McKearin 2003). Proper egg chamber packaging requires several signaling pathways including the Notch and Hedgehog pathways. For example, a mutation in *Delta* (Bender, Kooh et al. 1993), the main receptor for Notch signaling in the ovary, results in loss of stalk cells, which leads to fusion of adjacent egg chambers and formation of a mispackaged egg chamber similar to those produced in *aub-CycJ* mutants. Mutation of *Hedgehog* (Forbes, Lin et al. 1996) results in failure of germline cyst encapsulation by follicle cells, which produces a single mispackaged egg chamber located in the germarium, similar to those seen in *armi-CycJ* and *piwi-CycJ.* Previous studies have suggested that piRNA pathways may also be involved in proper egg chamber packaging, though the mechanisms are not known. For example, mutation of the piRNA pathway member *maelstrom* (Sato, Nishida et al. 2011) or the piRNA producing locus *flamenco* (Mevel-Ninio, Pelisson et al. 2007) was shown to produce mispackaged egg chambers. I also

observed a low frequency of mispackaged egg chambers in the *piwi* mutants, *aub* mutants, and *armi* nulls (Figure 12). Thus, it appears that mutation of *CycJ* exacerbates a preexisting packaging defect seen in these piRNA pathway mutants. How the piRNA pathway and *CycJ* affect the signaling pathways that are required for normal egg chamber packaging remains to be determined.

In conclusion, I have demonstrated strong genetic interactions between *CycJ* and three piRNA pathway members, *armi, piwi,* and *aub*. *CycJ* is not required for oogenesis under normal conditions but its role was uncovered in the *armi*, *piwi*, and *aub* mutants. The double mutants of *CycJ* and each of these genes have similar phenotypes that can be suppressed with *CycJ* transgenes. Taken together, these data suggest a nonredundant function for *CycJ* in regulating oogenesis when the piRNA pathways are compromised. The double mutant phenotypes suggest that *CycJ* may contribute to the role of the piRNA pathways in egg chamber production and/or maturation.

CHAPTER 3: CYCLIN J COOPERATES WITH THE SOMATIC piRNA PATHWAY TO CONTROL GERMLINE CONTENT AND PACKAGING OF EGG CHAMBERS

3.1 Introduction

Cyclin J (CycJ) is a poorly characterized highly conserved member of the cyclin superfamily of proteins. In Drosophila, CycJ is unique among the cyclins in that its expression is restricted to ovaries, suggesting a possible function in oogenesis (Figure 1) (Finley, Thomas et al. 1996; Kolonin and Finley 2000; Althoff, Viktorinova et al. 2009; Atikukke 2009; Atikukke, Albosta et al. 2014). Although *CycJ* is not essential for oogenesis, a *CycJ* null mutant genetically interacts with members of the piwi-associated RNA (piRNA) pathway. Mutants of the piRNA pathway members *piwi* or *armi* have oogenesis defects characterized by production of mispackaged egg chambers with too many germline cells, and mutation of *CycJ* in these mutants dramatically enhances the mispackaging defect (Atikukke, Albosta et al. 2014).

Piwi and Armi belong to a piRNA pathway that operates in both germline and germline-associated somatic cells in contrast to Ago3 and Aub, which function only in the germline (Figure 4). Piwi functions in part by entering the nucleus with its associated piRNAs and suppressing transposon transcription (Yin and Lin 2007; Huang, Yin et al. 2013). In somatic cells, a protein complex that includes Piwi, Armi, Zuc, Vret, and Yb functions in perinuclear Yb bodies to produce the antisense piRNAs that enter the nucleus with Piwi (Olivieri, Sykora et al. 2010; Murota, Ishizu et al. 2014). Piwi and Armi also facilitate production of piRNAs and suppression of transposons in the germline cells, though these cells lack Yb and Yb bodies. The requirement for Piwi and Armi, however, appears to differ significantly between somatic and germline cells. Previous studies have shown that somatic knock down or mutants of *piwi* have mispackaged egg

chambers and an excess of GSCs, which can be rescued with somatic expression of wild-type *piwi* (Cox, Chao et al. 1998; Jin, Flynt et al. 2013; Ma, Wang et al. 2014). Other pathway members that function only in somatic cells (e.g., (Yb)) or somatic and germline cells (e.g., Vreteno (Vret)) also limit GSC accumulation and egg chamber packaging from ovarian somatic cells (King, Szakmary et al. 2001; Swan, Hijal et al. 2001; Zamparini, Davis et al. 2011). In contrast, these studies show that germline-specific mutation of these piRNA pathway members does not result in GSC accumulation or egg chamber mispackaging. We have previously shown that both Armi and Piwi regulate egg chamber packaging and that CycJ contributes to this function, but it was unknown whether it is the germline or somatic functions of Armi and Piwi that interact with CycJ (Atikukke, Albosta et al. 2014).

Here I provide evidence that the somatic functions of *armi* and *piwi* regulate GSC accumulation and egg chamber packaging by limiting BMP signaling. *armi* and *piwi* mutants have an overabundance of GSCs in the germarium, decreased expression of the differentiation factor Bam, and mispackaged egg chambers. Double mutants of *CycJ* and either *armi* or *piwi* have a drastic increase of GSCs relative to single mutants, and a complete loss of egg chamber packaging in most cases. These defects could be suppressed with a loss of function mutation in the BMP ligand gene *dpp*, suggesting that increased BMP signaling is responsible for the excess GSCs and impaired egg chamber packaging. Somatic expression of *armi* in the *armi-CycJ* null suppressed the oogenesis defects, suggesting GSC accumulation and egg chamber packaging depend on the somatic functions of Armi and Piwi. These results show that GSCs are increased in somatic piRNA pathway mutants and CycJ is required when these cells accumulate,

suggesting that CycJ may be acting as a conserved stem cell regulator. *armi* and *armi-CycJ* null also had a reduction of mitotic follicle cells, but only *armi-CycJ* null was rescued by decreasing BMP signaling, indicating that *CycJ* promotes follicle cell proliferation by limiting BMP signaling in the absence of *armi*. My results suggest that CycJ cooperates with the somatic piRNA pathway to limit BMP signaling, thereby limiting GSCs and promoting egg chamber packaging and follicle cell proliferation.

3.2 Materials and Methods

3.2.1 *Drosophila* strains

All animals were raised at 25°C on standard food. I carried out all crosses at 25°C. *armi* null, *CycJ* null, *armi-CycJ* null were created as previously described (Atikukke, Albosta et al. 2014). w^{1118} was used for wild type in all of the control experiments. *UAS-GFP-armi* was obtained from William Therkauf. *c587-Gal4* was obtained from Ting Xie. Stocks for w^{1118}, *P{w[+mC]=GAL4::VP16-nos.UTR}MVD2 w[1118], y[1] w[*]*; P{w[+mW.hs]=en2.4-GAL4}e22c/SM5, *dpp[hr56] cn[1] bw[1]/SM6a*, w; Df(3L)Exel6095/TM6B Tb, balancer strains, P{ry[+t7.2]=PZ}piwi[06843] cn[1]/CyO; ry[506], w[1118] ; Df(2L)BSC145/CyO, were obtained from the Bloomington *Drosophila* Stock Center. All fly strains are listed in Appendix A.

3.2.2 Ovary dissection and staining

Aged mated well-fed female flies were anesthetized with CO_2, quickly dipped in 95% EtOH, then placed in 1X PBX [PBS:0.4% Triton-X 100] for dissection. Abdomens were first removed from the head and thorax. The abdomen was voided of all material except ovaries and ovarian tubules. All fixing, staining, and washing steps were conducted with 50 µL/fly at room temperature with gentle shaking. Ovaries and

abdomen shell were fixed in a microcentrifuge tube containing PBX/4% formaldehyde for 15 minutes. Fix was removed and ovaries were washed with PBX for 30 minutes, then PBS for 15 minutes. Ovaries were stained with primary antibodies in PBX for 60 minutes followed by overnight incubation at 4 C. Ovaries were washed with PBX for 60 minutes, then PBS for 15 minutes. Ovaries were incubated in secondary antibody in PBX for 60 to 120 minutes. Ovaries were washed with PBX for 30 minutes, PBS for 15 minutes, then counterstained with 1 µg/mL DAPI in PBX + 5% glycerol for 15 to 30 minutes. Ovaries were washed with PBX for 30 minutes, followed by PBS for 15 minutes. Ovaries were incubated in 1:1 glycerol:PBS solution for 15 minutes followed by final incubation in antifade solution containing 75% glycerol, PBS, and 207.7 mM DABCO (1, 4-Diazabicyclo[2.2.2]-octane). Ovaries were mounted on slides in antifade (15 to 25 µL/ovary pair) and cover slips were sealed with nail polish topcoat. Slides were store at 4°C. Primary mouse antibodies against spectrin (1B1), Bam, and engrailed were obtained from Developmental Studies Hybridoma Bank and diluted 1:50 in PBX for use. Primary rabbit antibody against phospho-Histone H3 (Ser10) was obtained from Upstate Biotechnology and diluted 1:10 in PBX. Primary rabbit antibody against pMad was a kind gift from Ed Laufer and was diluted 1:2000 in PBX. Secondary goat anti-mouse IgG H&L Alexa 594 was obtained form abcam and diluted 1:1000 in PBX. Secondary goat anti-rabbit IgG H&L FITC was obtained from Jackson ImmunoResearch Laboratories and diluted 1:1000 in PBX. DAPI was obtained from Sigma and diluted to 1µg/mL.

3.2.3 Phenotype quantification

To quantify oogenesis defects, females were aged for 2-4 days post eclosion and ovaries were extracted and stained with DAPI as described above. *piwi* mutant females were only aged for 0-1 day post eclosion due to rapid egg chamber loss. For spectrosome staining, I found that the numbers of spectrosomes in mutants was age dependent and determined that two to four day old females were ideal for revealing differences in spectrosome number with minimal age-related issues like egg chamber destruction. All flies were 1 to 2 days old for pMad and Bam staining quantification. All flies were 1 day old for pH3 staining quantification. All ovarian material was transferred to a slide and ovarioles were mechanically separated from one another with forceps or insulin syringes for analysis. The percent of compound egg chambers per fly was quantified and averaged for at least four flies per genotype. The number of cells in early germaria that express pMad, the number of round spectrosomes per germarium, the number of pH3 positive cells per ovariole, and the percent of germaria with detectable Bam expression were each quantified and averaged for at least two flies per genotype. Statistical differences between single mutants, double mutants, and *dpp* rescue for each phenotype were calculated using a type 3 student's T-test, which accounts for unequal sample sizes. Error bars represent standard error of the mean (SEM) calculated by dividing the standard deviation by the number of flies per genotype for each staining. n-values are indicated in each figure legend.

3.2.4 Identification of *p{HZ14-CycJ}* transgene genomic location with inverse PCR

Inverse PCR (iPCR) was performed to determine the insertion sites of *p{HZ14-CycJ}* transgenes (Table 3) and is a modified version of the original Berkeley Drosophila Genome

Table 3: Insertion site of *HZ14-CycJ* transgenes based on iPCR sequence data

Strain Name	Chromosome Location	Cytological Location	Closest gene to the left	Closest gene to the right
Q_54-1B	X:4812522	4D6	CG4041	CG6903
V_91-1A	X:3843508	3F9	Vap-33-1	Vap-33-1
J2_3-2	2R:11488022	52B1	CG8204	CG42524
J2_6-1	2L:5943984	26A3	Gpdh	Gpdh
J2_6-5	2L:5943991	26A3	Gpdh	Gpdh
J2_72-11	2R:19705365	60A2	CG4797	CG4797
J3_68-1	3R:19171530	94E13	pnt	pnt
J3_72-12	3L:6957858	65D5	sgl	CG10064
J3_72-5	3L:6958057	65D5	sgl	CG10064
J3_26-1	3R:10566646	88D2	eff	eff
J3_45-1	3L:17966383	75B1	Eip75B	Eip75B

Insertion sites of *p{HZ14-CycJ}* were determined by iPCR and are labeled with numbers corresponding to our records. Most insertion sites are intragenic, but there are insertion sites in regions of non-coding DNA for each chromosome. Insertion site in non-coding regions are preferable since it decreases the possibility of an artifact phenotype due to gene disruption. Insertion site information for J3_72-12 (*p{HZ14-CycJ}72-12*) was used for meiotic recombination to create an *armi* null chromosome (Figures 15, 16).

Project protocol of Jay Rehm (http://www.fruitfly.org/about/methods/inverse.pcr.html). Briefly, a restriction enzyme was used to cut within the genomically inserted transgene vector, which also digested at the nearest restriction site within the flaking genomic DNA. DNA fragments were ligated, purified, and subjected to PCR using primers specific to vector DNA, which also amplified the flanking genomic DNA in ligated circular DNA. PCR products were then sequenced to determine flanking DNA sequence. To do this, 15 adult flies were collected, placed in a 1.7 mL microcentrifuge tube, and frozen. Tubes were removed from the freezer and 400 µL of Buffer A was added followed by homogenization with a plastic pestle. Homogenates were incubated for 30 minutes at 65°C. 800 µL of 6M LiCl: 5M KAc solution was added, tubes were mixed by inversion, and incubated on ice for 10 minutes. Tubes were centrifuged for 15 minutes at 12,000 RPM and room temperature. The supernatant was transferred to another tube and recentrifuged. 1 mL of supernatant was transferred to another tube and 500 µL of 100% isopropanol was added, and then mixed by inversion. Tubes were centrifuged for 20 minutes at 12,000 RPM and room temperature. The supernatant was discarded and pellets were washed with 500 µL of 70% ethanol followed by centrifugation for 10 minutes at 12,000 RPM and 4°C. Supernatant was discarded and pellets were air dried and resuspended in 75 µL TE. DNA was then subjected to restriction digestion with the following reagents: 10 µl of DNA, 1X restriction buffer (NEB Buffer 1), 200 ng RNase A, 10 U Sau3AI restriction endonuclease (NEB R0169), 2.5 µg BSA, water to 25 µL. Mixture was incubated for 2.5 hours at 37°C followed by heat inactivation of enzyme for 20 minutes at 65°C. 5 µL of digestion was run on a 1% agarose gel to verify that there is only a smear of DNA indicating that digestion was complete. Digestion was then subject to religation as follows; 10 µL (~1 Fly) of digestion reaction

product was preheated at 65°C for 5 minutes followed by incubation on ice for 2 minutes. Digestion was then combined with 40 µL 10X Ligation Buffer [1M Tris-HCl, 1M MgCl2, 1M DTT, 100 mM ATP, H2O to 1.5 mL], 349 µL ddH_2O, and 1 µL (0.25 U) T4 DNA Ligase for a total of 400 µL/reaction. Mixture was incubated at 4°C overnight. This produced two circular pieces of DNA containing genomic DNA flanking the 5' end of the transgene insertion connected to 5' vector DNA and the same combination for the 3' end of the transgene insertion. Ligation product was precipitated with a mixture of 40 µL of 3M NaOAc and 1 mL EtOH at -80°C for 1 hour. Precipitate was centrifuged at 15000 rpm for 30 minutes at 4°C. Supernatant was discarded and pellets were washed with 0.5 mL cold 70% EtOH and spun at 15000 rpm for 15 minutes at 4°C. Supernatant was discarded and pellets were dried in a vacuum centrifuge without heat for 15 minutes. Pellets were resuspended in 150 µL TE for at least 1 hour at room temperature. Ligation products were amplified using PCR with primers specific for the vector used to insert the CycJ transgene. Two primer pairs were used targeting the 5' and 3' end of each insertion. 5' end primers were plac1/pwht1. 3' end primers were ey.3.f/ey.3.r. PCR reaction is designed to amplify a portion of the transgene vector and the flanking genomic DNA ligated into each circular DNA template. PCR products were examined on a 1.0% agarose gel to ensure there is only one amplification product. PCR reactions that produced a single product were prepared and sent for sequencing with either a primer for 5' end products, 5.sup.seq1, or a primer for 3' and products, ey.3.f. Sequencing results were used to map insertions to their genomic location based on flanking genomic DNA that was amplified. All primers are listed in Appendix B.

3.2.5 Generation of *armi* null on a *Df(3L)armi-J* chromosome with meiotic recombination

A new *armi* null chromosome was produced with meiotic recombination. This new chromosome 3 contained *Df(3L)armi-J* and a *p{HZ14-CycJ, mW}72-12* transgene (Figure 15). All matings were conducted in flies containing the *white* mutation on chromosome 1 resulting in white eyes, which allows for selection of recombinant chromosomes containing a *mini-white (mW)* transgene in the *p{HZ14-CycJ, mW}72-12* construct that produces orange eyes in a white-eyed background (Figure 16). The first round of matings was between white-eyed flies containing a balanced *Df(3L)armi-J* chromosome 3 and orange-eyed flies containing homozygous *p{HZ14-CycJ, mW}72-12* chromosome 3. The position of *Df(3L)armi-J* was known at 6.64 centimorgans (cM) from the telomere of chromosome 3 arm L and the insertion site of *p{HZ14-CycJ, mW}72-12* was determined with inverse PCR as described above (section 3.2.4, position in Table 3) to be 13.34 cM. Female progeny were selected based on the absence of Ser and used in the second mating. These females were orange-eyed (due to *mW*) transheterozygotes and should perform meiotic recombination at a frequency of 6.7% (13.34 cM – 6.64 cM) on chromosome 3 producing gametes containing *Df(3L)armi-J, p{HZ14-CycJ, mW}72-12* that also have orange eyes. The second mating is between transheterozygotes and a white-eyed marked balancer strain *TM3, Ser/Sb.* Balanced male progeny are selected based on Ser, orange eyes, and nSb. One male fly is used in the third mating with a balancer strain. Flies mated for nine days at room

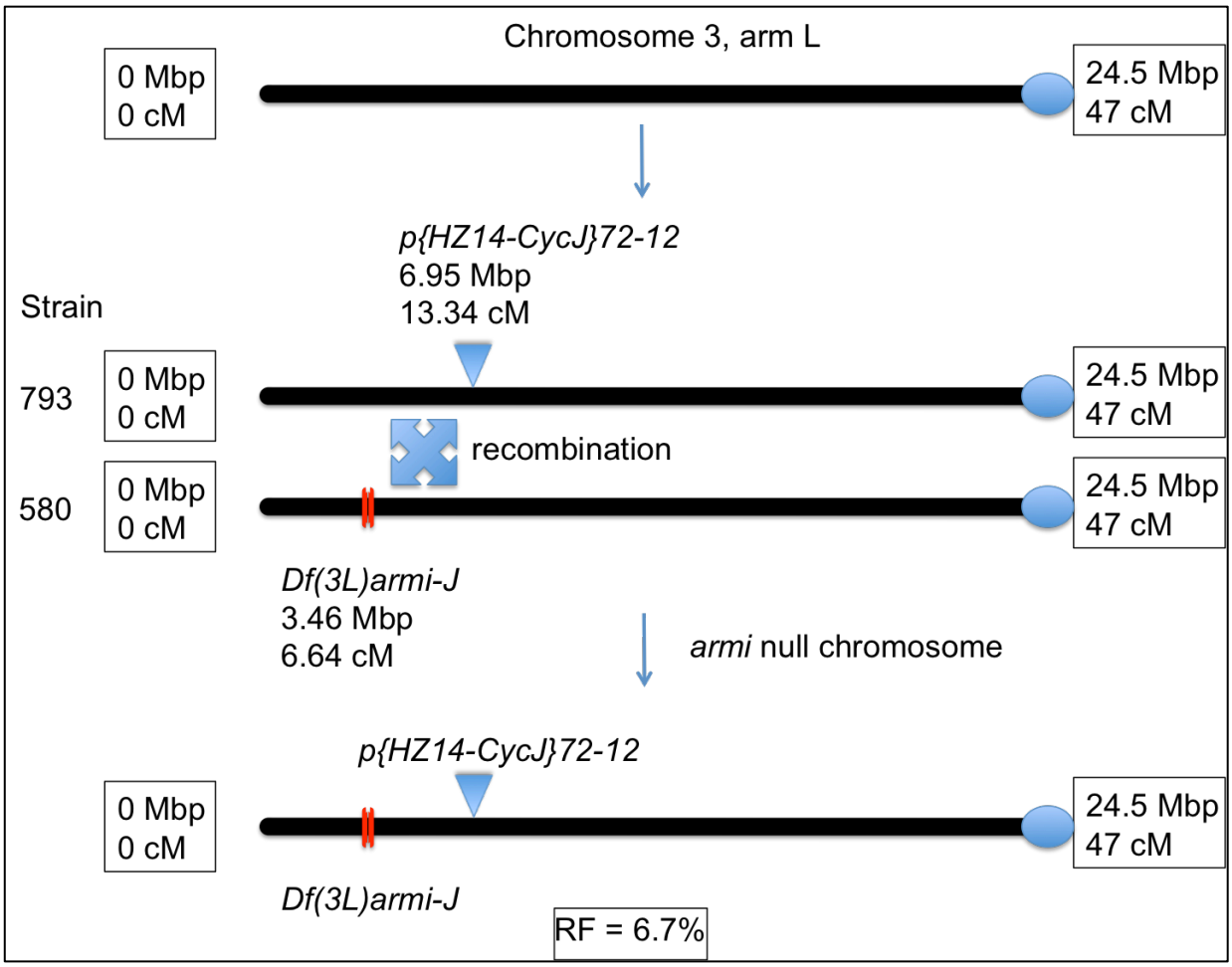

Figure 15: Production of a new chromosome 3 containing *Df(3L)armi-J* and *p{HZ14-CycJ, mW}72-12* using meiotic recombination. Meiotic recombination occurs at a known frequency in female *Drosophila* based on the distance between the two loci undergoing recombination. The recombination frequency has been experimentally determined and is represented in units known as centimorgans (cM). A distance of 1 cM between two loci represents a 1% recombination frequency. In this case, *Df(3L)armi-J* is at 6.64 cM in relation to the telomere and the desired *p{HZ14-CycJ, mW}72-12* site is at 13.34 cM. The recombination distance between the two is 13.34 cM – 6.64 cM = 6.7 cM or a recombination frequency of 6.7%. This approach was used to construct an *armi* null chromosome with the mating scheme shown in Figure 16.

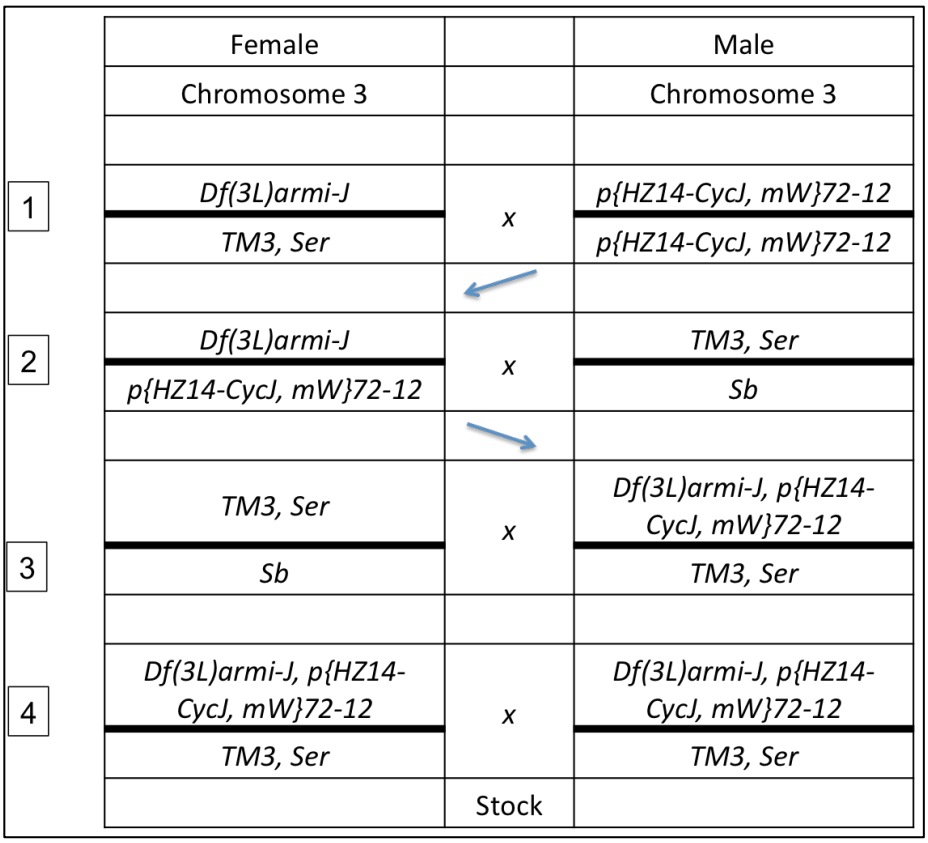

Figure 16: Mating scheme for meiotic recombination used to produce a new "*armi* null" chromosome 3. All matings are conducted in flies containing the *white* mutation on chromosome 1 (not shown), which allows for selection of recombinant chromosomes. The first round of matings is between white-eyed flies containing a balanced *Df(3L)armi-J* chromosome 3 and orange-eyed flies containing homozygous *p{HZ14-CycJ, mW}72-12* mapped to chromosome 3 using iPCR (as described in section 3.2.4, insertion sites listed in Table 3). Female progeny are selected based on the absence of Ser and used in the second mating. These females are orange-eyed transheterozygotes and should perform meiotic recombination at a frequency of 6.7% on chromosome 3 producing gametes containing *Df(3L)armi-J, p{HZ14-CycJ, mW}72-12* that have orange eyes. The second mating is between transheterozygotes and a white-eyed marked balancer strain *TM3, Ser/Sb.* Balanced male progeny are selected based on Ser, orange eyes, and nSb. One male fly is used in the third mating with a balancer strain. Flies mated for nine days at room temperature followed by DNA extraction of the male and diagnostic PCR to confirm the presence of both *Df(3L)armi-J* and *p{HZ14-CycJ, mW}72-12.* Matings that had a recombinant male were used to generate a stock in the fourth mating with Ser, nSb males and females. Diagnostic PCR for D*f(3L)armi-J* and *p{HZ14-CycJ, mW}72-12* contained one transposon-specific primer and one genomic primer as described previously. Recombinant flies were recovered at a rate of 2/31, or 6.45%, which is very close to the expected frequency of 6.7%.

temperature followed by DNA extraction of the male and diagnostic PCR to confirm the presence of both *Df(3L)armi-J* and *p{HZ14-CycJ, mW}72-12.* Matings that had a recombinant male were used to generate a stock in the fourth mating with Ser, nSb males and females. Diagnostic PCR for D*f(3L)armi-J* and *p{HZ14-CycJ, mW}72-12* contained one transposon-specific primer and one genomic primer. All fly strains are listed in Appendix A.

3.2.6 Tissue specific expression with *Gal4>UAS*

The *Gal4>UAS* system is described in section 2.2.8. This chapter utilized a germline specific *Gal4* construct *VP16::nos.UTR-Gal4* as well as ovarian somatic cell *Gal4* constructs *e22c-Gal4* and *c587-Gal4*. All fly strains are listed in Appendix A.

3.3 Results

3.3.1 *CycJ* cooperates with somatic *armi* to promote egg chamber packaging

Previous results showed that *piwi* and *armi* mutants have mispackaged egg chambers, and that *CycJ* mutation enhances these defects as described in Chapter 2 and (Atikukke, Albosta et al. 2014). Since *armi* and *piwi* have functions in both the somatic cells and in the germline, I set out to determine from which cell type they contribute to egg chamber packaging and to the *CycJ* interaction. To examine cell-specific requirements, I induced expression of *UAS-GFP.armi (UAS-armi*) either in the germline with *VP16::nos-Gal4* (*nos-Gal4)* or in ovarian somatic cells with *e22c-Gal4* or *c587-Gal4* in an *armi-CycJ* null background (Figure 17). Egg chambers were stained with DAPI to visualize nuclei and were considered mispackaged if they contained more than 15 nurse cell nuclei. As previously observed (Atikukke, Albosta et al. 2014), an *armi* null showed low levels of mispackaged egg chambers that rose dramatically with

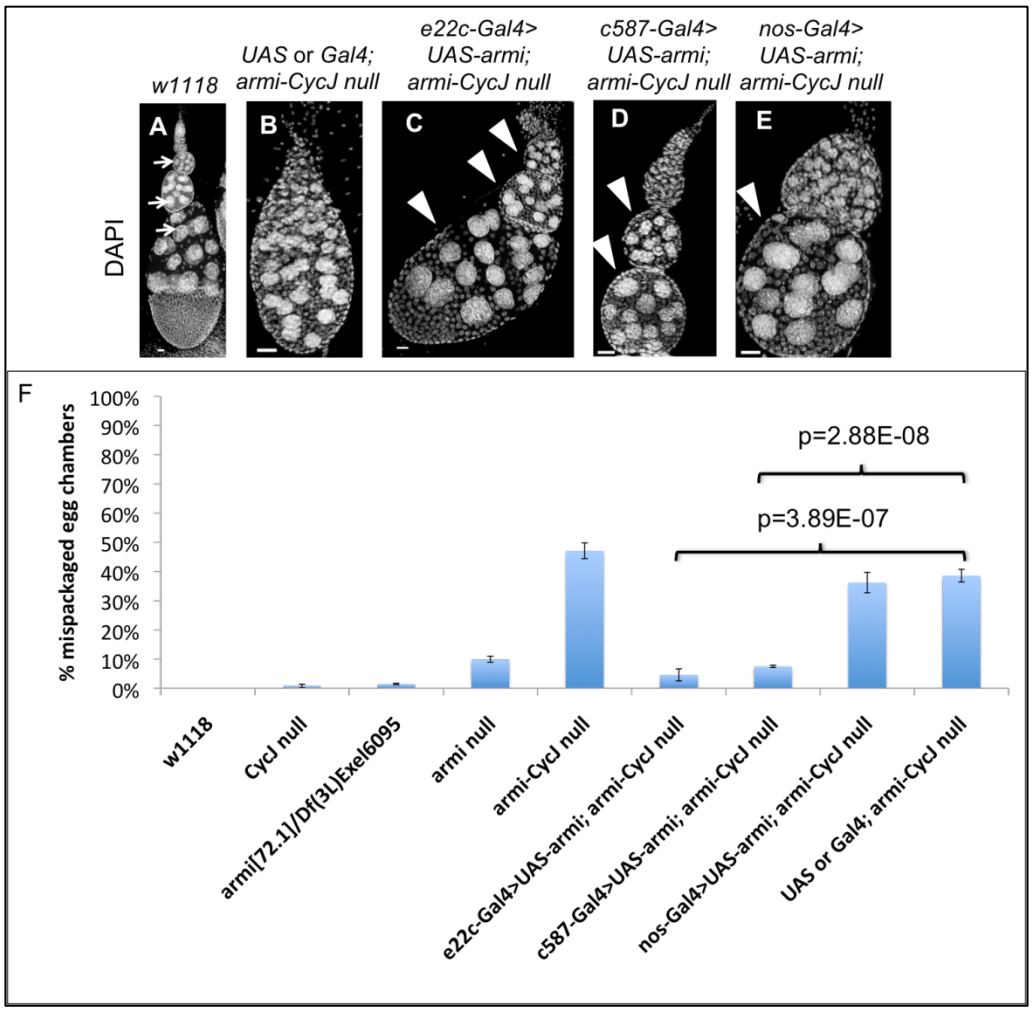

Figure 17: *CycJ* cooperates with somatic *armi* to promote egg chamber packaging. Packaging defects were quantified by counting the number of egg chambers with too many germline nuclei in DAPI stained ovaries. (A) a wild-type ovary represented by *w1118*. The ovariole includes a chain of developing egg chambers each with 15 germline cells, evident from the large polyploid nurse cell nuclei (arrows). (B) An *armi-CycJ* null ovariole with a single mispackaged egg chamber with an excess of germline cells. 40-50% of the egg chambers in *armi-CycJ* null mutant are similarly mispackaged. The example is a sibling of (C) that has *UAS-armi* or *e22c-Gal4* but not both. (C) An *armi-CycJ* null ovariole expressing *UAS-armi* in ovarian somatic cells with *e22c-Gal4*. (D) An *armi-CycJ* null ovariole expressing *UAS-armi* in ovarian somatic cells with *c587-Gal4*. (E) An *armi-CycJ* null ovariole expressing *UAS-armi* in germline cells with *nos-Gal4*. The ovarioles in C, D, and E have three, two, and one egg chamber(s) with the normal number of germline cells (arrow heads). (F) Quantification of mispackaged egg chambers. Phenotypes were compared to sibling controls that had either the *UAS* transgene or the Gal4 transgene but not both, in an *armi-CycJ* null background. Results are averages for at least 131 ovarioles per genotype. Error bars indicate SEM. P-values were calculated using a type 3 student's T-test. Size bars in A-E = 20 μm.

further removal of *CycJ* (Figure 17 B, F). Somatic expression of *UAS-armi* with either *e22c-Gal4* or *c587-Gal4* decreased the percent of mispackaged egg chambers from 38.6%±2.2% to 4.6%±2.1% ($p=3.89E^{-7}$) or 7.5%±0.4% ($p=5.37E^{-8}$), respectively, but germline expression of *UAS-armi* had no effect (Figure 17 C-F). These data suggest that *armi* regulates egg chamber packaging from the soma. Consistent with this somatic function of *armi*, an *armi* allele that is known to primarily affect germline *armi* (*armi[72.1]* (Olivieri, Sykora et al. 2010)), has a much less severe egg chamber packaging defect compared to the *armi* null (Figure 17 F). Combined, these data suggest that somatic *armi*, and not germline *armi*, regulates egg chamber packaging and that *CycJ* cooperates with the somatic function of *armi*. To further analyze tissue specific oogenesis regulation, I also quantified the number of egg chambers per ovariole in these flies. Flies were compared to sibling *armi-CycJ* null controls with either *UAS* or *Gal4,* but not both with 1.4±0.04 egg chambers per ovariole. Somatic expression of *UAS-armi* increased the number of egg chambers per ovariole to 2.6±0.3 and 2.8±0.2, but germline expression had little to no effect with 1.5±0.07 and 2.0±0.1. This further suggests that *armi* regulates egg chamber packaging from the soma and *CycJ* enhances this function. It also supports my observation that as mispackaging increases, total number of egg chambers decreases.

3.3.2 Somatic *armi* and *piwi* along with *CycJ* limit accumulation of GSC-like cells and promote egg chamber packaging

Several studies have indicated that somatic Piwi and the somatic-specific piRNA pathway act to limit the accumulation of GSCs in the germarium. For example, the accumulation of GSC-like cells seen in loss-of-function alleles of *vreteno* or *piwi* can be

suppressed by somatic expression of these genes (Zamparini, Davis et al. 2011; Jin, Flynt et al. 2013). Furthermore, a loss of function allele of the somatic-specific *fs(1)Yb* (*Yb^{72}*) results in germaria with too many GSC-like cells, whereas germline *Yb^{72}* clones do not (Swan, Hijal et al. 2001). To test whether *armi* or *CycJ* similarly contributes to regulating GSCs I used spectrin staining to examine spectrosomes, spherical structures found in GSCs and their daughter cystoblasts prior to further cell division and differentiation. Whereas normally germaria have 3 to 4 spectrosomes per germarium corresponding to the GSCs and cystoblasts (Figure 18 A, B), the piRNA pathway mutants *piwi* and *armi* exhibited an increase of spectrosomes (Figure 18 D, F, J) with 10.9±0.2 and 9.6±0.2 per germarium, respectively. When *CycJ* was removed from these mutants, there was a further increase of spectrosomes to 17.0±0.6 in *piwi-CycJ* and 17.8±0.6 in *armi-CycJ* (Figure 18 E, G, J). Interestingly, neither *aub[QC42]/aub[HN]* transheterozygotes (*aub)* nor *aub-CycJ* double mutants exhibited increased spectrosomes (data not shown). Somatic expression of *UAS-armi* with either *e22c-Gal4* or *c587-Gal4* in *armi-CycJ* reduced spectrosomes to 12.0±0.6 ($p=1.51E^{-13}$) and 6.7±0.1 ($p=3.39E^{-31}$) respectively (Figure 18 J). Consistent with previous data with *piwi* and *Yb*, these data indicate that the somatic piRNA pathway regulates the accumulation of spectrosome containing GSC-like cells. Furthermore, it appears that CycJ cooperates with the somatic piRNA pathway to limit GSC-like cell accumulation.

Maintenance of germline stem cells depends on bone morphogenetic protein (BMP) signaling from the somatic cells that comprise the stem cell niche (Figures 3, 18 A). To test whether the excess GSCs that I observe in the *armi*, *piwi*, and *CycJ* double mutants depends on BMP signaling I introduced a loss of function allele of *dpp*

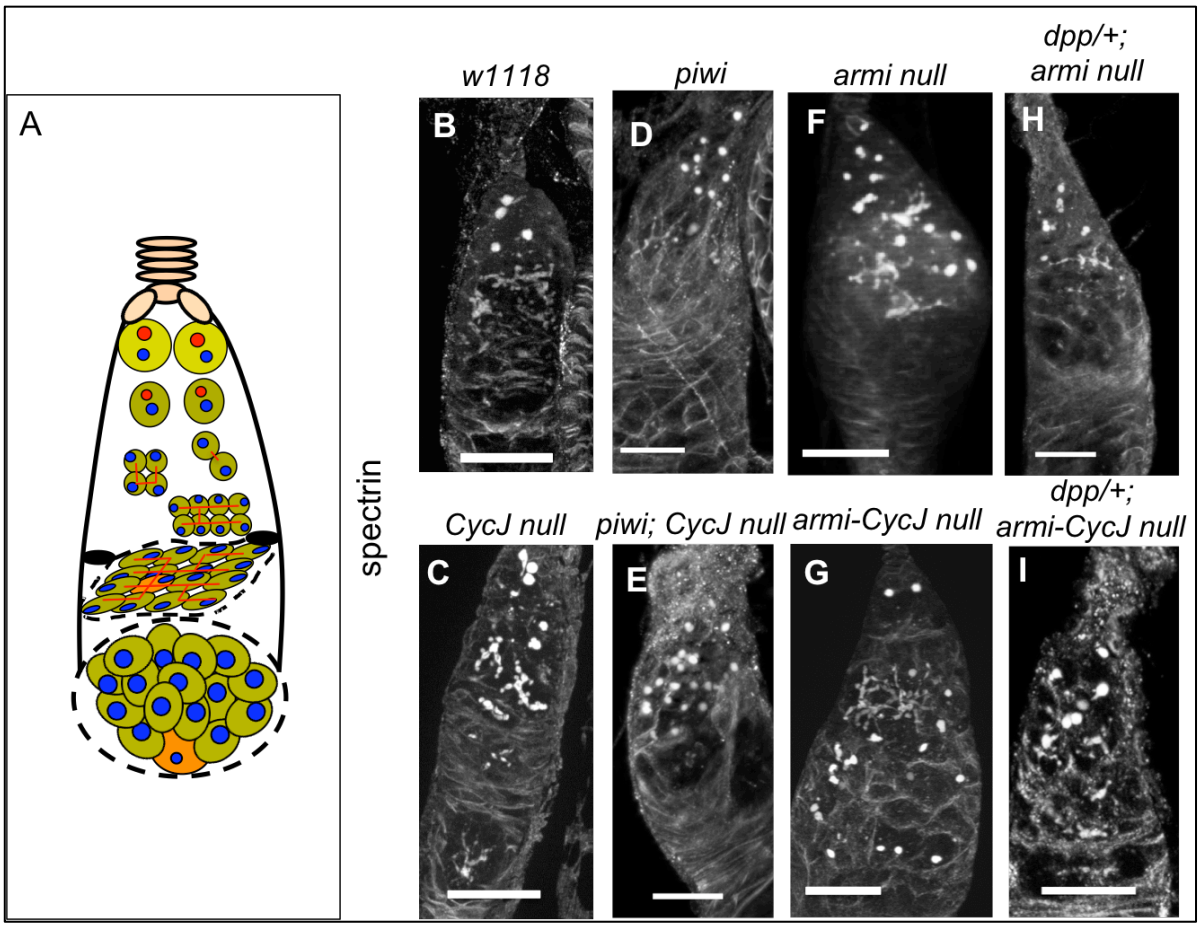

Figure 18: Somatic *armi* and *piwi* along with *CycJ* limit accumulation of GSC-like cells

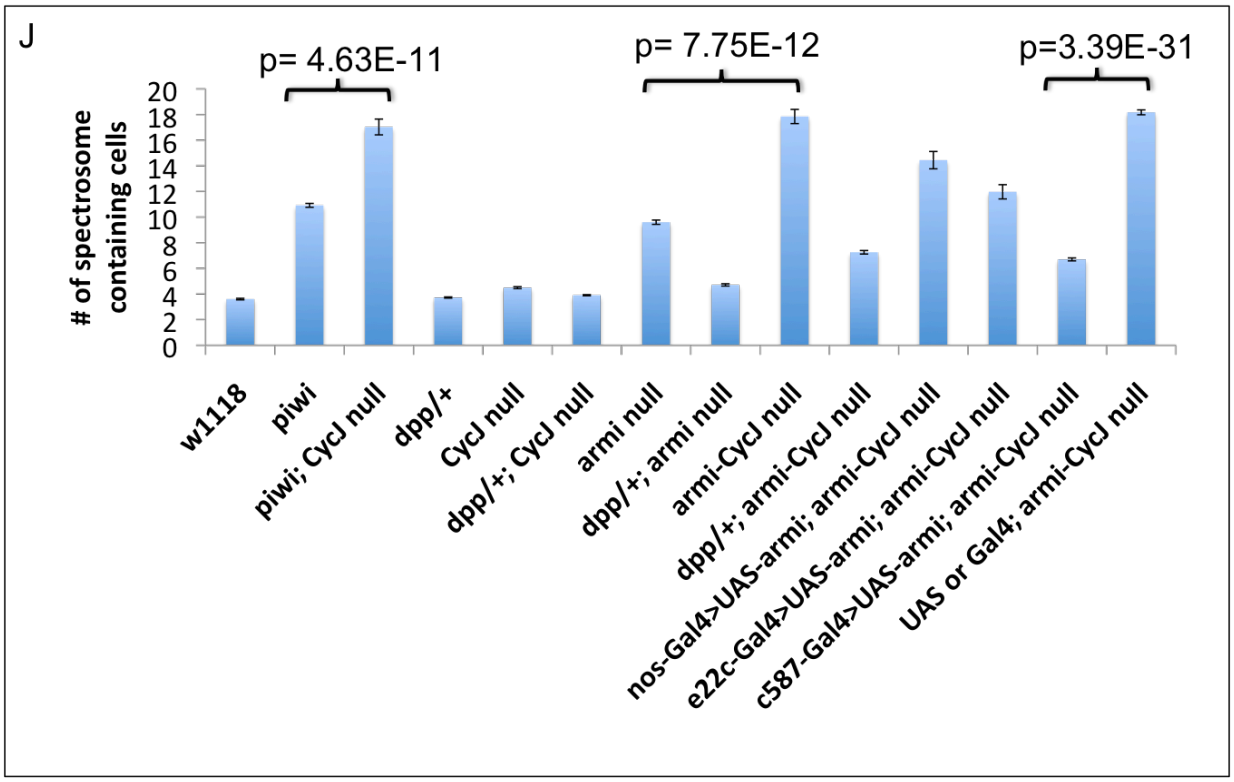

Figure 18: Somatic *armi* and *piwi* along with *CycJ* limit accumulation of GSC-like cells. Spectrin staining was used to visualize the round spectrosomes found in GSC and cystoblasts. (A) A diagram representing a normal germarium with anterior terminal filament cells at the top and a stage 1 egg chamber at the bottom. GSCs produce daughter cell that differentiate and become surrounded by follicle cells to form an egg chamber. A single spectrosome (red sphere) is normally found in the 2-3 GSCs (yellow cells) in the niche and in adjacent daughter cystoblasts (light green cells), resulting in 3-4 spectrosomes per germarium. Wild type represented by w1118 (B) and *CycJ* null (C) had normal numbers of spectrosomes. The piRNA pathway mutants of either *piwi* (D) or *armi* (F) had an increase in spectrosomes, while removal of *CycJ* from the *piwi* mutant (E) or the *armi* mutant (G) resulted further significant increases in the number of spectrosomes. Introduction of a loss of function *dpp[hr56]* (*dpp*) allele to the *armi* null (H) or *armi-CycJ* double mutant (I) resulted in a significant decrease of spectrosomes ($p \leq 1.24E^{-37}$). The mean number of spectrosomes per germarium from at least 66 germaria for each genotype is plotted in H. Error bars represent SEM. P-values were calculated using a type 3 student's T-test. Size bars in B-I = 20 μm.

(*dpp[hr56]*) and quantified spectrosomes per germarium (Figure 18). Introduction of the *dpp* allele to the *armi* null reduced the number of spectrosomes from 9.6±0.2 to 4.7±0.1 ($p=3.44^{-52}$) (Figure 18 F, H, J). Adding the *dpp* allele to *armi-CycJ* null also drastically reduced the number of spectrosomes from 17.8±0.6 to 7.3±0.1 ($p=2.12^{-17}$) (Figure 18 G, I, J). Thus reduction of Dpp reduces GSC-like cell accumulation in *armi* and *armi-CycJ* mutants. These data support the conclusion that *CycJ* and members of the somatic piRNA pathway cooperate to limit GSC-like cell accumulation.

The number of GSC-like cells correlates directly with the frequency of mispackaged egg chambers in the *armi*, *piwi* and *CycJ* double mutants (Figures 17, 18, and (Atikukke, Albosta et al. 2014)). To further examine the correlation between extra GSC-like cells and egg chamber mispackaging, I introduced the *dpp* mutant into single and double mutants and analyzed egg chamber packaging. I confirmed that *piwi* and *armi* mutants had a mild increase of mispackaged egg chambers, which was significantly more severe when *CycJ* was also removed (Figure 19). Combination of the *dpp* allele with the *armi* null resulted in a reduction of mispackaged egg chambers from 24.3%±3.4% to 6.8%±1.3% (p=0.0023). Addition of *dpp* to the *armi-CycJ* double null reduced the percent of mispackaged egg chambers from 49.8%±4.9% to 6.2%±1.4% ($p=5.90E^{-05}$). These data show that the egg chamber packaging defect observed in *armi* and *armi-CycJ* mutants also depends on BMP signaling. These results also suggest that mispackaged egg chambers results at least in part from excess GSC in the germarium.

3.3.3 Somatic *armi* and *piwi* limit GSC accumulation by limiting BMP signaling

A reduction in Dpp suppressed the excess GSC-like cells and mispackaged egg chambers in *armi* and *armi-CycJ* suggesting the possibility that these genes affect BMP

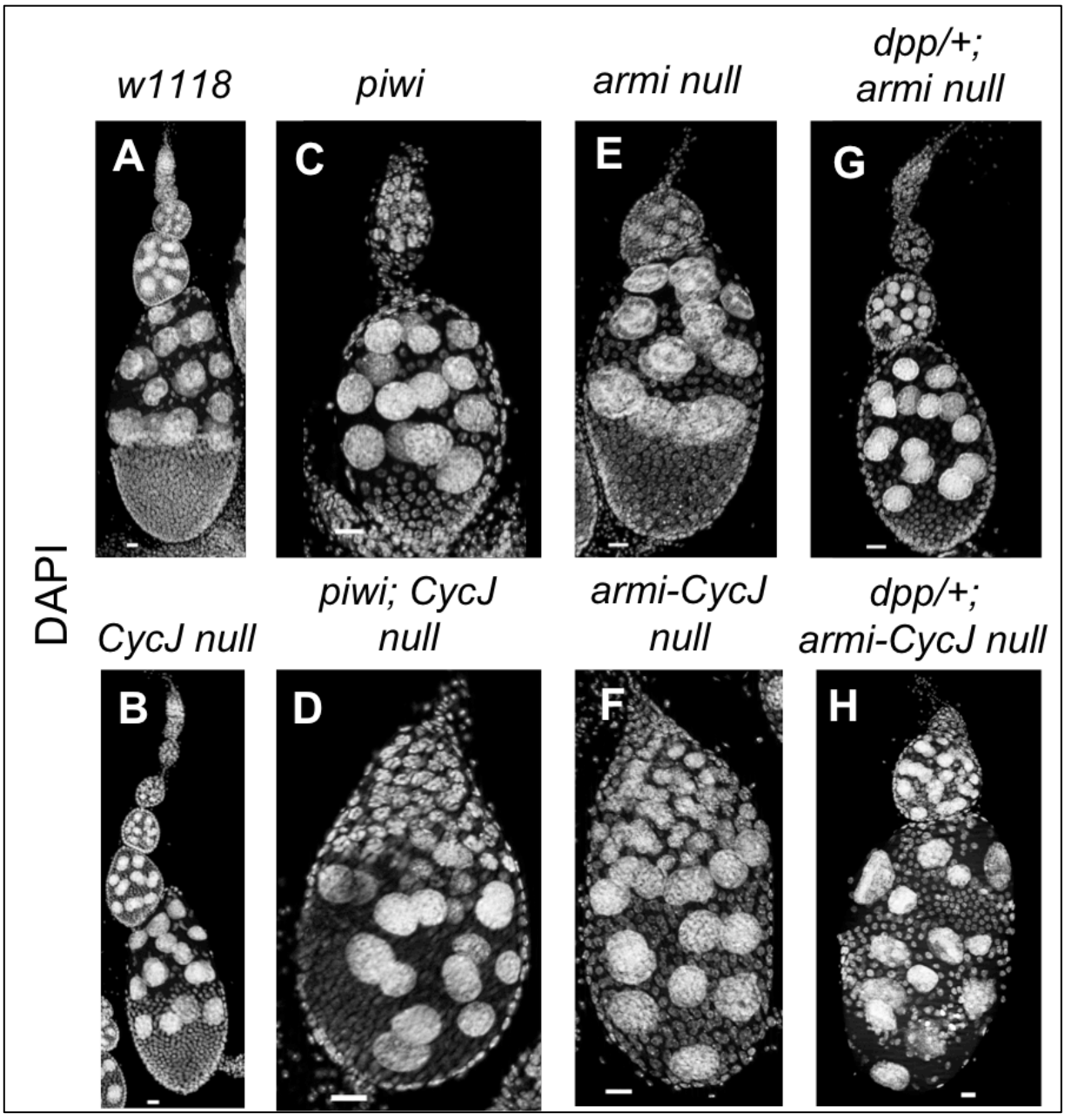

Figure 19: Somatic *armi* and *piwi* along with *CycJ* permit egg chamber packaging by limiting BMP signaling

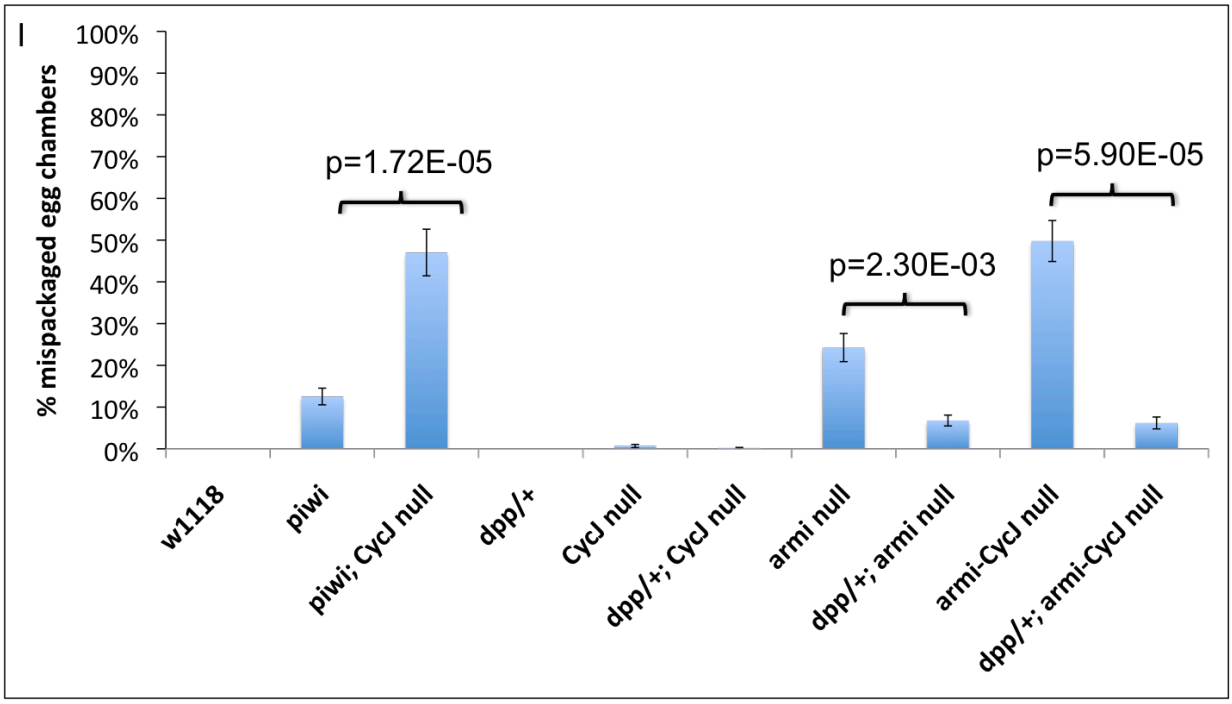

Figure 19: Somatic *armi* and *piwi* along with *CycJ* permit egg chamber packaging by limiting BMP signaling. Egg chamber packaging was assessed by DAPI staining nuclei and quantifying the percent of egg chambers with too many germline cells. Wild type (A) and *CycJ* null (B) had normal egg chamber packaging with very few, if any, mispackaged egg chambers. piRNA pathway mutants (C and E) had an increase of mispackaged egg chambers indicated graphically (I), though the images represent the most common ovarioles. *CycJ*-piRNA pathways double mutants (D and F) had a drastic increase of mispackaged egg chambers representing ~50% of all egg chambers per fly. Addition of a loss of function *dpp* allele to *armi* null (G) or *armi-CycJ* null (H) reduced the percent of mispackaged egg chambers compared to sibling *armi* and *armi-CycJ* null ($p \leq 0.0023$). Quantified data is represented graphically (I). The percent of mispackaged egg chambers per ovariole was calculated from at least 145 ovarioles for each genotype. Error bars represent SEM. P-values were calculated using a type 3 student's T-test. Size bars = 20 μm.

signaling. To investigate this, I stained for the activated transcription factor in the BMP signaling pathway, phosphorylated Mad (pMad), which is normally present in GSCs and absent from the differentiating cystoblasts (Figure 20). As shown in Figure 20, the number of pMad staining cells in germaria of wild type was 2.2±0.03, but was increased in mutants of *piwi* to 3.1±0.03 or *armi* to 3.1±0.02 and to a greater extent when *CycJ* was also removed to 4.5±0.1 ($p=6.18E^{-08}$) and 4.6±0.07 ($p=3.43E^{-10}$), respectively. The pMad activation indicates that at least some of the excess spectrosome-containing cells in these mutants are GSCs because they also contain activated BMP signaling. To confirm that BMP signaling was increased in the mutant germaria I stained for the differentiation factor Bam, which is normally repressed by BMP signaling in the GSCs, but expressed in differentiating cystoblasts (Song, Wong et al. 2004). I found that single and double mutants of the piRNA pathway and *CycJ* had a drastic reduction in the percent of Bam-expressing germaria (Figure 21). Taken together, these data show that BMP signaling is increased in *armi* and *piwi* mutants, and that removal of *CycJ* exacerbates this defect.

These results demonstrate that BMP signaling is increased in *CycJ*-piRNA pathway double mutants as well as *piwi* and *armi* single mutants, but they fail to show whether this is a somatic or germline function. Previous data show that somatic loss of *piwi* results in increased BMP signaling (Jin, Flynt et al. 2013; Ma, Wang et al. 2014). To examine a tissue-specific role for limiting BMP signaling, I expressed *UAS-armi* in somatic cells with either *e22c-Gal4* or *c587-Gal4* in *armi-CycJ* followed by pMad staining. Somatic expression of *armi* reduced pMad positive cells in *armi-CycJ* mutants, suggesting that somatic *armi* regulates BMP signaling (Figure 20 Q). Somatic

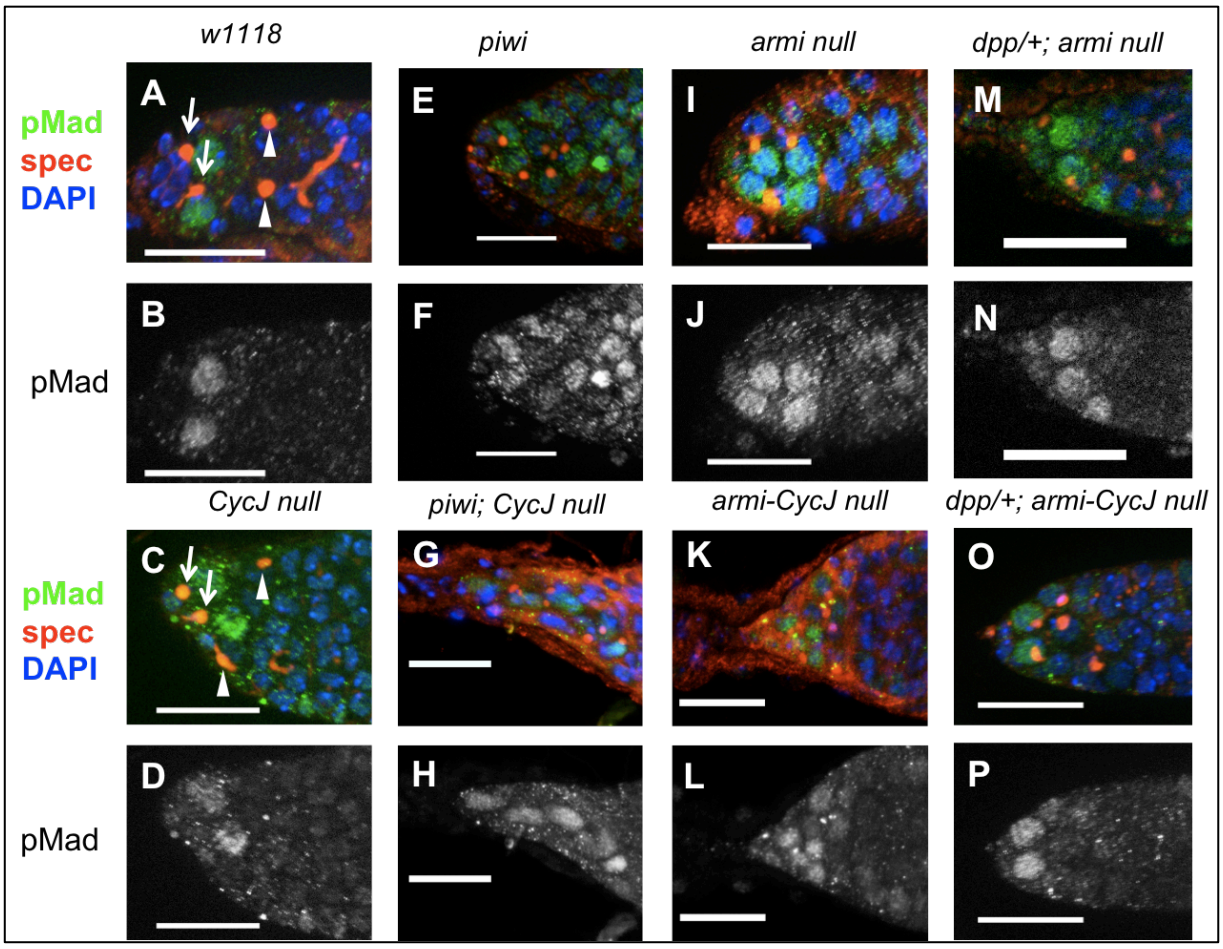

Figure 20: *CycJ* and the somatic piRNA pathway cooperate to limit BMP signaling

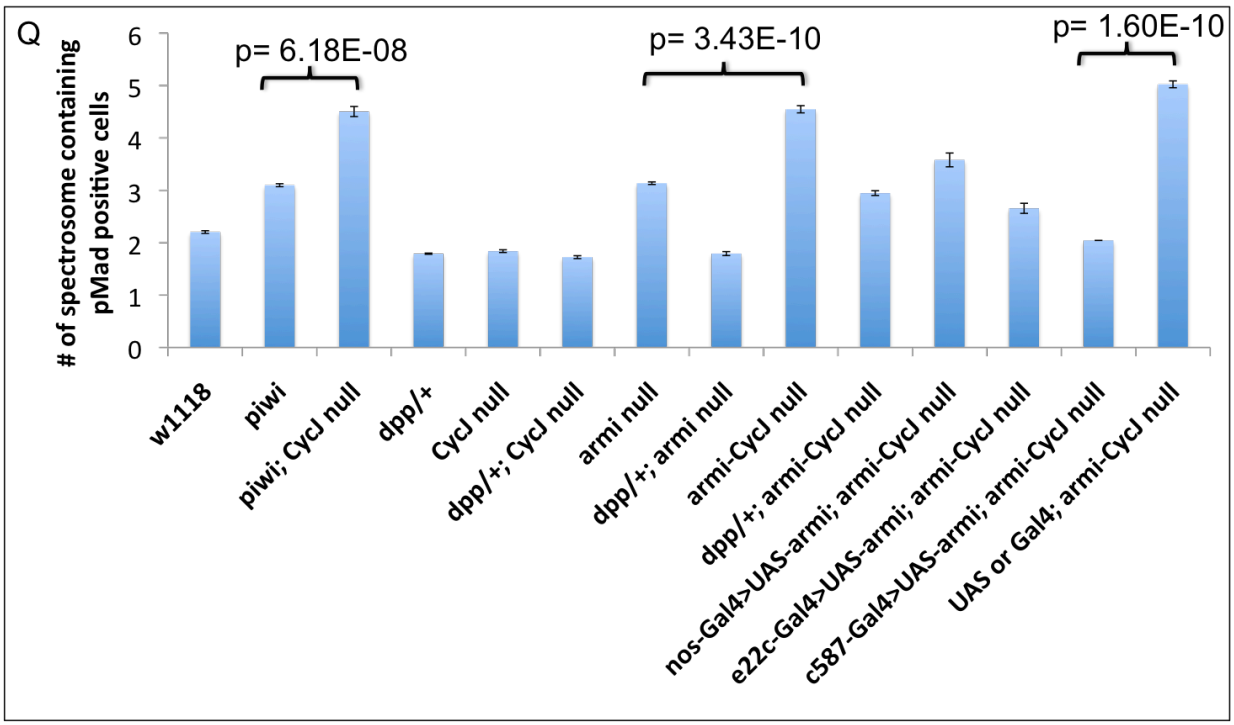

Figure 20: *CycJ* and the somatic piRNA pathway cooperate to limit BMP signaling. Germaria stained for pMad as an indicator of BMP activity, for spectrin to visualize spectrosomes, and DAPI. (Q) Quantification of the number of pMAD-positive, spectrosome-containing cells per germarium. Wild type (A, B) and *CycJ* null (C, D) germaria usually contain two pMad positive cells, each with a round spectrosome (arrow), indicating that they are GSCs. They also contain 1-2 pMAD-negative cells that have round spectrosomes (arrowhead); these are differentiating cystoblasts. Mutants of *piwi* (E, F) or *armi* (I, J) exhibited a significant increase in pMad positive cells with spectrosomes, indicating that the extra cells are GSCs. Double mutants of *CycJ* and either *piwi* (G, H) or *armi* (K, L) had more drastic increases in pMad positive cells with spectrosomes. Introduction of a single *dpp* allele to *armi* null (M, N) or *armi-CycJ* (O, P) significantly reduced the number of pMad positive cells ($p \leq 4.65E^{-05}$). Quantification of these and additional controls (Q) represents at least 47 germaria for each genotype. $p=3.43E^{-10}$ is comparing *armi* null to *armi-CycJ* null. Error bars represent SEM. P-values were calculated using a type 3 student's T-test. Size bars in A-P = 20 μm.

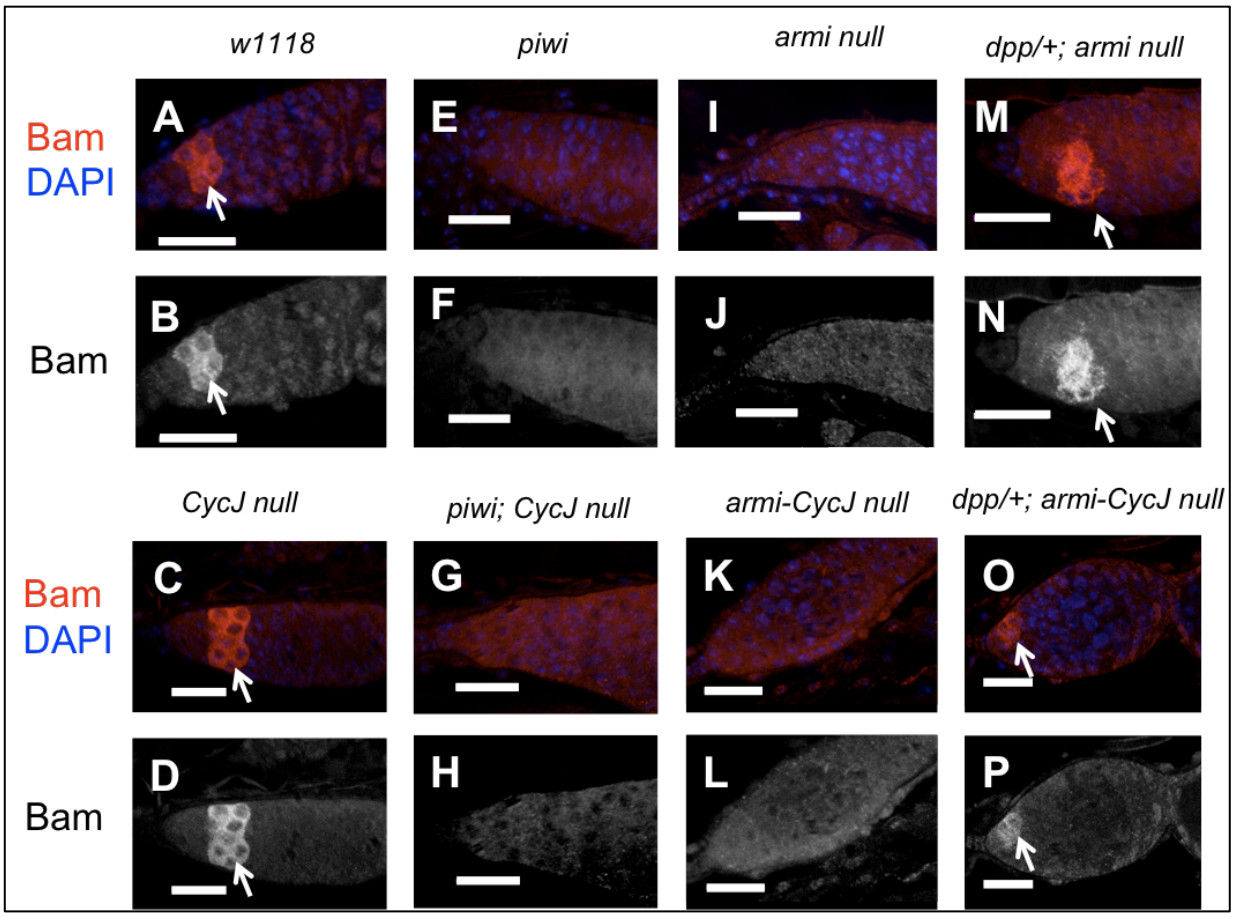

Figure 21: Bam expression is reduced in mutants of *piwi*, *armi*, *piwi-CycJ*, and *armi-CycJ*

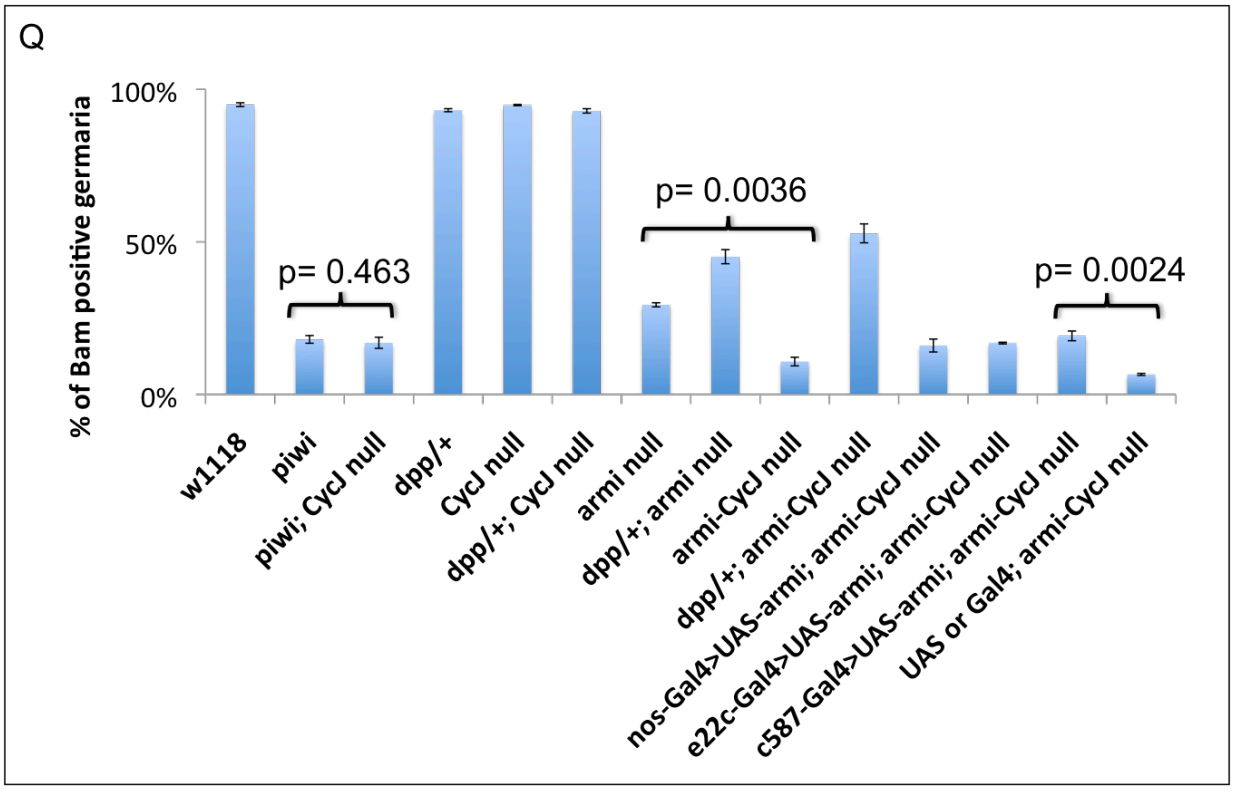

Figure 21: Bam expression is reduced in mutants of *piwi*, *armi*, *piwi-CycJ*, and *armi-CycJ*. Downstream effects of BMP signaling were analyzed by staining and quantifying germaria for Bam protein expression. Bam protein is identified with arrows and was expressed in a subset of germaria for all mutants and controls. Wild type (A & B), *dpp/+* (M & N), and *CycJ* null (C & D) had Bam expression in most germaria. Most germaria in CycJ-piRNA pathway single and double mutants (E-L) did not express Bam. Addition of a loss of function *dpp* allele to *armi* (M & N) and *armi-CycJ* null (O & P) was able to rescue Bam expression in most germaria ($p \leq 0.01$ for *dpp* rescue of both *armi* null and *armi-CycJ* null). Quantification of these and additional control genotypes is shown in (Q) from at least 65 germaria for each genotype. p=0.0036 is comparing *armi* null to *armi-CycJ* null. Error bars represent SEM. P-values were calculated using a type 3 student's T-test. Size bars in A-P = 20 μm.

expression of *UAS-armi* was also able to increase Bam expression in *armi-CycJ* (Figure 21 Q). Since egg chambers in the single and double mutants contain large nurse cell nuclei (Figure 19), it is expected that some of these GSCs eventually escape excess BMP signaling and differentiate. These data also suggest that CycJ and the somatic piRNA pathway cooperate to limit GSC accumulation by limiting BMP signaling.

One possible mechanism of increasing BMP signaling in the germarium is through expanding the canonical niche by increasing the number of cap cells, which have characteristic expression of *engrailed* (*en*) (Ward, Shcherbata et al. 2006). I examined cap cells by staining germaria of single and double mutants for *en*, but these cells did not appear to be increased (Figure 22). These data suggest that *CycJ* cooperates with somatic *armi* and *piwi* to limit BMP signaling in the early germarium by a mechanism other than expanding the canonical niche. However, I cannot exclude the possible expansion of other cells that can act as niche cells, like escort cells (Kirilly and Xie 2007).

BMP signaling in germline cells is triggered by Dpp production in adjacent somatic niche cells (Xie and Spradling 1998; Song, Wong et al. 2004). Based on this and my previous results, I attempted to reduce BMP signaling in *CycJ*-piRNA pathway single and double mutants by introducing the *dpp* allele, which significantly reduced the number of pMad positive cells (Figure 20 M-Q). Reducing BMP signaling with a *dpp* allele also rescued Bam expression in *armi* and *armi-CycJ* mutants, indicating that the reduced Bam expression in these mutants is due to the increased BMP signaling (Figure 21 M-Q). These results support the conclusion that the somatic function of *armi* and *piwi* are required to limit BMP signaling and GSC accumulation.

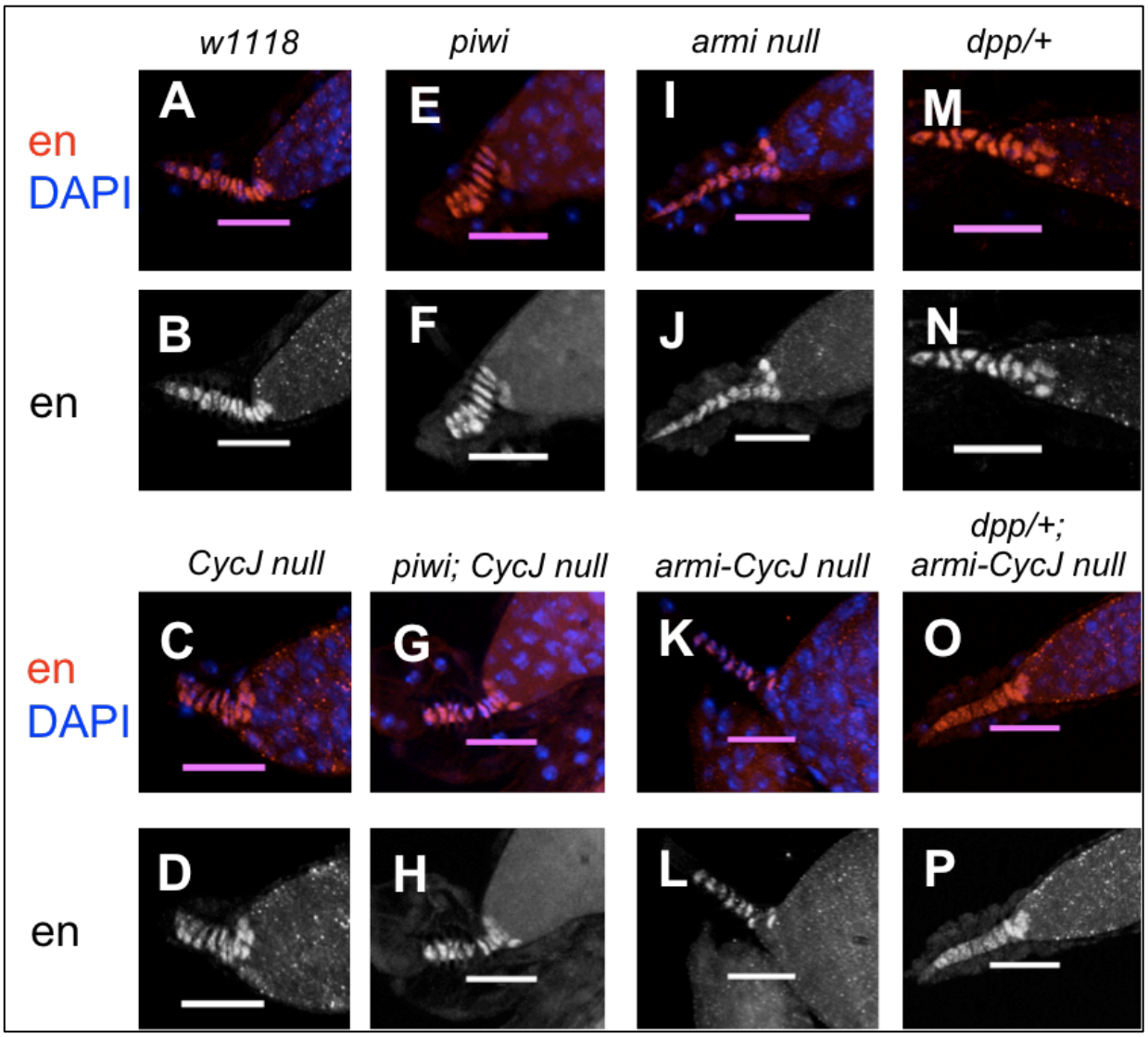

Figure 22: Engrailed expression in terminal filament and cap cells is not altered by *CycJ, armi, piwi,* or the *dpp* allele. Engrailed (en) protein expression is characteristic of the canonical GSC niche terminal filament and cap cells and can indirectly drive expression of *dpp*. To examine if the GSC niche was expanded in double mutants, germaria were stained for en. It does not appear that en expression is expanded in any single or double mutants (A-P). Size bars = 20 μm.

3.3.4 *CycJ* promotes follicle cell proliferation by limiting BMP signaling in the absence of *armi*

Egg chamber packaging also requires proper proliferation of the follicle cells that will surround each developing cyst. It has been shown that mutations of *hedgehog* result in decreased follicle cell proliferation and production of mispackaged egg chambers similar to those produced by *CycJ*-piRNA pathway mutants (Forbes, Lin et al. 1996). To test whether *armi* and *armi-CycJ* double mutants have decreased somatic cell proliferation, I stained ovaries of one-day-old flies for the mitotic marker phospo-Histone H3 (pH3) and quantified the number of mitotic cells per ovariole (Figure 23). I observed that the *armi* null had a decreased number of pH3 positive cells and further removal of *CycJ* reduced the number of pH3 positive cells from 12.8±0.9 to 6.3±0.3 ($p=8.20E^{-9}$). Thus, follicle cell proliferation is decreased in *armi* and *armi-CycJ* mutants, which may contribute to the mispackaging of too many germline cells into individual egg chambers. To my surprise, somatic expression of *armi* was not able to rescue follicle cell proliferation, whereas germline expression resulted in a minor increase of pH3 positive cells (Figure 24). Furthermore, a *dpp* mutant rescued follicle cell proliferation in *armi-CycJ* mutants, but not *armi* null. On the other hand, somatic expression of *CycJ* was able to increase the number of pH3 positive cells in *armi-CycJ* null. These data demonstrate that *armi* promotes somatic cell proliferation, possibly from the germline and independent of BMP signaling. They also suggest that somatic expression of *CycJ* can promote somatic cell proliferation in the absence of *armi*. It has been shown that BMP signaling promotes follicle stem cell self-renewal and proliferation, but not proliferation of later stage follicle cells surrounding fully formed egg chambers

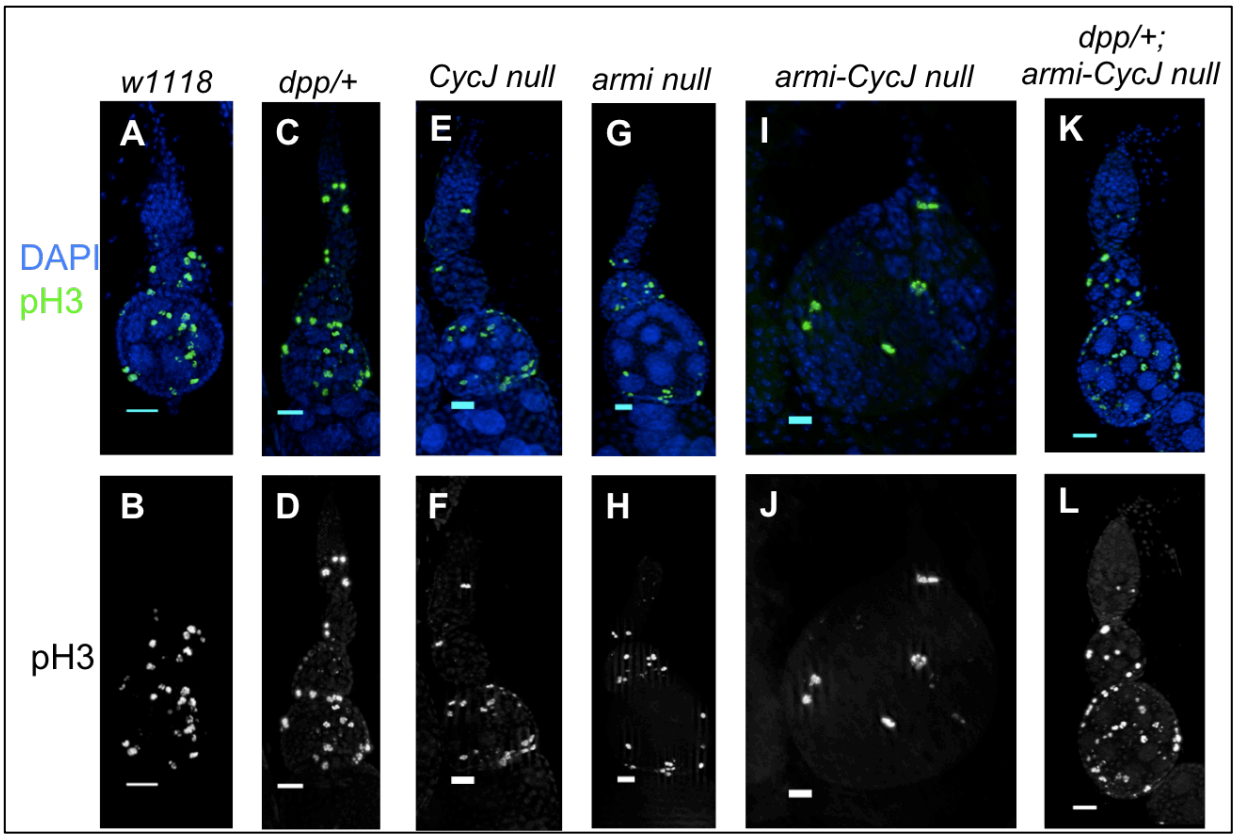

Figure 23: *CycJ* promotes proliferation of follicle cells in ovarioles by limiting BMP signaling in the absence of *armi*

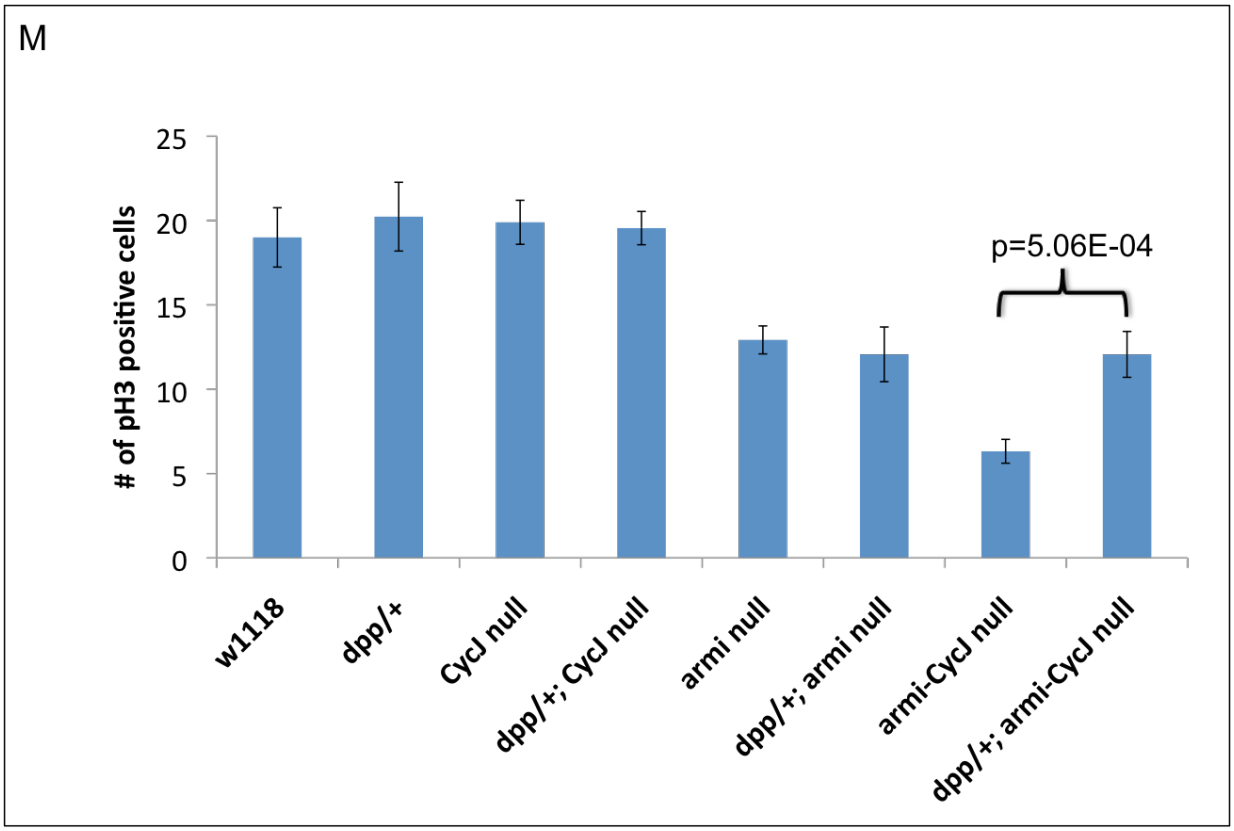

Figure 23: *CycJ* promotes proliferation of follicle cells in ovarioles by limiting BMP signaling in the absence of *armi*. The number of mitotic somatic cells in *CycJ-armi* double and single mutants was analyzed by staining for phospho-Histone H3 (pH3) and quantifying the average number of positively stained cells per ovariole. Wild type (A and B), *dpp*/+ (C and D), and *CycJ* null (E and F) had had about 20 pH3 positive cells per ovariole respectively. *armi* null (G and H) exhibited a decreased number of pH3 positive cells, which was further decreased when *CycJ* was also removed (I and J). Introduction of a loss of function *dpp* allele to *armi-CycJ* null (K and L) was able to increase the number of pH3 positive cells ($p=5.06E^{-04}$), but had no effect in *armi* null. Quantification of these and additional control genotypes is shown in (M) from at least 59 ovarioles for each genotype. Error bars represent SEM. P-values were calculated using a type 3 student's T-test. Size bars in A-L = 20 μm.

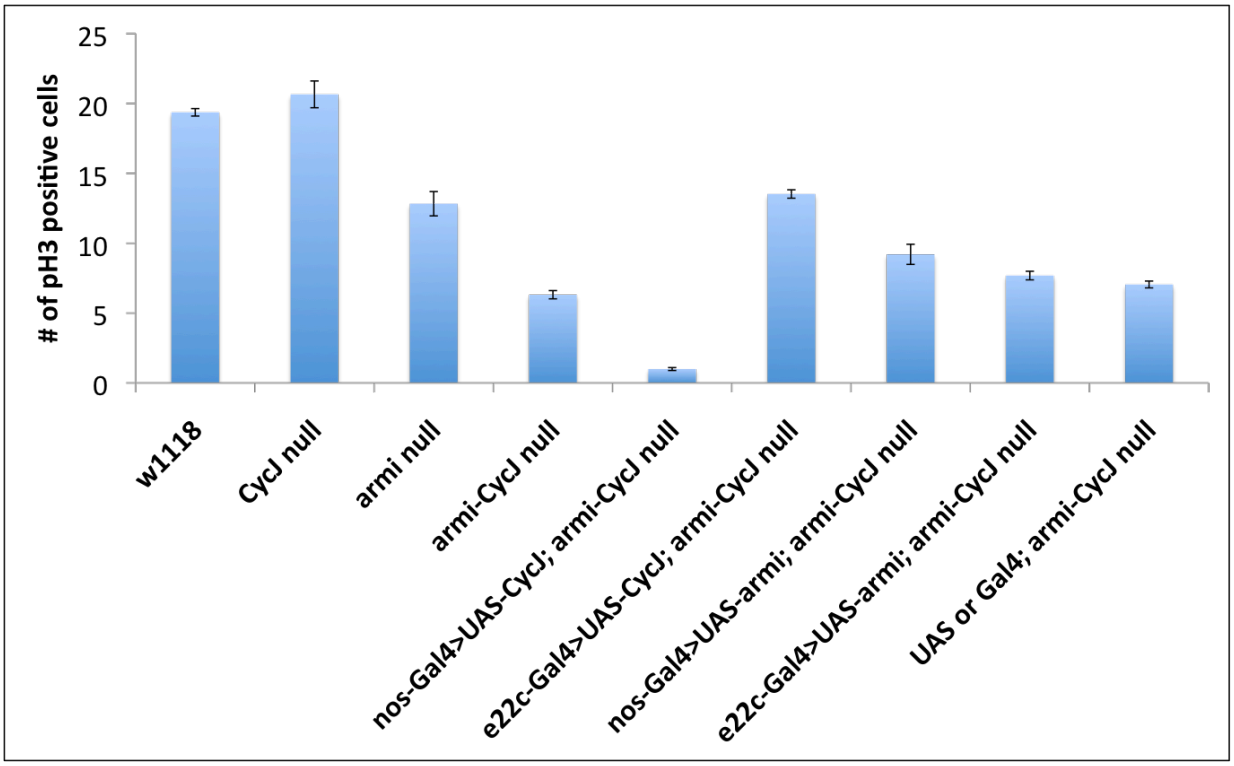

Figure 24: Somatic expression of *CycJ* increases follicle cell proliferation in the absence of *armi*. Mitotic somatic cells per ovariole in *CycJ-armi* expressing tissue-specific *UAS-CycJ* or *UAS-armi* were analyzed by staining for phospho-Histone H3 (pH3) and quantified. Wild type, *CycJ* null, *armi* null, and *armi-CycJ* double null were previously quantified and are shown for reference. Somatic expression was driven by *e22c-Gal4* and germline expression by *VP16::nos-Gal4.* Somatic expression of *UAS-CycJ* was the condition able to increase the number of pH3 positive cells to 12.6±0.6 compared to sibling controls with either *UAS* or *Gal4*, but not both, in *armi-CycJ* at 7.0±0.7.

(Kirilly, Spana et al. 2005). Thus, it remains unclear and unlikely that BMP signaling is affecting somatic cells directly, but may regulate them indirectly through disrupted germline-soma communication due to the excess of GSCs. It is also possible that *CycJ* and the piRNA pathway are regulating other signals, like Hedgehog, that directly regulate follicle cell proliferation. Further analyses of these possibilities are required.

3.4 Discussion and Summary

CycJ was previously shown to promote egg chamber packaging and maturation in the absence of the piRNA pathway, though the mechanism was poorly understood (Atikukke, Albosta et al. 2014). One key observation is that *CycJ*-piRNA pathway double mutants produce mispackaged egg chambers with too many germline cells. Here, I interrogated the identity of these cells by staining for spectrosomes and pMad, which are characteristic of GSCs. I found that there is an accumulation of GSCs that contain spectrosomes and pMad in the piRNA pathway mutants *piwi* and *armi,* which was exacerbated when *CycJ* was also removed. Furthermore, a loss of function *dpp* allele was able to rescue this accumulation, indicating that BMP signaling is responsible. Other piRNA pathway mutants produce a similar accumulation of GSCs. Mutants of *fs(1)Yb, piwi,* and *vreteno* all exhibit excess GSCs (Swan, Hijal et al. 2001; Zamparini, Davis et al. 2011; Jin, Flynt et al. 2013; Ma, Wang et al. 2014). Furthermore, *piwi* mutants have a concomitant increase of BMP signaling (Ma, Wang et al. 2014). I find this to be the case for the *piwi* mutant used in this study, as well as the *armi* null, which had not been described previously. The finding that *armi* also regulates BMP signaling from somatic cells is consistent with a model where it functions together with Piwi, Yb, and Vret in the somatic piRNA pathway.

A pressing question that comes out of these findings is how do *CycJ* and the piRNA pathway limit BMP signaling? Regulation can occur either by directly moderating production of morphogens, influencing extracellular diffusion of morphogens, participation in the BMP signaling pathway in GSCs, or through regulation of other pathways that effect BMP signaling. Previous studies demonstrate that *dpp* transcript levels increase 10 fold in escort cells after *piwi* knockdown, indicating that *piwi* is regulating production of the morphogen *dpp* (Ma, Wang et al. 2014). Since *piwi* and *armi* appear to be functionally similar in my hands, it is attractive to speculate that *armi* may also regulate *dpp* production, but this remains to be tested. It is more difficult to speculate about *CycJ.* One scenario includes overproduction of Dpp in piRNA pathway mutants followed by increased diffusion when *CycJ* is removed. In other words, *CycJ* may be responding to increased Dpp and acting to limit its diffusion, but there is no evidence to support this claim. Future work is required to determine how *CycJ* and the piRNA pathway regulate BMP signaling.

I also demonstrate that *CycJ* and the piRNA pathway regulate egg chamber packaging and mitotic follicle cell number by limiting BMP signaling. My analyses of these phenotypes fail to address whether BMP signaling is directly or indirectly responsible. *CycJ*-piRNA pathway double mutants generally contain one mispackaged egg chamber with an overabundance of undifferentiated GSCs and a terminal filament, indicating that packaging has completely failed and the germarium has become the only egg chamber. A key aspect of proper packaging is that a differentiated cyst signals to somatic stem cells in the middle of the germarium followed by production of follicle cells that migrate across the germarium and participation in encapsulation of the cyst (Nystul

and Spradling 2010). A possible explanation for these mispackaged egg chambers is that accumulation of GSCs in the germarium displaces differentiated cysts and disrupts the normal signaling between cysts and somatic stems cells. Without the proper signals, the somatic stem cells might not produce cells that migrate across the germarium and encapsulate cysts. This model would explain both mispackaging and a decrease of mitotic somatic cells in ovarioles. Since the *dpp* allele rescues both egg chamber packaging and mitotic somatic cells, it is also possible that BMP signaling is directly affecting the proliferation of somatic stem cells and follicle cells.

In conclusion, I have demonstrated that *CycJ* limits BMP signaling in the absence of the somatic piRNA pathway. It appears that *CycJ* is enhancing a function of the somatic piRNA pathway that limits BMP signaling and regulates multiple aspects of oogenesis including GSCs, egg chamber packaging, and mitotic follicle cell number. My data show that expressing *UAS-armi* in ovarian somatic cells promotes egg chamber packaging in *armi-CycJ* null, suggesting that it is the somatic function of the piRNA pathway that is regulating these aspects of oogenesis. Taken together, these data suggest that CycJ cooperates with the somatic piRNA pathway to limit BMP signaling, limit GSC accumulation, promote egg chamber packaging, and promote mitotic follicle cell number. These results show that GSCs are increased in somatic piRNA pathway mutants and CycJ is required when these cells accumulate, suggesting that CycJ may be acting as conserved stem cell regulator.

CHAPTER 4: CONCLUSIONS AND FUTURE DIRECTIONS

4.1 Conclusions

Multiple studies, including this one, demonstrate that *CycJ* is dispensable for oogenesis under normal conditions (Althoff, Viktorinova et al. 2009; Atikukke 2009; Atikukke, Albosta et al. 2014). However, *CycJ* is required for egg chamber packaging and maturation in the absence of the piRNA pathways represented by *piwi, armi,* and *aub*. Qualitative and quantitative differences in the genetic interactions suggest that *CycJ* interacts more strongly with piRNA pathway members that function in both the germline and somatic cells (*piwi* and *armi)* compared to those that function in the germline only (*aub*). I went on to demonstrate that it is the somatic function of *piwi* and *armi* with which *CycJ* genetically interacts to regulate egg chamber packaging. These data demonstrate that *CycJ* cooperates with somatic *piwi* and *armi* to limit BMP signalling, limit GSC accumulation, promote egg chamber packaging, and promote follicle cell proliferation.

4.1.1 *CycJ* genetically interacts with the piRNA pathways to regulate egg chamber packaging and maturation

The purpose of oogenesis in *Drosophila* is to produce an egg chamber and facilitate its maturation to a normal stage 14 oocyte, and the piRNA pathways are able to regulate both of these processes (Table 2). Egg chamber production (packaging) seems to be regulated by a function of the piRNA pathway in somatic cells (Figure 17), whereas maturation to a normal stage 14 oocyte is regulated by the ability of the piRNA pathway to promote axis specification in germline cells (Table 1). Previous data show that mutations of either *Yb* and *Vret,* which both function in the soma, produce egg

chambers with an excess of differentiated germline cells, whereas mutation of germline specific piRNA pathway members like *aub* do not (King, Szakmary et al. 2001; Swan, Hijal et al. 2001; Althoff, Viktorinova et al. 2009; Atikukke 2009; Zamparini, Davis et al. 2011; Atikukke, Albosta et al. 2014; Ma, Wang et al. 2014). On the other hand, axis specification appears to be a germline function of piRNA pathways (Cook, Koppetsch et al. 2004; Klattenhoff, Bratu et al. 2007). My data support these differing roles for piRNA pathway members by showing that mutations of *armi* and *piwi* have more severe egg chamber packaging defects compared to *aub*, whereas all three have oocyte maturation defects including axis misspecification and/or reduced stage 14 oocyte production (Tables 1, 2). Furthermore, ovaries from *armi[72.1]* mutants (which primarily affects germline Armi (Olivieri, Sykora et al. 2010)) had much less severe egg chamber packaging defects compared to the *armi* null, supporting the conclusion that egg chamber packaging is regulated by the somatic function of piRNA pathway members (Figure 17). This is the first study to characterize and quantify mispackaged egg chambers in either *armi* or *piwi* mutants. My data show that *armi* and *piwi* regulate egg chamber packaging and maturation, whereas *aub* has a much more definitive role regulating maturation.

My data also show that *CycJ* is interacting with both of these piRNA pathway functions, but the mechanisms remain poorly understood. It is possible that CycJ regulates egg chamber maturation by a mechanism related to axis misspecification in piRNA pathway mutants, which is associated with DNA damage accumulation (Cook, Koppetsch et al. 2004; Klattenhoff, Bratu et al. 2007). In other words, CycJ might be responding to DNA damage in piRNA pathway mutants. The activity of some cyclins

are inhibited under DNA damage conditions, and it is attractive to speculate that CycJ is under similar regulation when the piRNA pathways are inhibited and DNA damage checkpoints are activated. Typically, DNA damage response and checkpoints act to arrest the cell cycle (Wang and Kalderon 2009). It appears that CycJ is acting opposite to characterized checkpoints in that it is promoting egg chamber maturation during piRNA pathway inhibition. CycJ also regulates egg chamber packaging in the absence of the somatic function, but not germline function, of the piRNA pathway as discussed in the following sections.

4.1.2 *CycJ* and the somatic piRNA pathway cooperate to limit GSC accumulation

One feature of mispackaged egg chambers in *CycJ*-piRNA pathway double mutants was an anterior population of small germline cells located where GSCs normally reside. Upon investigation, I found that these cells were excess GSCs in *piwi* or *armi* single mutants and mutation of *CycJ* further increased the quantity of these cells, and this was rescued with somatic expression of *armi*. Recently multiple piRNA pathway mutants and/or somatic knockdowns including *piwi, vret,* and *Yb* were shown to accumulate GSCs, which supports our finding with *piwi* (Swan, Hijal et al. 2001; Zamparini, Davis et al. 2011; Jin, Flynt et al. 2013; Ma, Wang et al. 2014). My data also demonstrate for the first time that somatic Armi is also acting to limit accumulation of GSCs. Together, these data support a function for the piRNA pathway in somatic cells limiting GSC accumulation.

GSC accumulation in *piwi* or *armi* mutants leads to a requirement for CycJ, which is acting to limit these GSCs. One interpretation of these data is that CycJ is responding to GSC accumulation. This requirement for CycJ is supported by data

showing that *CycJ* expression is increased in ovaries from *Bam* mutant or *dpp* over-expression flies that result in germaria filled with GSC (Kai, Williams et al. 2005). More strikingly, *CycJ* expression is induced in fly testes (where it is not normally detected) of *bgcn* mutant or *bgcn* mutant over-expressing the Jak/STAT ligand *Os* that result in excess GSC production and differentiation inhibition (Terry, Tulina et al. 2006). Together, these data suggest that *CycJ* is expressed in stem cell populations. Furthermore, my data indicate that CycJ may be acting to limit further expansion of stem cells when they are in excess. This is particularly fascinating considering that in humans, *CCNJ* is also up-regulated in induced pluripotent stem cells and embryonic stem cells (Ohi, Qin et al. 2011). Together, these data suggest that CycJ may be a conserved stem cell regulator.

4.1.3 The somatic piRNA pathway cooperates with *CycJ* to permit egg chamber packaging by limiting BMP signaling

My data show that *CycJ* cooperates with the somatic piRNA pathway to limit BMP signaling. BMP signaling is increased in piRNA pathway single mutants and mutation of *CycJ* enhances this defect. This phenotype could be suppressed with a loss of function *dpp* allele or by somatic expression of *armi*, suggesting that the somatic function of Armi is acting to limit BMP signaling. Recent data show that mutation and somatic knockdown of *piwi* results in a 10-fold increase of *dpp* transcript levels (Jin, Flynt et al. 2013). My data also show that increased BMP signaling results in GSC accumulation in mutants of *piwi*, *armi*, *piwi-CycJ*, or *armi-CycJ* (Figures 18, 20). These data support a role for somatic Piwi limiting *dpp* production, and suggest that somatic

Armi has a similar role limiting *dpp* and that *CycJ* is also regulating BMP signaling, though the mechanism remains elusive and requires further investigation.

Increased BMP signaling in single and double mutants also correlates with mispackaged egg chambers. This can be interpreted in a few ways. First, BMP signaling may be directly responsible for the process of egg chamber packaging, i.e., surrounding of germline cysts with follicle cells. There are data showing that increased BMP signaling facilitated by over-expression of *dpp* results in mispackaged egg chambers similar to those in my study. (Muzzopappa and Wappner 2005). A causal relationship between BMP signaling and egg chamber packaging, however, has not been demonstrated. Typically, egg chamber packaging is thought to be facilitated by Notch signaling (Nystul and Spradling 2010). It is possible that BMP signaling is affecting Notch signaling to regulate egg chamber packaging. Previously, BMP signaling has been shown to both promote and inhibit Notch signaling in a context-dependent manner (Miyazono, Maeda et al. 2005). However, the relationship between BMP signaling and Notch signaling remains unclear. Finally, it is possible that the increase of GSCs that results from increased BMP signaling is disrupting the normal cell-cell signaling that must take place between differentiated germline cysts and somatic stem cells that facilitate egg chamber packaging. I favor this explanation since GSCs in single and double mutants appear to displace cysts in the germarium and it is likely that GSCs can not send the same signals as cysts. This would explain how egg chamber mispackaging is a consequence of excess GSCs. This would also support the primary role of CycJ as a stem cell regulator, but these hypotheses require further analysis.

4.1.4 The somatic piRNA pathway and *CycJ* regulate oogenesis from ovarian somatic cells and promote proliferation of follicle cells

My data indicate that somatic expression of either *CycJ* or *armi* in *armi-CycJ* null can promote egg chamber packaging, suggesting that these genes may regulate this process from within these cells (Figures 13, 18). It has been shown that mutation of genes like *hedgehog* that regulate proliferation of follicle stem cells and follicle cells actively involved in cyst encapsulation results in loss of egg chamber packaging, producing mispackaged egg chambers similar to those in my study (Forbes, Lin et al. 1996). I found that *armi* mutants had reduced follicle cell proliferation and this defect was enhanced when *CycJ* was also mutated, suggesting that these genes are cooperating to promote follicle cell proliferation. Interestingly, somatic expression of *CycJ*, but not *armi*, was able to rescue follicle cell proliferation (Figure 24). Most of the pH3 positive follicle cells were surrounding egg chambers that were distinct from germaria, so these follicle cells would be expected to contribute to egg chamber maturation rather than to packaging. Moreover, while Hedgehog is known to promote the proliferation of follicle cells involved in packaging, it does not affect the follicle cells that I examined around maturing egg chambers (Forbes, Lin et al. 1996). Therefore, the regulation of these follicle cells may be independent of egg chamber packaging and might indicate yet another function of *armi* and *CycJ*, though further analyses are required.

4.1.5 A working model for the role of CycJ during oogenesis

All of the data thus far indicate that CycJ may be acting as a conserved stem cell regulator (Figure 25). We have demonstrated that *CycJ* is only required for oogenesis

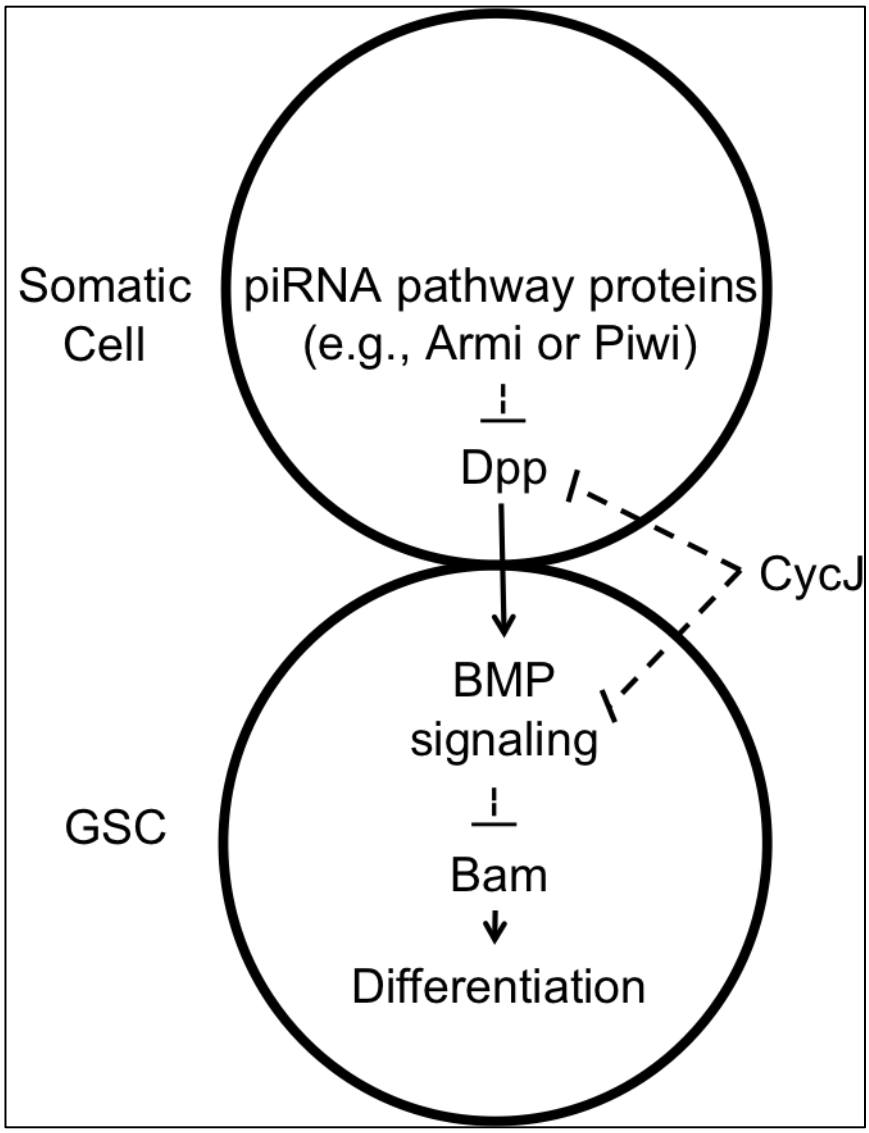

Figure 25: Model – CycJ cooperates with the somatic piRNA pathway to limit GSC accumulation. Germline stem cells (GSCs) are normally maintained as stem cells by production and secretion of Dpp from adjacent ovarian somatic cells. Dpp activates BMP signaling in the GSCs thereby inhibiting their differentiation. One of the functions of piRNA pathway proteins in ovarian somatic cells is to limit production of Dpp. When the piRNA pathway members are mutated, Dpp production is increased and GSC differentiation is inhibited resulting in excess GSCs. It appears that CycJ is limiting these excess GSCs by limiting Dpp, BMP signaling, and/or GSC proliferation. It remains unclear from which cell type CycJ is functioning.

when the piRNA pathways are inhibited. Under this condition, loss of *CycJ* enhances BMP signaling, accumulation of GSCs, egg chamber mispackaging, and decreased follicle cell proliferation. The fact that reducing *dpp* rescues all of these defects suggests that regulation of Dpp is the primary function of at least the somatic piRNA pathway and possibly CycJ during oogenesis. Previous data show that Piwi limits *dpp* in somatic cells, and our data support this conclusion as well as suggest that Armi is involved in the same process (Jin, Flynt et al. 2013; Ma, Wang et al. 2014). It is possibe that CycJ acts to attenuate the consequences of BMP signaling in GSCs by limiting GSC proliferation. This role for CycJ is supported by protein expression data that demonstrates a germline-specific pattern for CycJ-GFP fusions, but the precise expression pattern of CycJ normally as well as in the absence of the piRNA pathways remains to be determined (Althoff, Viktorinova et al. 2009). CycJ might actually be responding to the Dpp/BMP signaling that is increased by defects in the somatic piRNA pathway mutants. This model suggests that CycJ may be acting as a conserved stem cell regulator by acting in conjunction with the BMP signaling pathway. This is an attractive model since *CycJ* is up-regulated in some stem cell populations, as well as when stem cells are induced, a feature which is conserved from *Drosophila* to humans (Kai, Williams et al. 2005; Terry, Tulina et al. 2006; Ohi, Qin et al. 2011). How and from where CycJ is regulating BMP signaling and GSCs remains to be determined.

4.2 Future Directions

4.2.1 Under what condition is CycJ required for oogenesis?

All of our data show that CycJ is only required in the absence of the piRNA pathways, which suggests that piRNA pathway inhibition is creating some condition

under which CycJ is required for oogenesis. Inhibition of the piRNA pathways leads to many defects, including male and female sterility, transposon derepression, target gene derepression, DNA damage accumulation, GSC dysregulation, increased BMP signaling, egg chamber mispackaging, decrease of heterochromatin production, and defective axis specification (Cox, Chao et al. 1998; Vagin, Sigova et al. 2006; Klattenhoff, Bratu et al. 2007; Yin and Lin 2007; Klattenhoff and Theurkauf 2008; Atikukke 2009; Malone, Brennecke et al. 2009; Zamore 2010; Rangan, Malone et al. 2011; Jin, Flynt et al. 2013; Atikukke, Albosta et al. 2014). It is possible that one of these consequences of piRNA pathway inhibition is creating a requirement for CycJ. To address this possibility, these conditions would need to be examined independent of piRNA pathway inhibition in the absence of *CycJ*.

First, CycJ could be responding to increased transposon activity. To examine this possibility, transposons could be derepressed without mutating a piRNA pathway member in a *CycJ* null. This is possible with a fly strain mutant for the *flamenco* (*flam*) locus, which is a piRNA producing locus. *flam* mutants have characteristic derepression of transposons as well as sterility and oogenesis defects similar to our *armi* and *piwi* mutants (Pelisson, Song et al. 1994; Mevel-Ninio, Pelisson et al. 2007). If double mutants of *CycJ* and *flam* resulted in mispackaged egg chambers similar to those in *armi-CycJ* or *piwi-CycJ*, this would suggest that transposon derepression is a major contributing factor of these genetic interactions and may be the condition to which CycJ is responding. Alternatively, if there was no interaction between *CycJ* and *flam*, it would suggest that CycJ is not responding to transposon upregulation or DNA damage associated with transposon up-regulation.

CycJ could also be responding to increased DNA damage in piRNA pathway mutants. To examine this hypothesis, DNA damage could be induced in wild type and *CycJ* null flies independent of the piRNA pathway or transposon derepression. There are many methods for inducing DNA damage in flies, including feeding flies the mutagen MMS, or exposure to gamma radiation (Vogel and Natarajan 1979; Mittler 1982). If more severe mispackaged egg chambers were produced in *CycJ* null treated with one of these DNA damaging agents compared to treated wild type, it would suggest that DNA damage is the condition to which CycJ is responding. Alternatively, egg chamber packaging could be unaffected, suggesting that CycJ is not responding to DNA damage. One pitfall is that DNA damage would be induced in the entire organism, which could dysregulate other processes required for oogenesis, e.g., insulin signaling (Hsu, LaFever et al. 2008).

Finally, CycJ may be responding to increased BMP signaling in somatic piRNA pathway mutants. There are data to support that this may be the case since *CycJ* expression is increased in ovaries over-expressing *dpp*, suggesting that CycJ is playing some role in these ovaries (Kai, Williams et al. 2005). To examine this possibility, BMP signaling could be increased in *CycJ* null. This can be accomplished with over-expression of BMP signaling pathway components, like Dpp, or over-expression of factors that increase BMP signaling, like Dally. Production of mispackaged egg chambers with these conditions in *CycJ* null would suggest that CycJ is responding to increased BMP signaling, whereas if mispackaging was unaffected it would suggest that CycJ is not responding to increased BMP signaling. These over-expression condtions are known to produce germaria filled with GSCs, which may already be

devoid of developing egg chambers (Xie and Spradling 1998; Guo and Wang 2009). It is possible that mutation of *CycJ* under these conditions would result in expansion of GSC populations without a noticeable effect on packaging, since there may not be packaging in over-expression conditions alone. This would still suggest that CycJ is responding to increased BMP signaling. A pitfall for this approach is that *dally* has been shown to limit diffusion of Dpp, and increased diffusion may not be sufficient for a CycJ response.

4.2.2 How do CycJ and the somatic piRNA pathway regulate BMP signaling?

Previous studies show that *piwi* regulates BMP signaling by limiting *dpp* production in escort cells, which are somatic cells that surround developing cysts and can act as a local differentiation niche (Kirilly, Wang et al. 2011). This experiment was done by isolating enhancer trap-labelled escort cells with FACS (Jin, Flynt et al. 2013). It has been determined in these studies that escort cells are regulated by the somatic piRNA pathway and are acting as a noncanonical niche that can promote GSC accumulation. I have speculated that *armi* may also directly regulate *dpp* production, but do not have any evidence to support this claim. To address this possibility, escort cells could be isolated with FACS in *armi* null followed by qRT-PCR to examine *dpp* transcript levels. These results would be compared to wild type escort cell *dpp* transcript levels to show that Armi either does or does not increase *dpp* transcripts.

It is possible that *CycJ* also regulates *dpp* transcript levels in the absence of either *piwi* or *armi*, so qRT-PCR could also be done on escort cells of double mutants. Results would simply be compared to single mutants and controls to show that *dpp* is either increased or not increased in these mutants. It is also possible that *CycJ* is

regulating BMP signaling by limiting diffusion of the morphogen Dpp, thereby restricting BMP signaling in the absence of the somatic piRNA pathway. To address this, Dpp would need to be visualized with antibodies or transgenic constructs like fluorescent fusion proteins. For example, fly strains expressing a *dpp-lacZ* fussion are available (Bloomington stock # 8412) and could be used to visualize Dpp in *CycJ*-piRNA pathway mutants. Dpp localization would have to be compared to single mutants. If Dpp diffusion was increased in double mutants compared to single mutants, it would suggest that CycJ is regulating this phenotype. One pitfall is that visualizing Dpp may not be sensitive enough to show increased diffusion. Alternatively, CycJ could be directly regulating GSC numbers, and expansion of GSCs might signal to escort cells to produce Dpp. Therefore, increased Dpp levels or diffusion may be a result of GSC accumulation, making these results difficult to interpret.

4.2.3 In what cells is CycJ required?

I have demonstrated that expressing *CycJ* in ovarian somatic cells can rescue *armi-CycJ* null oogenesis defects back to an *armi* null phenotype. One problem with this is that there is no evidence that *CycJ* is normally expressed in ovarian somatic cells. In fact, data using GFP-CycJ concluded that it is expressed in the germline, but not in the ovarian somatic cells (Althoff, Viktorinova et al. 2009). Nevertheless, I hypothesize that *CycJ* is expressed and required in ovarian somatic cells. One way to address a requirement for *CycJ* in somatic cells is to knock down *CycJ* in these cells in an *armi* null and screen for a genetic interaction resulting in mispackaged egg chambers similar to those in double mutants. Another approach is to knock down both *CycJ* and *armi* in somatic cells at the same time. If either of these mutant-knock down or double knock

down conditions resulted in severely mispackaged egg chambers, this would suggest that both CycJ and Armi are required in somatic cells for this process. However, if severe mispackaging was not observed, it could be attributed to incomplete knockdown and would therefore be inconclusive. I have preliminary data targeting both *Yb* and *CycJ* for knock down by expressing shRNA with the somatic *c587-Gal4* driver (Figure 26 and Table 4). *Yb* knockdown resulted in mispackaged egg chambers similar to those observed in *armi* and *piwi* mutants, but double knockdown with *CycJ* did not result in an obvious enhancement of these mispackaged egg chambers (Figure 26 and Table 4). It is possible that *CycJ* knockdown was not sufficient to result in a genetic interaction. It is also possible that *CycJ* is required in a different subset of somatic cells. To address this, double knockdown could be done with other ovarian somatic cell drivers like *e22c-Gal4*, but the same caveats apply. The ideal demonstration that CycJ is expressed in ovarian somatic cells is by antibody detection, but a suitable antibody would have to be created.

I have also demonstrated that mispackaged egg chambers of *armi-CycJ* null are partially rescued by expression of *UAS-CycJ* open reading frame driven by the germline-specific *nos-Gal4* (Figure 13). This suggests that CycJ may be required in germline cells for regulation of egg chamber packaging. One way to test this possibility is to drive the expression of short hairpin RNAs (shRNAs) targeting *CycJ* and piRNA pathway members with the germline-specific maternal triple driver (*MTD-Gal4*). For example, in preliminary experiments, I compared ovary phenotypes in single knockdowns with those in double knockdowns (Figure 26 and Table 4). There were significant changes in double knockdowns of *CycJ* and either *armi, aub, Spindle-E*

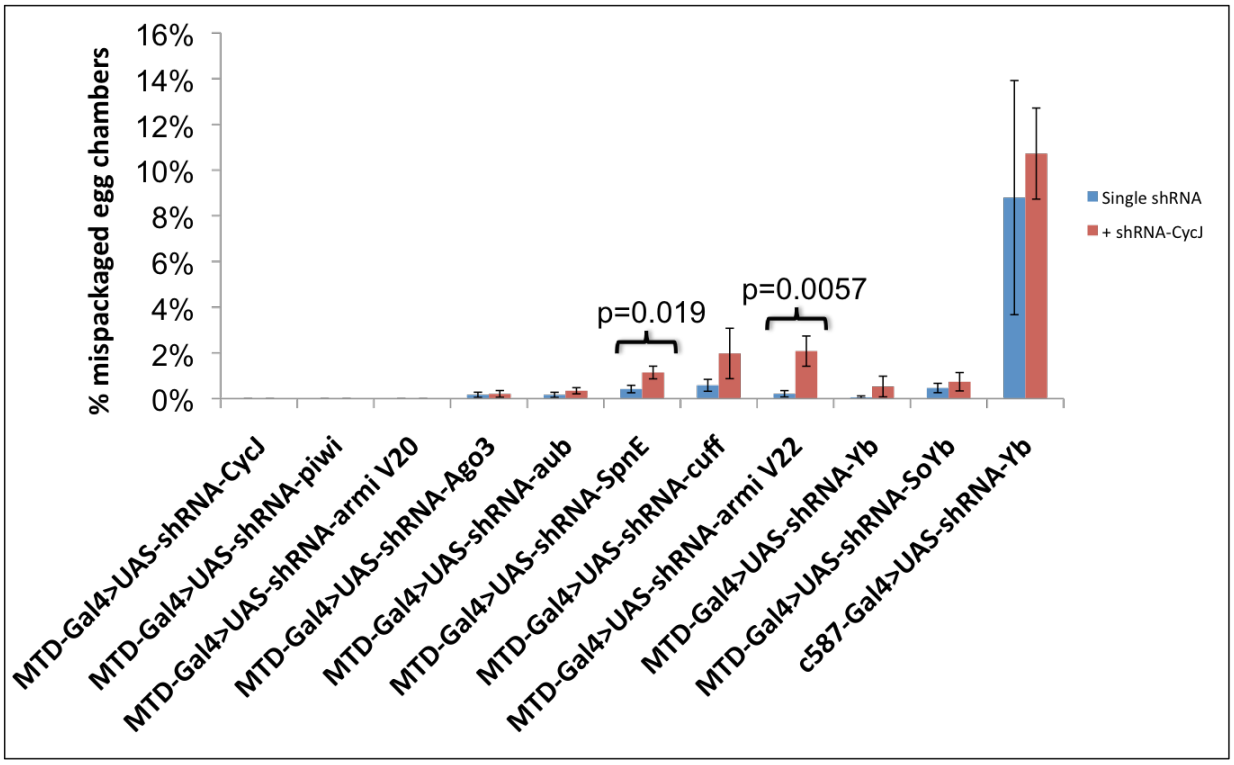

Figure 26: Double RNAi in the germline resulted in an increase of egg chambers with too many germline cells. Driving the expression of shRNAs targeting both *CycJ* and piRNA pathway members results in an increase of egg chambers with too many germline cells. Pairs of *UAS-shRNA* were expressed in the germline with the *Maternal Triple Driver (MTD-Gal4)* and in somatic cells with *c587-Gal4.* Female progeny containing the driver and both shRNA transgenes were DAPI stained and examined for oogenesis defects. They were compared to siblings containing the driver and one shRNA transgene. Knockdown of both *piwi* and *armi20* (*UAS-VALIUM20.armi,* a transgene optimized for somatic cell expression) resulted in agametic germarium that did not contain any identifiable germline cells. Double knockdown of *CycJ* and either *SpnE* or *armi22 (UAS-VALIUM22.armi,* a transgene optimized for germline cell expression) resulted in a significant increase of egg chambers with too many germline cells. This increase was small (3% of egg chambers with too many germline cells.) compared to null and mutant genetic interactions (~50% of egg chambers with too many germline cells). *Yb* was used as a negative control from germline knockdown and a positive control for somatic knockdown, since it is expressed only in the somatic cells and is known to regulate egg chamber packaging. Knocking down *CycJ* in *Yb* knockdown conditions did not significantly increase egg chamber mispackaging. Quantification values and significant p-values are in Table 4. All fly lines are listed in Appendix A.

Table 4: Driving the expression of shRNAs targeting both *CycJ* and piRNA pathway members results in multiple oogenesis defects

Genotype[a]	Knockdown Alias	# of mature oocytes per fly[b]		# of egg chambers per ovariole[b]		% mispackaged egg chambers[b]	
Wild Type	WT	30.4	$p=6.32^{-7}$	4.5	p=0.41	0.0	p=1
MTD>V20.CycJ	*CycJ*	7.3		4.4		0.0	
MTD>V20.piwi	***Piwi***	0.0	p=1	0.0	p=1	0.0	p=1
MTD>V20.piwi, V20.CycJ	***Piwi-CycJ***	0.0		0.0		0.0	
MTD>V20.armi	***Armi20***	0.0	p=1	0.0	p=1	0.0	p=1
MTD>V20.armi, V20.CycJ	***Armi20-CycJ***	0.0		0.0		0.0	
MTD>V20.Ago3	***Ago3***	16.6	p=0.28	4.4	p=0.40	.2	p=0.42
MTD>V20.Ago3, V20.CycJ	***Ago3-CycJ***	13.5		4.5		.2	
MTD>V22.aub	***Aub***	29.8	p=0.026	3.8	p=0.36	.2	p=0.16
MTD>V22.aub, V20.CycJ	***Aub-CycJ***	16.7		4.0		.3	
MTD>V22.Yb	***Yb***	20.9	p=0.25	4.5	p=0.13	.1	p=0.16
MTD>V22.Yb, V20.CycJ	***Yb-CycJ***	17.7		4.6		.5	
MTD>V22.SoYb	***SoYb***	25.3	p=0.43	4.4	p=0.011	.5	p=0.28
MTD>V22.SoYb, V20.CycJ	***SoYb-CycJ***	24.1		4.7		.7	
MTD>V22.SpnE	***SpnE***	10.6	p=0.42	4.6	p=0.048	.4	p=0.019
MTD>V22.SpnE, V20.CycJ	***SpnE-CycJ***	9.8		3.9		1.1	
MTD>V22.Cuff	***Cuff***	16.4	p=0.40	4.3	p=0.17	.6	p=0.12
MTD>V22.Cuff, V20.CycJ	***Cuff-CycJ***	17.8		4.0		2.0	
MTD>V22.armi	***armi22***	5.5	$p=6.22^{-4}$	4.2	p=0.44	.2	p=0.0057
MTD>V22.armi, V20.CycJ	***armi22-CycJ***	19.1		3.8		3.0	
c587>V22.Yb	***Yb***	21.3	p=0.17	2.3	p=0.20	8.8	p=0.37
c587>V22.Yb, V20.CycJ	***Yb-CycJ***	13.3		2.9		10.7	

[a.] Comparison of wild-type ovaries to ovaries expressing shRNA using Gal4 driven by the germline-specific promoters in the *Maternal Triple Driver* (*MTD*-Gal4) or the somatic-specific promoter *c587-Gal4*. shRNAs are expressed from *UAS* constructs containing the VALIUM20 (V20) vector, which is optomized for expressing miRNA-like short hairpin RNAs (shRNA) in the soma, or VALIUM20 (V20) vector, which is optomized for shRNA expression in the germline. Expression of shRNA targeting both *piwi* and *armi* resulted in agametic germaria producing no germline cells in either single or double shRNA expression. Interestingly, expression of the *CycJ* shRNA and *armi* shRNA from the VALIUM22 vector, which is optimized for the germline, resulted in statistically significant changes in all three oogenesis parameters quantified, similar to but less severe than the double null. It is also important to note that number of mature oocytes changed in the opposite direction compared to double null flies. The screen also reproduced *aub* as a genetic interactor and identified *SoYb* and *SpnE* as potential novel genetic interactors. Although these defects were statistically significant, the overall changes are small compared to double null flies and positive control somatic *Yb* shRNA expression. [b.] p-values were calculated using a type 3 student's t-test comparing single and double shRNA expressing ovaries.

(Spn-E), or *Sister of Yb (SoYb)*, but defects were much less severe compared to double mutants (Figures 11, 12, and Table 2). Only double knockdowns of *CycJ* and either *Spn-E* or *armi* resulted in more severe egg chamber packaging defects, but overall levels of egg chamber mispackaging were low. As a negative control, I attempted to knockdown the soma-specific *Yb* in the germline with *MTD-Gal4*, which did not result in oogenesis defects. Due to a lack of proper controls, these RNAi results are considered preliminary. One major pitfall of this approach is that multiple lines of evidence suggest that it is the somatic function of the piRNA pathway that regulates egg chamber packaging, so knockdown in the germline is not the appropriate condition. An alternative approach would be to knockdown *CycJ* in the germline of either *armi* or *piwi* mutants, but knockdown efficiency would have to be verified. For any of these knockdown experiments, it would be ideal to perform analysis of transcript levels to demonstrate efficiency of knockdown.

4.2.4 What is the mechanism for production of mispackaged egg chambers in these mutants?

The question of how mispackaged egg chambers are produced in single and double mutants still remains. My data suggest that *CycJ* and the somatic piRNA pathway cooperate to regulate egg chamber packaging by limiting BMP signaling. But it is also possible that they are regulating other pathways involved in egg chamber packaging. Aside from BMP signaling, Notch signaling is another major regulator of these two processes. Therefore, *CycJ* and the somatic piRNA pathway may be regulating Notch signaling to facilitate egg chamber packaging. I examined Notch signaling in single and double mutants by staining for Cut, which is negatively regulated

in somatic cells by Notch signaling, and Hindsight (Hnt), which is positively regulated in somatic cells by Notch signaling (Figure 27). I found that signaling appears to be fine in single mutants, but Cut appears to be absent in *armi-CycJ* double nulls, suggesting that Notch signaling is increased.

One way to further analyze Notch signaling, is to create clonal *armi-CycJ* mutant cell populations by inducing mitotic recombination in actively dividing cells using the Flp-FRT recombination technique (diagram and matings in Figure 28). Recombinant cells lose GFP, indicating that they are homozygous for *armi-CycJ* null. This technique can create clonal mutant germline cells, somatic cells, or both. In preliminary experiments, I made mutant clones and stained ovarioles in red for desired Notch pathway protein, green for GFP (non-clonal cell marker), and blue for DAPI (nuclei). Arrows in these figures indicate the same clonal follicle cell patch in a given row. I found that nuclear localization of Cut is indeed lost in somatic clones (Figure 29 A-D), suggesting that Notch signaling was increased in the absence of *CycJ* and *armi*. To my surprise, I found that Hnt appeared to be increased in somatic clones, further supporting that Notch signaling was increased (Figure 29 E-H). I next wanted to look upstream at activated Notch signaling by staining for the Notch Intracellular Domain (NICD) and found that NICD appeared to be increased in clonal somatic cells, again supporting that Notch signaling was increased in the absence of *armi* and *CycJ* (Figure 29 I-L). These experiments lacked the control wild type, *CycJ* null, and *armi* null clones so results should be considered preliminary. Based on staining with these antibodies in *CycJ* and *armi* null, I expect that these controls would not demonstrate increased Notch signaling (Figure 27). Evidence suggests that Notch signaling and BMP signaling directly

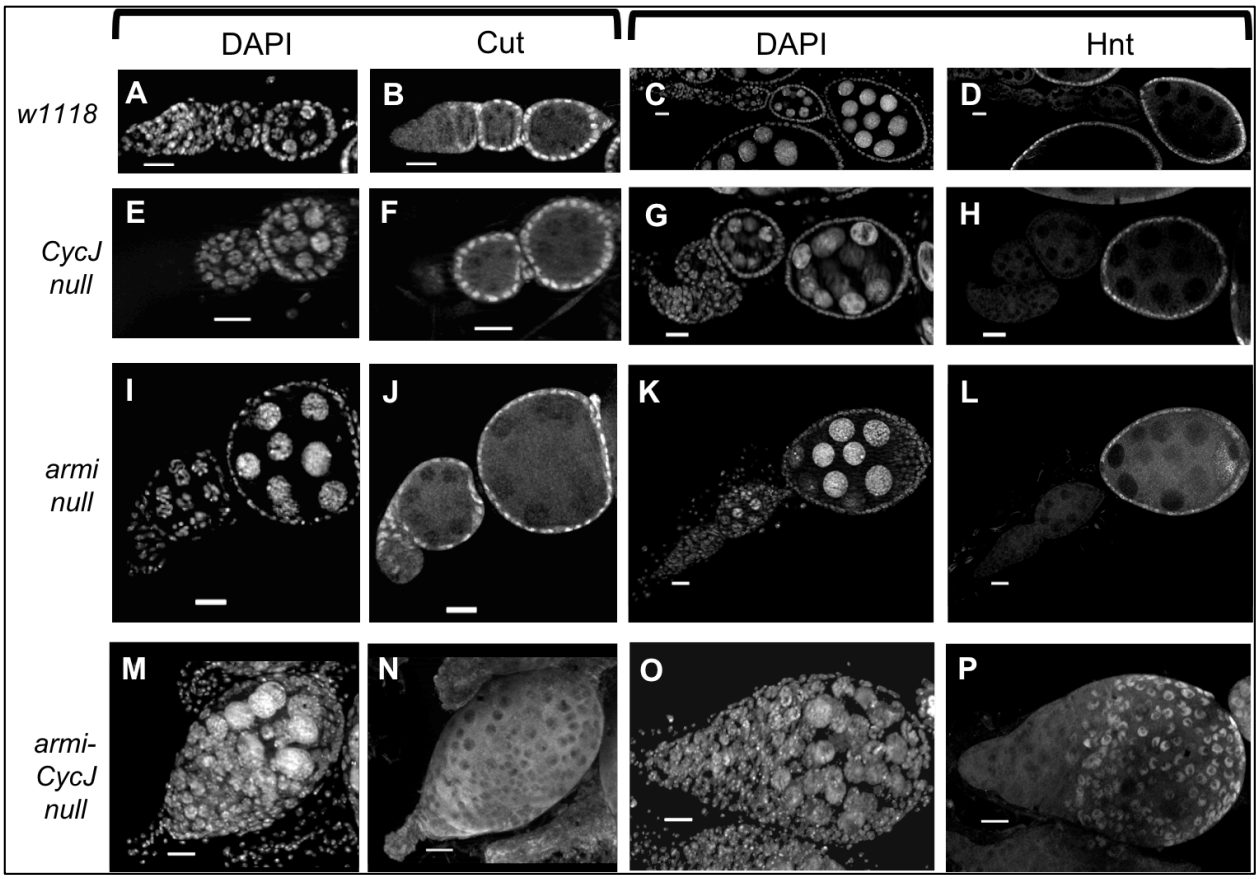

Figure 27: *CycJ* and the somatic piRNA pathway cooperate to limit Notch signaling. To analyze Notch signaling in somatic cells of single and double mutants, I used markers for the absence (Cut) and presence (Hnt) of Notch signaling. I stained for Cut, which is expressed in young egg chambers where Notch signaling is absent, and Hindsight (Hnt), which is expressed in later egg chambers where Notch signaling is present. Wild type (w1118), *CycJ* null, and *armi* null all exhibited the appropriate patterns of both Cut and Hnt expression (A-L). *armi-CycJ* double null, on the other hand, had reduced expression of Cut (N, M is the same ovariole with DAPI counterstaining) and potentially normal levels of Hnt (O and P). All images are paired to show ovarioles of indicated genotypes counterstained with DAPI followed by the same ovariole stained for either Cut (B, F, J, N) or Hnt (D, H, L, P). All size bars = 20 μm.

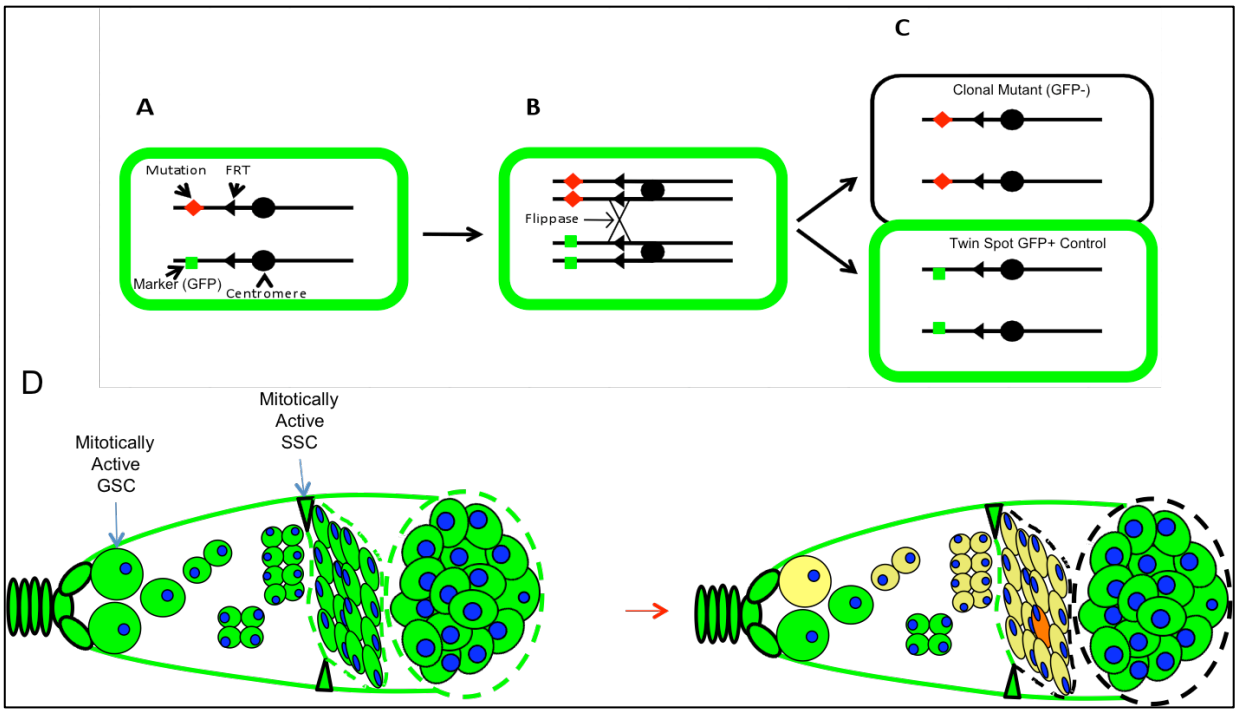

Figure 28: Mutant cell populations can be produced in mitotically active cells of the ovary using FLP/FRT recombination. Groups of mutant cells can be produced in heterozygous cells containing a mutation, a marker, and recombination targets using FLP/FRT mitotic recombination. FLP/FRT recombination relies on the enzyme Flippase (FLP), which facilitates recombination between DNA sequences known as Flippase Recombination Targets (FRTs) oriented in the same direction. Recombination takes place in A) mitotically active cells B) after DNA synthesis, but before mitosis. C) When mitosis occurs and sister chromatids segregate, a cell is produced with two copies of the mutation lacking the marker (GFP in this case, green cells) and its sister is produced with two copies of GFP. D) This can be used in ovaries to create mutant populations of germline stem cells, germline cells, somatic stem cells, or somatic cells. Mutants are depicted as lacking GFP.

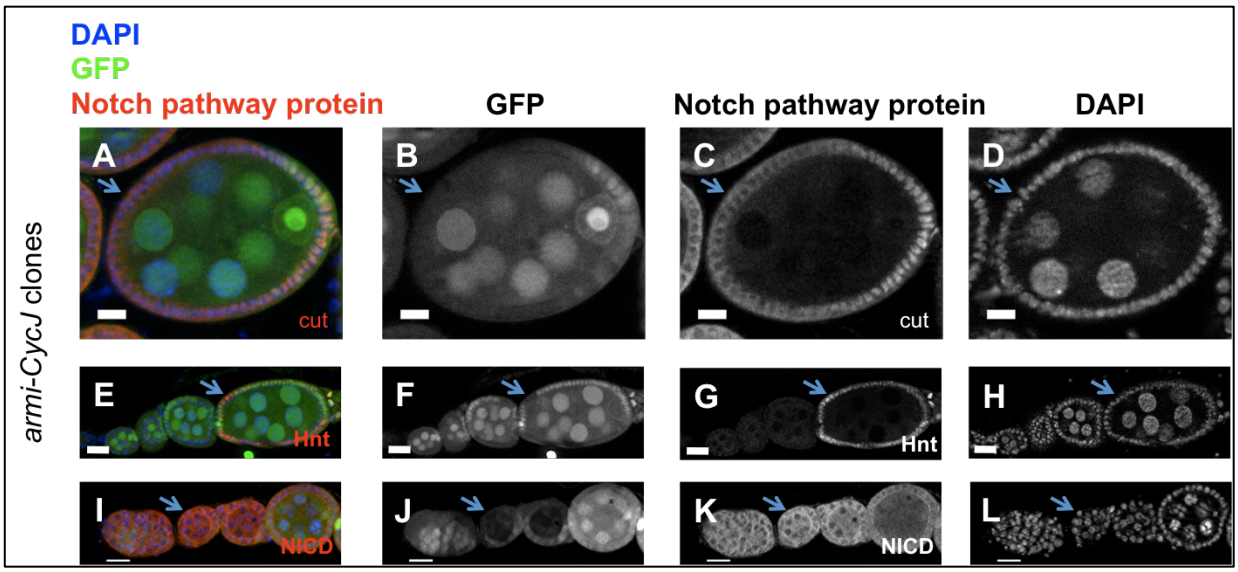

Figure 29: Notch signaling is increased in *armi-CycJ* null somatic clones. Heat shock was used to induce mitotic recombination in *hsFlp; Df(3L)armi-J, FRT80B/Ubi-GFP, FRT80B* flies. Clonal cells that are homozygous *Df(3L)armi-J* are identified by lack of GFP (B, F, and J). Protein expression is compared directly to adjacent somatic cells that express GFP and have at least one copy of *armi* and *CycJ.* In these mutant somatic cell clones, Cut has lost nuclear localization (C). Clonal mutants also appear to have increased Hnt expression (G). Finally, NICD, the active component of Notch signaling, appears to be increased in mutant clones (K). Each row is a single set of images for the same ovariole with the indicated staining or counterstain. All size bars = 20 μm.

correlate in the early germarium, so this result is not entirely unexpected in light of increased BMP signaling in double mutants (Song, Call et al. 2007; Tseng, Kao et al. 2014). If these results are true, they suggest that *CycJ* is acting to limit Notch signaling in the absence of *armi*. Based on previous data, increased Notch signaling may be decreasing follicle cell proliferation by promoting the switch to endocycles (reviewed in (Roth 2001)). This could explain the decreased somatic cell proliferation I observed in *armi-CycJ* mutants. However, I expect increased Notch signaling in the germarium would increase packaging, but my data suggest that packaging is decreased (Grammont and Irvine 2001). It is possible that there is a confounding effect of increased BMP signaling and GSC accumulation in *CycJ*-piRNA pathway mutants, which reduces egg chamber packaging and ameliorates the role of Notch in the packaging process. Nevertheless, the functional consequence of increased Notch signaling in these mutants has yet to be determined.

APPENDICES

Appendix A: List of flies

Name	Genotype	Finley Lab #	Stock Center #	Reference
Three-gene deletion	*Df(3L)armi-J/ TM6C, Tb, Sb*	580	-	Atikukke 2009
CycJ null	P{armi}, Df(3L)armi-J/TM6C, Tb Sb	624	-	Atikukke 2009
armi null	w; p{CycJ_HZ14}72-12, Df(3L)armi-J/TM6C, Tb Sb	1027	-	This study
p{CycJ}	w; p{CycJ} ; Sb/TM3, Ser	897	-	Atikukke 2009
p{HZ14-CycJ}54-1	P{CycJ HZ14}Q54-1B; CyO/Sp	846	-	This study
p{HZ14-CycJ}91-1	P{CycJ HZ14}V91-1A	848	-	This study
p{HZ14-CycJ}3-2	w; P{CycJ HZ14}3-2/CyO; TM3, Ser/Sb	823	-	Atikukke, Albosta et al. 2014
p{HZ14-CycJ}6-1	P{CycJ HZ14}6-1/CycO; TM3, Ser/Sb	828	-	This study
p{HZ14-CycJ}6-5	P{CycJ HZ14}6-5/CyO; TM3, Ser/Sb	829	-	Atikukke, Albosta et al. 2014
p{HZ14-CycJ}6-6	P{CycJ HZ14}6-6/CyO; TM3, Ser/Sb	830	-	Atikukke, Albosta et al. 2014
p{HZ14-CycJ}72-11	P{CycJ HZ14}72-11/CyO; TM3, Ser/Sb	833	-	Atikukke, Albosta et al. 2014
p{HZ14-CycJ}68-1	CyO/Sp; P{CycJ HZ14}68-1/TM3, Ser	837	-	This study
p{HZ14-CycJ}72-12	CyO/Sp; P{CycJ HZ14}72-12/TM3, Ser	840	-	This study
p{HZ14-CycJ}72-5	CycO/Sp; P{CycJ HZ14}72-5/TM3, Ser	842	-	This study
p{HZ14-CycJ}26-1	CycO/Sp; P{CycJ HZ14}26-1/TM3, Ser	834	-	This study
p{HZ14-CycJ}45-1	CyO/Sp; P{CycJ HZ14}45-1/TM3, Ser	835	-	This study
p{armi}	p{armi}5 / CyO; TM3Ser / Sb	501	-	Atikukke 2009
p{armi}	p{armi}3; TM3Ser/Sb	497	-	Atikukke 2009
p{CG14971}	p{CG14971}_4	520	-	Atikukke 2009
UAS-CycJ	y w; {UAS-Myc-CycJ}51C/CyO	801	-	Atikukke, Albosta et al. 2014
UAS-armi	UAS-GFP-armi/CyO ; armi72.1/TM3 Ser	127	-	Cook, Koppetsch et al. 2004
Wild Type	w[1118]	55	5905	Hazelrigg, Levis et al. 1984
armi 72.1	CyO/Sp; armi[72.1]/TM3 Ser	257	-	Cook, Koppetsch et al. 2004
mnkP6	w dpb [mnkP6w+]pxsp / CyO	578	-	Takada, Kelkar et al. 2003
Flippase	hsFLP, y, w; Dr/TM3, Sb	870	26902	Golic 1991

Name	Genotype	Finley Lab #	Stock Center #	Reference
aub QC42	w; aub[QC42] cn[1] bw[1]/CyO	544	4968	Schupbach and Wieschaus 1991
aub HN	aub[HN] cn[1] bw[1]/CyO	542	8517	Schupbach and Wieschaus 1991
eIF5B 09143	eIF5B[09143]/TM3, Sb Ser	118	11735	-
VP16::nos-Gal4	w VP16-nos.UTR_Gal4	854	7303	Van Doren, Williamson et al. 1998
e22c-Gal4	y w; e22c-Gal4	1030	1973	Lawrence, Bodmer et al. 1995 and Barth, Hafen et al. 2012
c587-Gal4	c587-Gal4	1010	-	Song and Xie 2003
Exel6094	w; Df(3L)Exel6094/TM6B, Tb[1]	146	7573	Parks, Cook et al. 2004
Exel6095	w; Df(3L)Exel6095/TM6B, Tb	232	7574	Parks, Cook et al. 2004
Balancer	w; CyO/Sp; TM3, Ser/Sb	41	-	Van Berkum Lab, WSU
Balancer	w; CyO/Sp; TM6, Tb Sb/Dr	1024	-	This study
phiC31 integrase	y w vas-phiC31; RFP attp-51C	609	24482	Bischof, Maeda et al. 2007
piwi 06843	piwi[06843] cn/CyO; ry	792	12225	Lin and Spradling 1997
BSC145	w; Df(2L)BSC145/CyO	906	9505	Cook, Christensen et al. 2012
dpp hr56	dpp[hr56] cn bw/SM6a	998	36528	Irish and Gelbart 1987
MTD-Gal4	w otu-Gal4; nos-Gal4; VP16::nos.UTR-Gal4	895	31777	Ni, Zhou et al. 2011
shRNA-CycJ	y sc v; UAS_VALIUM20_shRNA-CycJ attP40	987	37521	Ni, Zhou et al. 2011
shRNA-piwi	y sc v; UAS_VALIUM20_shRNA-piwi attP2	916	33724	Ni, Zhou et al. 2011
shRNA-armi V20	y sc v; UAS_VALIUM20_shRNA-armi attP2	920	34789	Ni, Zhou et al. 2011
shRNA-Ago3	y sc v; UAS_VALIUM20_shRNA-Ago3 attP2	921	34815	Ni, Zhou et al. 2011
shRNA-aub	y sc v; UAS_VALIUM22_shRNA-aub attP2	922	35201	Ni, Zhou et al. 2011
shRNA-SpnE	y sc v; UAS_VALIUM22_shRNA-spnE attP2	924	35303	Ni, Zhou et al. 2011
shRNA-cuff	y sc v; UAS_VALIUM22_shRNA-cuff attP2	925	35318	Ni, Zhou et al. 2011
shRNA-armi V22	y sc v; UAS_VALIUM22_shRNA-armi attP2	926	35343	Ni, Zhou et al. 2011
shRNA-Yb	y sc v; UAS_VALIUM22_shRNA-Yb attP2	1001	35181	Ni, Zhou et al. 2011
shRNA-SoYb	y sc v; UAS_VALIUM22_shRNA-SoYb attP2	1003	36881	Ni, Zhou et al. 2011

Appendix B: List of primers

Lab #	Name	Target	Use	Sequence (5' to 3')
907	PA01F	CycJ	PCR and RTPCR	TGACCATGAGGGAGCAAGAACTCA
908	PA01R	CycJ	PCR and RTPCR	ACAGCCTTGTACTCGAATGCCGTA
909	PA02F	armi	PCR and RTPCR	AGCTCAGCGGATTTGGTGACAAAG
910	PA02R	armi	PCR and RTPCR	GTTCGGTGCATTGACCAGCTTCAT
911	PA03	CG14971	PCR and RTPCR	TGCCCATTTCCCTCTACACCATGA
912	PA03	CG14971	PCR and RTPCR	TGCAAGCCTAGCTTCGATTTCTGC
901	RF305	Left end of Df(3L)armi-J	Sequencing	AGATACGCACACGCGACGCC
900	RF304	Right end of Df(3L)armi-J	Sequencing	CACAACCCGATCCCGCCGAG
918	PARB1	Internal left of Df(3L)armi-J	Sequencing	CAACTTTGGCACATATCAATATTATGCTCTCGAC
920	PAXP1	Internal right of Df(3L)armi-J	Sequencing	GGTCAGACATTTAAAAGGAGGCGACTC
951	6094Gpfor	Exel deficiency	diagnostic PCR	CGAGGCCGGAACCAAGGAGC
952	6094Gprev	Exel deficiency	diagnostic PCR	CCGCAATCCGGAAAGTTTTTCG
953	6095Gpfor	Exel deficiency	diagnostic PCR	GCCAAGTTGGCAGGTGGGCA
954	6095Gprev	Exel deficiency	diagnostic PCR	AGCGCCTAAGCAGTTGCAGCA
950	TnRight	Exel deficiency	diagnostic PCR	TTTACTCCAGTCACAGCTTTG
949	TnLeft	Exel deficiency	diagnostic PCR	TACTATTCCTTTCACTCGCACTTATTG
962	RB	Df(3L)armi-J	diagnostic PCR	GCATCAAAGAACAAGCCGGCCAAG
923	PA_Df(3L)armiJ_R	Df(3L)armi-J	diagnostic PCR	TAACTGTCGAGCGAATGGAAGCGA
906	plac1	5' end iPCR inserts	Inverse PCR	CACCCAAGGCTCTGCTCCCACAAT
905	pwht1	5' end iPCR inserts	Inverse PCR	GTAACGCTAATCACTCCGAACAGGTACCA
903	ey.3.f	3' end iPCR inserts & Seq	Inverse PCR & Seq	CCTTTCACTCGCACTTATTG
904	ey3.r	3' end iPCR inserts	Inverse PCR	GTGAGACAGCGATATGATTGT
902	5.sup.seq1	5' end iPCR insert sequencing	Inverse PCR Seq	TCCAGTCACAGCTTTGCAGC

REFERENCES

Abdu, U., M. Brodsky, et al. (2002). "Activation of a meiotic checkpoint during Drosophila oogenesis regulates the translation of Gurken through Chk2/Mnk." Curr Biol 12(19): 1645-1651.

Akbari, O. S., I. Antoshechkin, et al. (2013). "The developmental transcriptome of the mosquito Aedes aegypti, an invasive species and major arbovirus vector." G3 (Bethesda) 3(9): 1493-1509.

Althoff, F., I. Viktorinova, et al. (2009). "Drosophila Cyclin J is a mitotically stable Cdk1 partner without essential functions." Dev Biol 333(2): 263-272.

Aravin, A. A., G. J. Hannon, et al. (2007). "The Piwi-piRNA pathway provides an adaptive defense in the transposon arms race." Science 318(5851): 761-764.

Aravin, A. A., M. S. Klenov, et al. (2004). "Dissection of a natural RNA silencing process in the Drosophila melanogaster germ line." Mol Cell Biol 24(15): 6742-6750.

Arbeitman, M. N., E. E. Furlong, et al. (2002). "Gene expression during the life cycle of Drosophila melanogaster." Science 297(5590): 2270-2275.

Ashburner, M. (1989). Drosophila. Cold Spring Harbor, N.Y., Cold Spring Harbor Laboratory.

Atikukke, G. (2009). Cyclin J cooperates with the piRNA to regulate early oocyte development in *Drosophila*. Ph.D., Wayne State University.

Atikukke, G., P. Albosta, et al. (2014). "A role for Drosophila Cyclin J in oogenesis revealed by genetic interactions with the piRNA pathway." Mechanisms of development 133: 64-76.

Bender, L. B., P. J. Kooh, et al. (1993). "Complex function and expression of Delta during Drosophila oogenesis." Genetics 133(4): 967-978.

Bischof, J., R. K. Maeda, et al. (2007). "An optimized transgenesis system for Drosophila using germ-line-specific phiC31 integrases." Proc Natl Acad Sci U S A 104(9): 3312-3317.

Brand, A. H. and N. Perrimon (1993). "Targeted gene expression as a means of altering cell fates and generating dominant phenotypes." Development 118(2): 401-415.

Brodsky, M. H., B. T. Weinert, et al. (2004). "Drosophila melanogaster MNK/Chk2 and p53 regulate multiple DNA repair and apoptotic pathways following DNA damage." Mol Cell Biol 24(3): 1219-1231.

Cao, L., F. Chen, et al. (2014). "Phylogenetic analysis of CDK and cyclin proteins in premetazoan lineages." BMC Evol Biol 14: 10.

Carrera, P., O. Johnstone, et al. (2000). "VASA mediates translation through interaction with a Drosophila yIF2 homolog." Mol Cell 5(1): 181-187.

Chen, D. and D. McKearin (2003). "Dpp signaling silences bam transcription directly to establish asymmetric divisions of germline stem cells." Curr Biol 13(20): 1786-1791.

Chintapalli, V. R., J. Wang, et al. (2013). "Data-mining the FlyAtlas online resource to identify core functional motifs across transporting epithelia." BMC Genomics 14: 518.

Cook, H. A., B. S. Koppetsch, et al. (2004). "The Drosophila SDE3 homolog armitage is required for oskar mRNA silencing and embryonic axis specification." Cell 116(6): 817-829.

Cox, D. N., A. Chao, et al. (1998). "A novel class of evolutionarily conserved genes defined by piwi are essential for stem cell self-renewal." Genes & Development 12(23): 3715-3727.

de Cuevas, M., M. A. Lilly, et al. (1997). "Germline cyst formation in Drosophila." Annu Rev Genet 31: 405-428.

Evans, T., E. T. Rosenthal, et al. (1983). "Cyclin: a protein specified by maternal mRNA in sea urchin eggs that is destroyed at each cleavage division." Cell 33(2): 389-396.

Feliciano, A., J. Castellvi, et al. (2013). "miR-125b acts as a tumor suppressor in breast tumorigenesis via its novel direct targets ENPEP, CK2-alpha, CCNJ, and MEGF9." PLoS One 8(10): e76247.

Finley, R. L., Jr. and R. Brent (1994). "Interaction mating reveals binary and ternary connections between Drosophila cell cycle regulators." Proc Natl Acad Sci U S A 91(26): 12980-12984.

Finley, R. L., Jr., B. J. Thomas, et al. (1996). "Isolation of Drosophila cyclin D, a protein expressed in the morphogenetic furrow before entry into S phase." Proc Natl Acad Sci U S A 93(7): 3011-3015.

Forbes, A. J., H. Lin, et al. (1996). "hedgehog is required for the proliferation and specification of ovarian somatic cells prior to egg chamber formation in Drosophila." Development 122(4): 1125-1135.

Giaever, G., D. D. Shoemaker, et al. (1999). "Genomic profiling of drug sensitivities via induced haploinsufficiency." Nat Genet 21(3): 278-283.

Gonzalez-Reyes, A., H. Elliott, et al. (1997). "Oocyte determination and the origin of polarity in Drosophila: the role of the spindle genes." Development 124(24): 4927-4937.

Gonzalez-Reyes, A. and D. St Johnston (1994). "Role of oocyte position in establishment of anterior-posterior polarity in Drosophila." Science 266(5185): 639-642.

Goode, S., D. Wright, et al. (1992). "The neurogenic locus brainiac cooperates with the Drosophila EGF receptor to establish the ovarian follicle and to determine its dorsal-ventral polarity." Development 116(1): 177-192.

Grammont, M. and K. D. Irvine (2001). "fringe and Notch specify polar cell fate during Drosophila oogenesis." Development 128(12): 2243-2253.

Graveley, B. R., A. N. Brooks, et al. (2011). "The developmental transcriptome of Drosophila melanogaster." Nature 471(7339): 473-479.

Gunawardane, L. S., K. Saito, et al. (2007). "A slicer-mediated mechanism for repeat-associated siRNA 5' end formation in Drosophila." Science 315(5818): 1587-1590.

Guo, Z. and Z. Wang (2009). "The glypican Dally is required in the niche for the maintenance of germline stem cells and short-range BMP signaling in the Drosophila ovary." Development 136(21): 3627-3635.

Haase, A. D., S. Fenoglio, et al. (2010). "Probing the initiation and effector phases of the somatic piRNA pathway in Drosophila." Genes Dev 24(22): 2499-2504.

Hadwiger, J. A., C. Wittenberg, et al. (1989). "A family of cyclin homologs that control the G1 phase in yeast." Proc Natl Acad Sci U S A 86(16): 6255-6259.

Harvey, R. C., C. G. Mullighan, et al. (2010). "Identification of novel cluster groups in pediatric high-risk B-precursor acute lymphoblastic leukemia with gene expression profiling: correlation with genome-wide DNA copy number alterations, clinical characteristics, and outcome." Blood 116(23): 4874-4884.

Hillenmeyer, M. E., E. Fung, et al. (2008). "The chemical genomic portrait of yeast: uncovering a phenotype for all genes." Science 320(5874): 362-365.

Hochegger, H., S. Takeda, et al. (2008). "Cyclin-dependent kinases and cell-cycle transitions: does one fit all?" Nat Rev Mol Cell Biol 9(11): 910-916.

Horton, L. E. and D. J. Templeton (1997). "The cyclin box and C-terminus of cyclins A and E specify CDK activation and substrate specificity." Oncogene 14(4): 491-498.

Hsu, H. J., L. LaFever, et al. (2008). "Diet controls normal and tumorous germline stem cells via insulin-dependent and -independent mechanisms in Drosophila." Dev Biol 313(2): 700-712.

Huang, X. A., H. Yin, et al. (2013). "A major epigenetic programming mechanism guided by piRNAs." Dev Cell 24(5): 502-516.

Huynh, J. R. (2000). Fusome as a Cell-Cell Communication Channel of Drosophila ovarian cyst Austin, TX, Landes Bioscience.

Jeffrey, P. D., A. A. Russo, et al. (1995). "Mechanism of CDK activation revealed by the structure of a cyclinA-CDK2 complex." Nature 376(6538): 313-320.

Jin, Z., A. S. Flynt, et al. (2013). "Drosophila piwi mutants exhibit germline stem cell tumors that are sustained by elevated Dpp signaling." Curr Biol 23(15): 1442-1448.

Kai, T., D. Williams, et al. (2005). "The expression profile of purified Drosophila germline stem cells." Dev Biol 283(2): 486-502.

King, F. J. and H. Lin (1999). "Somatic signaling mediated by fs(1)Yb is essential for germline stem cell maintenance during Drosophila oogenesis." Development 126(9): 1833-1844.

King, F. J., A. Szakmary, et al. (2001). "Yb modulates the divisions of both germline and somatic stem cells through piwi- and hh-mediated mechanisms in the Drosophila ovary." Mol Cell 7(3): 497-508.

Kirilly, D., E. P. Spana, et al. (2005). "BMP signaling is required for controlling somatic stem cell self-renewal in the Drosophila ovary." Dev Cell 9(5): 651-662.

Kirilly, D., S. Wang, et al. (2011). "Self-maintained escort cells form a germline stem cell differentiation niche." Development 138(23): 5087-5097.

Kirilly, D. and T. Xie (2007). "The Drosophila ovary: an active stem cell community." Cell research 17(1): 15-25.

Klattenhoff, C., D. P. Bratu, et al. (2007). "Drosophila rasiRNA pathway mutations disrupt embryonic axis specification through activation of an ATR/Chk2 DNA damage response." Developmental cell 12(1): 45-55.

Klattenhoff, C. and W. Theurkauf (2008). "Biogenesis and germline functions of piRNAs." Development 135(1): 3-9.

Klenov, M. S., O. A. Sokolova, et al. (2011). "Separation of stem cell maintenance and transposon silencing functions of Piwi protein." Proc Natl Acad Sci U S A 108(46): 18760-18765.

Kobayashi, H., E. Stewart, et al. (1992). "Identification of the domains in cyclin A required for binding to, and activation of, p34cdc2 and p32cdk2 protein kinase subunits." Mol Biol Cell 3(11): 1279-1294.

Kolonin, M. G. and R. L. Finley, Jr. (2000). "A role for cyclin J in the rapid nuclear division cycles of early Drosophila embryogenesis." Dev Biol 227(2): 661-672.

Lantz, V., J. S. Chang, et al. (1994). "The Drosophila orb RNA-binding protein is required for the formation of the egg chamber and establishment of polarity." Genes & Development 8(5): 598-613.

Lees, E. M. and E. Harlow (1993). "Sequences within the conserved cyclin box of human cyclin A are sufficient for binding to and activation of cdc2 kinase." Mol Cell Biol 13(2): 1194-1201.

Li, C., V. V. Vagin, et al. (2009). "Collapse of germline piRNAs in the absence of Argonaute3 reveals somatic piRNAs in flies." Cell 137(3): 509-521.

Lim, S. and P. Kaldis (2013). "Cdks, cyclins and CKIs: roles beyond cell cycle regulation." Development 140(15): 3079-3093.

Lin, H., L. Yue, et al. (1994). "The Drosophila fusome, a germline-specific organelle, contains membrane skeletal proteins and functions in cyst formation." Development 120(4): 947-956.

Ma, X., S. Wang, et al. (2014). "Piwi is required in multiple cell types to control germline stem cell lineage development in the Drosophila ovary." PLoS One 9(3): e90267.

Mairiang, D., H. Zhang, et al. (2013). "Identification of new protein interactions between dengue fever virus and its hosts, human and mosquito." PLoS One 8(1): e53535.

Malone, C. D., J. Brennecke, et al. (2009). "Specialized piRNA pathways act in germline and somatic tissues of the Drosophila ovary." Cell 137(3): 522-535.

Masrouha, N., L. Yang, et al. (2003). "The Drosophila chk2 gene loki is essential for embryonic DNA double-strand-break checkpoints induced in S phase or G2." Genetics 163(3): 973-982.

McKearin, D. and B. Ohlstein (1995). "A role for the Drosophila bag-of-marbles protein in the differentiation of cystoblasts from germline stem cells." Development 121(9): 2937-2947.

Mevel-Ninio, M., A. Pelisson, et al. (2007). "The flamenco locus controls the gypsy and ZAM retroviruses and is required for Drosophila oogenesis." Genetics 175(4): 1615-1624.

Minshull, J., J. J. Blow, et al. (1989). "Translation of cyclin mRNA is necessary for extracts of activated xenopus eggs to enter mitosis." Cell 56(6): 947-956.

Mittler, S. (1982). "Effect of hyperthermia on radiation-induced chromosome loss in female Drosophila melanogaster." Journal of Heredity 73(6): 451-456.

Miyazono, K., S. Maeda, et al. (2005). "BMP receptor signaling: transcriptional targets, regulation of signals, and signaling cross-talk." Cytokine Growth Factor Rev 16(3): 251-263.

Muerdter, F., P. M. Guzzardo, et al. (2013). "A genome-wide RNAi screen draws a genetic framework for transposon control and primary piRNA biogenesis in Drosophila." Mol Cell 50(5): 736-748.

Murota, Y., H. Ishizu, et al. (2014). "Yb integrates piRNA intermediates and processing factors into perinuclear bodies to enhance piRISC assembly." Cell Rep 8(1): 103-113.

Murray, A. W. (2004). "Recycling the cell cycle: cyclins revisited." Cell 116(2): 221-234.

Murray, A. W., M. J. Solomon, et al. (1989). "The role of cyclin synthesis and degradation in the control of maturation promoting factor activity." Nature 339(6222): 280-286.

Muzzopappa, M. and P. Wappner (2005). "Multiple roles of the F-box protein Slimb in Drosophila egg chamber development." Development 132(11): 2561-2571.

Nishimasu, H., H. Ishizu, et al. (2012). "Structure and function of Zucchini endoribonuclease in piRNA biogenesis." Nature 491(7423): 284-287.

Nystul, T. and A. Spradling (2010). "Regulation of epithelial stem cell replacement and follicle formation in the Drosophila ovary." Genetics 184(2): 503-515.

Ohi, Y., H. Qin, et al. (2011). "Incomplete DNA methylation underlies a transcriptional memory of somatic cells in human iPS cells." Nat Cell Biol 13(5): 541-549.

Olivieri, D., M. M. Sykora, et al. (2010). "An in vivo RNAi assay identifies major genetic and cellular requirements for primary piRNA biogenesis in Drosophila." EMBO J 29(19): 3301-3317.

Parrish, J. R., T. Limjindaporn, et al. (2004). "High-throughput cloning of Campylobacter jejuni ORfs by in vivo recombination in Escherichia coli." Journal of proteome research 3(3): 582-586.

Pelisson, A., S. U. Song, et al. (1994). "Gypsy transposition correlates with the production of a retroviral envelope-like protein under the tissue-specific control of the Drosophila flamenco gene." EMBO J 13(18): 4401-4411.

Pines, J. and T. Hunt (1987). "Molecular cloning and characterization of the mRNA for cyclin from sea urchin eggs." EMBO J 6(10): 2987-2995.

Qi, H., T. Watanabe, et al. (2011). "The Yb body, a major site for Piwi-associated RNA biogenesis and a gateway for Piwi expression and transport to the nucleus in somatic cells." J Biol Chem 286(5): 3789-3797.

Rangan, P., C. D. Malone, et al. (2011). "piRNA production requires heterochromatin formation in Drosophila." Curr Biol 21(16): 1373-1379.

Robinson, D. N., K. Cant, et al. (1994). "Morphogenesis of Drosophila ovarian ring canals." Development 120(7): 2015-2025.

Rojas-Rios, P., I. Guerrero, et al. (2012). "Cytoneme-mediated delivery of hedgehog regulates the expression of bone morphogenetic proteins to maintain germline stem cells in Drosophila." PLoS Biol 10(4): e1001298.

Roth, S. (2001). "Drosophila oogenesis: coordinating germ line and soma." Curr Biol 11(19): R779-781.

Rubin, G. M. and A. C. Spradling (1982). "Genetic transformation of Drosophila with transposable element vectors." Science 218(4570): 348-353.

Sato, K., K. M. Nishida, et al. (2011). "Maelstrom coordinates microtubule organization during Drosophila oogenesis through interaction with components of the MTOC." Genes Dev 25(22): 2361-2373.

Schupbach, T. and E. Wieschaus (1991). "Female sterile mutations on the second chromosome of Drosophila melanogaster. II. Mutations blocking oogenesis or altering egg morphology." Genetics 129(4): 1119-1136.

Schupbach, T., E. Wieschaus, et al. (1978). "Study of Female Germ Line in Mosaics of Drosophila." Wilhelm Rouxs Archives of Developmental Biology 184(1): 41-56.

Sienski, G., D. Donertas, et al. (2012). "Transcriptional silencing of transposons by Piwi and maelstrom and its impact on chromatin state and gene expression." Cell 151(5): 964-980.

Siomi, M. C., K. Sato, et al. (2011). "PIWI-interacting small RNAs: the vanguard of genome defence." Nat Rev Mol Cell Biol 12(4): 246-258.

Slaidina, M. and R. Lehmann (2014). "Translational control in germline stem cell development." J Cell Biol 207(1): 13-21.

Song, J. J., S. K. Smith, et al. (2004). "Crystal structure of Argonaute and its implications for RISC slicer activity." Science 305(5689): 1434-1437.

Song, X., G. B. Call, et al. (2007). "Notch signaling controls germline stem cell niche formation in the Drosophila ovary." Development 134(6): 1071-1080.

Song, X., M. D. Wong, et al. (2004). "Bmp signals from niche cells directly repress transcription of a differentiation-promoting gene, bag of marbles, in germline stem cells in the Drosophila ovary." Development 131(6): 1353-1364.

Spradling, A. C. (1993). "Germline cysts: communes that work." Cell 72(5): 649-651.

Stanyon, C. A., G. Liu, et al. (2004). "A Drosophila protein-interaction map centered on cell-cycle regulators." Genome biology 5(12): R96.

Swan, A., S. Hijal, et al. (2001). "Identification of new X-chromosomal genes required for Drosophila oogenesis and novel roles for fs(1)Yb, brainiac and dunce." Genome Res 11(1): 67-77.

Takada, S., A. Kelkar, et al. (2003). "Drosophila checkpoint kinase 2 couples centrosome function and spindle assembly to genomic integrity." Cell 113(1): 87-99.

Terry, N. A., N. Tulina, et al. (2006). "Novel regulators revealed by profiling Drosophila testis stem cells within their niche." Dev Biol 294(1): 246-257.

Ting, H. J., J. Messing, et al. (2013). "Identification of microRNA-98 as a therapeutic target inhibiting prostate cancer growth and a biomarker induced by vitamin D." J Biol Chem 288(1): 1-9.

Tseng, C. Y., S. H. Kao, et al. (2014). "Notch signaling mediates the age-associated decrease in adhesion of germline stem cells to the niche." PLoS Genet 10(12): e1004888.

Vagin, V. V., A. Sigova, et al. (2006). "A distinct small RNA pathway silences selfish genetic elements in the germline." Science 313(5785): 320-324.

Vogel, E. and A. T. Natarajan (1979). "The relation between reaction kinetics and mutagenic action of mono-functional alkylating agents in higher eukaryotic systems. II. Total and partial sex-chromosome loss in Drosophila." Mutat Res 62(1): 101-123.

Wang, Z. A. and D. Kalderon (2009). "Cyclin E-dependent protein kinase activity regulates niche retention of Drosophila ovarian follicle stem cells." Proc Natl Acad Sci U S A 106(51): 21701-21706.

Ward, E. J., H. R. Shcherbata, et al. (2006). "Stem cells signal to the niche through the Notch pathway in the Drosophila ovary." Curr Biol 16(23): 2352-2358.

Wieschaus, E. and J. Szabad (1979). "The development and function of the female germ line in Drosophila melanogaster: a cell lineage study." Dev Biol 68(1): 29-46.

Winzeler, E. A., D. D. Shoemaker, et al. (1999). "Functional characterization of the S. cerevisiae genome by gene deletion and parallel analysis." Science 285(5429): 901-906.

Xie, T. and A. C. Spradling (1998). "decapentaplegic is essential for the maintenance and division of germline stem cells in the Drosophila ovary." Cell 94(2): 251-260.

Yin, H. and H. Lin (2007). "An epigenetic activation role of Piwi and a Piwi-associated piRNA in Drosophila melanogaster." Nature 450(7167): 304-308.

Zamore, P. D. (2010). "Somatic piRNA biogenesis." EMBO J 29(19): 3219-3221.

Zamparini, A. L., M. Y. Davis, et al. (2011). "Vreteno, a gonad-specific protein, is essential for germline development and primary piRNA biogenesis in Drosophila." Development 138(18): 4039-4050.

Zhang, J. and L. Li (2005). "BMP signaling and stem cell regulation." Dev Biol 284(1): 1-11.

ABSTRACT

DROSOPHILA CYCLIN J AND THE SOMATIC piRNA PATHWAY COOPERATE TO REGULATE GERMLINE STEM CELLS

by

PAUL MICHAEL ALBOSTA

May 2015

Advisor: Dr. Russell L. Finley, Jr.

Major: Molecular Biology and Genetics

Degree: Doctor of Philosophy

Cyclin J (CycJ) is a highly conserved cyclin that is uniquely expressed specifically in ovaries in *Drosophila*. Deletion of the genomic region containing *CycJ* and adjacent genes resulted in a genetic interaction with neighboring piRNA pathway gene, *armitage (armi)*. Here I assessed oogenesis in *CycJ* null in the presence or absence of mutations in *armi* or other piRNA pathway genes. Although *CycJ* null flies had decreased egg laying and hatching rates, ovaries appeared normal indicating that *CycJ* is dispensable for oogenesis under normal conditions. Further double mutant analysis of *CycJ* and neighbor *armi,* as well as two other piRNA pathway members (*piwi* and *aub*), revealed that *CycJ* genetically interacts with the piRNA pathways by enhancing their ability to regulate oogenesis. Double mutants of *CycJ* and mutants of *piwi* or *armi* produced mispackaged egg chambers containing an overabundance of germline cells, while double mutants of *CycJ* and *piwi* or *armi* had more severe defects. *CycJ* mutants also genetically interacted with mutants of the germline piRNA pathway member *aub*, resulting in unique oogenesis defects, though they were less severe than defects in double mutants of *CycJ* and *piwi* or *armi*. Piwi and Armi are known to function in both

the germline and germline-associated somatic cells. Here I show that the somatic function of *armi* and *piwi* promote egg chamber packaging in part by limiting BMP signaling and the accumulation of excess germline stem cells (GSCs) and that *CycJ* appears to cooperate with the somatic piRNA pathway. The increase of GSCs in *armi*, *piwi*, or *CycJ* double mutants depends on increased BMP signaling. Finally, *CycJ* promotes follicle cell proliferation in the absence of *armi*. My results suggest that *CycJ* genetically interacts with the somatic piRNA pathway to promote egg chamber packaging, limit BMP signaling, limit GSC accumulation, and promote proliferation of follicle cells.

AUTOBIOGRAPHICAL STATEMENT

PAUL MICHAEL ALBOSTA

EDUCATION:

2009-2015 Ph.D. in Molecular Biology and Genetics, Wayne State University, Detroit, MI, USA

2005-2008 B.S. in Biology, Saginaw Valley State University, University Center, MI, USA

HONORS AND AWARDS:

Rumble Fellowship, August 2012 to August 2013, Wayne State University

1st place poster presentation, CMMG retreat 2010

1st place oral presentation, Wayne State University GSRD 2013

PROFESSIONAL MEMBERSHIPS:

Genetics Society of America

PROFESSIONAL EXPERIENCE:

2006-2008 Head Assistant Laboratory Technician, Biology Department, Saginaw Valley State University, University Center, MI, USA

PUBLICATIONS:

G. Atikukke*, **P. Albosta***, H. Zhang, R.L. Finley Jr. **A role for *Drosophila* Cyclin J in oogenesis revealed by genetic interactions with the piRNA pathway**. *Mechanisms of Development.* 133: 64-76, 2014. *co-first authorship